Universidad Autónoma de Madrid
Departamento de Bioquímica

Doctoral Thesis

In vivo Elucidation of PIM Kinase Role in Tumourigenesis

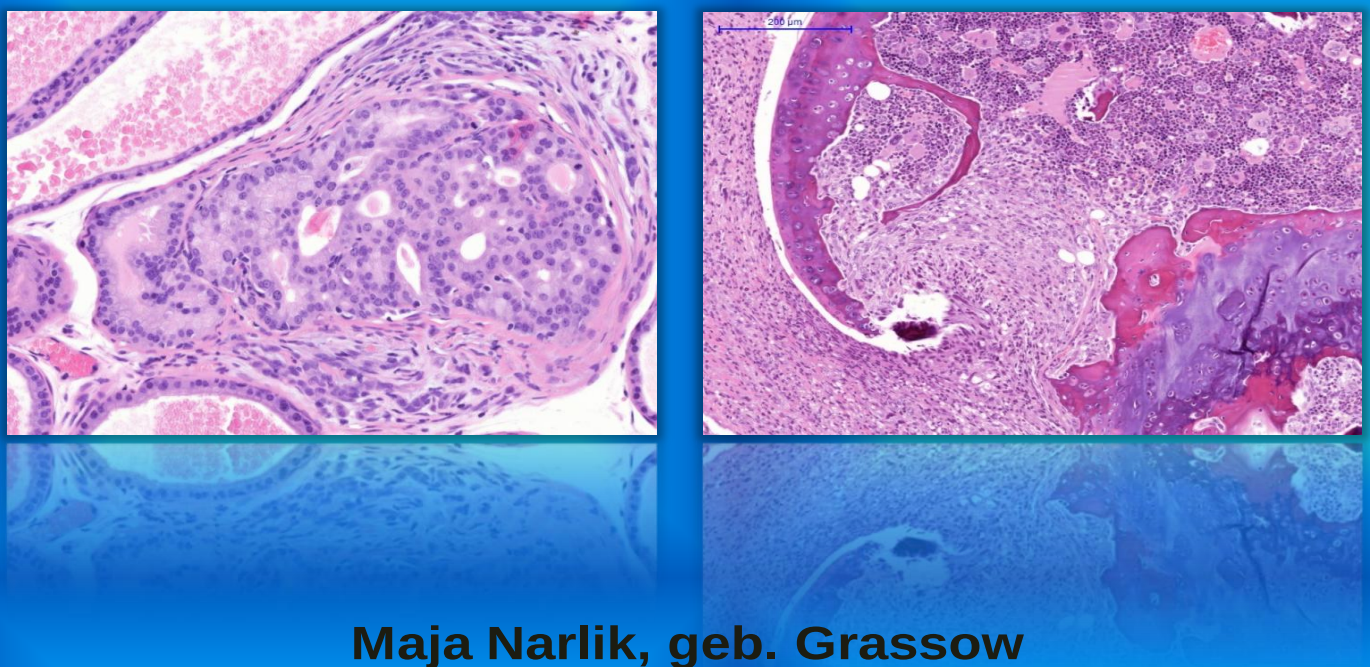

Maja Narlik, geb. Grassow

Madrid, 2012

DEPARTAMENTO DE BIOQUÍMICA

FACULTAD DE MEDICINA

UNIVERSIDAD AUTÓNOMA DE MADRID

In vivo Elucidation of PIM Kinase Role in Tumourigenesis

Maja Narlik, geb. Grassow; Licenciada en Biología

Directores: Dr. Amancio Carnero Moya y
Dra. Carmen Blanco Aparicio

Centro Nacional de Investigaciones Oncológicas

(CNIO)

El trabajo experimental presentado en esta memoria ha sido realizado en el grupo de Farmacología Molecular, del Departamento de Terapias Experimentales del Centro Nacional de Investigaciones Oncológicas (CNIO) bajo la dirección de los **Dres. Amancio Carnero Moya y Carmen Blanco Aparicio.**

Ha sido realizado con una beca de formación de personal universitario (FPU) del Ministerio de Educación y Ciencia.

Madrid, septiembre de 2011

A la comisión de doctorado de la UAM:

La finalidad de esta carta es informar a la comisión de doctorado de la Universidad Autónoma de Madrid sobre la doctoranda Maja Narlik Grassow que ha realizado su trabajo de Tesis Doctoral en el laboratorio de la sección de Desarrollo de Ensayos/Farmacología Molecular del Programa de Terapias Experimentales del Centro Nacional de Investigaciones Oncológicas (CNIO) en Madrid, desde el Marzo de 2006 hasta Febrero de 2011. Durante este tiempo ha llevado adelante el trabajo experimental de su tesis doctoral de manera responsable y exitosa. La doctoranda Maja Narlik Grassow ha planeado y llevado a cabo sus experimentos con gran motivación y eficacia y también ha destacado por la correcta interpretación y valoración de los resultados obtenidos. Estos resultados son sólidos y coherentes y constituyen un aporte relevante a la investigación científica, además serán publicados próximamente.

Durante la realización de este trabajo Maja Narlik Grassow ha adquirido gran conocimiento sobre cáncer, biología celular, genética y transducción de señales. Así mismo ha adquirido una gran competencia técnica que la habilita para desarrollar cualquier trabajo científico en el futuro.

En suma, tanto la capacidad de trabajo y las aptitudes mostradas por Maja Narlik Grassow durante el desarrollo de su proyecto de tesis, como los resultados de su investigación resumidos en esta memoria, pensamos que acreditan a Maja como merecedora del grado de Doctora. Por la tanto, mediante la presente autorizamos a Maja a leer su tesis doctoral ante el tribunal que ustedes consideren oportuno para optar al título de doctor.

Sin más, muy atentamente

Amancio Carnero Moya
Director de tesis

Carmen Blanco Aparicio
Directora de tesis

Juan Carlos Lacal Sanjuan
Tutor y Profesor Honorario, UAM
Departamento de Bioquímica/Facultad de Medicina

Acknowledgements

First of all, I want to thank my thesis directors Amancio and Carmen.

Amancio, thanks for letting me join your group and giving me the opportunity to write my thesis about a subject I like - mice. You pushed me when I needed it and taught me a lot, although I still do not believe that “life is hard” and for that you get the biggest thanks! Thanks for believing that I can do this, even when I thought I couldn’t. Because of you, I still love to be in a lab, just now I actually feel that I know what I’m doing. Thank you!

Carmen, you “adopted” me when Amancio left the CNIO and I cannot thank you enough for everything you have done, for all the work you put in. You taught me a lot of little things that in the end really make a difference in quality. Thank you!

I also want to thank the members of the Molecular Pharmacology Group, although a lot of them left the CNIO a while ago.

Oli, you were my “social services” during the first two years – thank you for all your help beginning the journey down the “PIM signalling pathway”, you have been a great teacher and I’m glad Amancio put me to work with you. Even on the worst days, there was still something to laugh about (if everything fails – we still can wait tables and drive a taxi).

Sandra and Bea, what can I say, you were like “Charlie´s Angels” - always there to listen and give advice; always willing to help. I don’t know how I would have done it without you. I hope at my next workplace I’ll find friends and colleagues like you.

Mer, thanks for your help and your cheering me up, you’ll always be my “enana favorita”. Vicky, Lidia, Natasha, Fabian, Irene, Wolf, Belen and Nuria: thanks for sharing part of the way and showing me some useful tricks that made work easier. Jesús, thanks for the chats and ideas about my PCR problems, you helped me a lot.

Huge thanks to Yoli, the best animal technician one could dream of. *Eres la más mejor del mundo mundial!* Thanks for your help and your ideas: most of what I learned about mice and handling them I learned from you!

Thanks to the other people of the animal facility: Isabel Blanco, whose door was always open, Delfi who was always there when I needed something, Sergio who jeopardized his fingers helping me identify pyelonephritis and all the others who did a great job every day so I could do mine.

Thanks to Narciso and Javier from the Biosecurity Unit, who made mouse irradiation less dreadful.

Thanks to Sagrario Ortega and Marta Riffo of the Transgenic Mice Unit, who helped me with any doubts I had about transgenic mouse generation.

Thanks to Marta Cañamero and her girls of the Comparative Pathology Unit for their excellent work; especially Virginia Alvarez, Maria del Carmen Arriba, Elvira Gil, Maria Gomez, Patricia Gonzalez and Natalia Matesanz. Special thanks to Marta for her help with the prostate and bladder grading and her ideas to putting everything together.

To my favourite “witches” from lab 105A: thanks for being my nutritionists, my psychologists and my friends. You made hard times a lot easier.

Marcie, thanks for the English editing and the endless coffee conversations during the years.

Last but not least the biggest thank you goes to my family. They supported me no matter what, and put up with me leaving home for so long. They told me that I have a choice, and knowing that helped me through the bad times.

But most importantly I want to thank the one person that stood by my side. Ibo my dear, thank you for everything, for bearing the bitching, the crying, the late nights and weekends without any complaint. Thanks for putting my feet back on the ground and your loving support. This is your work as much as mine. I cannot wait to start the next part of our life. Sonsuza dek beraber!

Resumen en Español

Las PIM quinasas son una familia de serina/treonina quinasas constituida por 3 isoformas diferentes (PIM1, PIM2 y PIM3) que son altamente homólogas. Su expresión esta mediada por la vía de señalización JAK/STAT que proporciona señales de supervivencia y de transición del ciclo celular. Actualmente, se están desarrollando activamente inhibidores de las PIM quinasas para el desarrollo de medicamentos contra el cáncer. Pero se sabe poco de la contribución relativa de las 3 isoformas en el proceso tumorigénico *in vivo* y como la inhibición individual de cada una podría afectar al crecimiento tumoral. Usando ratones modificados genéticamente, por un lado, hemos explorado si la inhibición específica de las isoformas de Pim es necesaria para prevenir la formación de sarcomas inducidos mediante el tratamiento carcinogénico con 3-metilcolantreno. Por otro lado, hemos determinado como la sobreexpresión de *PIM1* en la próstata de ratones transgénicos influye en la aparición de tumores en envejecimiento o en respuesta a un tratamiento hormonal. También hemos investigado la posible cooperación de la sobreexpresión de *PIM1 con la* pérdida de un alelo de *Pten* en la neoplasia prostática inducida por envejecimiento o por tratamiento hormonal.

Hemos determinado que la ausencia de *Pim2* y *Pim3* reduce mucho el crecimiento de los sarcomas, en similar medida a la ausencia de las 3 isoformas. Este modelo de sarcoma suele producir invasión del hueso por parte de las células tumorales. La ausencia de *Pim2* y *Pim3* reduce la invasión del hueso inducida por el tumor en un 70%, lo que es comparable con la reducción de la invasión del hueso en ausencia de las 3 isoformas. Se obtuvieron resultados similares en MEFs (fibroblastos embrionarios de ratón) derivados de los ratones "knockout" (KO), los MEFs doble KO *Pim2/3* mostraron una proliferación reducida y fueron resistentes a la transformación oncogénica por el oncogén *RAS*. Nuestros datos también sugieren un papel importante de la fosforilación de Gsk3β en el proceso de la tumorigénesis.

Con respecto a la sobreexpresión de *PIM1* en próstata hemos determinado que *PIM1* aumenta la formación de neoplasia intraepitelial en próstata (mPIN) inducida por hormonas, lo que correlaciona con inflamación debido a que los ratones que sobreexpresan *PIM1* mostraron niveles significativamente aumentados de inflamación. *PIM1* parece cooperar con la pérdida de un alelo de *Pten* en lesiones mPIN inducidas por hormonas, dado que el grado de mPIN está aumentado en estos animales. Por otro lado, en ratones de 10 meses la sobreexpresión de *PIM1* solo inducía grados bajos de mPIN. En ratones de 10 meses *PIM1* tampoco cooperaba con la pérdida de *Pten*. Hemos mostrado que *PIM1* también está expresado en vejiga después del tratamiento hormonal, induciendo hiperplasia urotelial moderada o severa, nuevamente relacionado con un entorno inflamatorio. En resumen nuestro trabajo muestra que las PIM quinasas siguen siendo dianas interesantes implicadas en muchos aspectos del proceso tumorigénico.

Summary in English

PIM kinases are a family of serine/threonine kinases composed of three different isoforms (PIM1, PIM2 and PIM3) that are highly homologous. Their expression is mediated by the JAK/STAT signalling pathway, providing survival and cell cycle transition signals. PIM kinases are heavily targeted for anticancer drug discovery. However, very little is known about the relative contribution of the different isoforms to the tumourigenesis process *in vivo*, and how their individual inhibition might affect tumour growth. Taking advantage of genetically modified mice, on one hand we explored whether the inhibition of specific *Pim* isoforms is required to prevent sarcomas induced by 3-methylcholanthrene carcinogenic treatment. On the other hand, we determined how overexpression of *PIM1* in prostate influenced the induction of prostatic neoplasia in aging and under hormone treatment in transgenic mice. We also investigated a possible cooperation of *PIM1* overexpression and heterozygous *Pten* loss in prostate in hormone- and aging-induced neoplasia.

We found that absence of *Pim2* and *Pim3* greatly reduced sarcoma growth, to a similar extent to the absence of all 3 isoforms. This model of sarcoma generally produces bone invasion by the tumour cells. Lack of *Pim2* and *Pim3* reduced tumour-induced bone invasion by 70 %, which is comparable with the reduction of tumour-induced bone invasion in the absence of all 3 isoforms. Similar results were obtained in MEFs derived from these knockout mice, where double *Pim2/3* knockout MEFs already showed reduced proliferation and were resistant to oncogenic transformation by the *H-RAS* oncogene. Our data also suggest an important role of Gsk3β phosphorylation in the process of tumourigenesis.

With regard to *PIM1* overexpression in prostate we determined that *PIM1* increased formation of hormone-induced prostate intraepithelial (mPIN) lesions, correlating with inflammation, since mice overexpressing *PIM1* showed significantly increased inflammation. *PIM1* seems to cooperate with loss of one *Pten* allele in hormone treatment-induced mPIN lesions, as mPIN severity is increased in these animals. In 10-month old mice on the other hand, *PIM1* overexpression only induced low-grade mPIN lesions. Also, in 10-month old mice, *PIM1* did not cooperate with *Pten* loss. We also showed that *PIM1* is expressed in bladder after hormone treatment inducing moderate to severe bladder hyperplasia, again correlating with an inflammatory environment. Taken together we showed in this work that PIM kinases are an interesting anticancer drug target which is involved in many aspects of tumourigenesis.

Indices

Index of Contents

Directory of Tables

Directory of Figures

Abreviations

ABL	Abelson leukaemia virus tyrosine kinase
AKT/PBK	murine thymoma viral oncogene homolog1 / Protein Kinase B
APS	ammoniumperoxodisulphate
ARF	alternate reading frame
AR	androgen receptor
BAD	BCL-2 associated death
BAX	BCL-2 associated X
BCL-2	B-cell lymphoma 2
BCR	break point cluster region
bh-grade	bladder hyperplasia grade
BTG1	B-cell translocation protein 1
CDK	cyclin dependent kinase
cDNA	complementary desoxyribonucleic acid
CDC25A	cell division cycle 25 homolog A
cKIT	feline sarcoma viral oncogene homolog
cTAK	CDC25C associated kinase
Cre	Cre-recombinase
CXRC4	chemokine receptor 4
CYR61	cystine-rich protein 61
dH_2O	distilled water
DKO	double knock-out
4E-BP	eukaryotic initiation translation factor 4E- binding protein
EPLIN	epithelial protein lost in neoplasm
ER	estrogen receptor
EtOH	ethanol
FLICE	FADD-like interleukin 1beta converting enzyme
FLIP	FLICE inhibitory protein
G-CSF	granulocyte colony stimulating factor
GFI-1	growth factor independent transcription repressor
GSK3β	glycogen synthase kinase 3β
HIF1α	hypoxia-inducible factor 1α-subunit
HP1	heterochromatin protein 1
HSP70	heat shock protein 70
IGFBP	insulin-like growth factor binding protein

IgG	immunogloblulin gamma
IHQ	immunohistochemistry
KI	knock-in
KI67/MKI67	proliferation related KI-67 antigen
KO	knock-out
LB medium	Luria broth medium
MARK	microtubule-affinity-regulating kinase
MIC	macrophage inhibiting cytokine
MMP9	matrix metallopeptidase 9
MYB	v- Myb-avian myeloblastosis - viral oncogene homologue
MYC	v- Myc –avian myelocytomatosis - viral oncogene homologue
3MC	3-Methylcholanthrene
MEF	mouse embryonic fibroblast
$MgCl_2$	magnesium chloride
mPIN	mouse prostate intraepithelial neoplasia
N-CAM	neural cell adhesion molecule
N-FATc1	nuclear factor of activated T-cells cytoplasmic 1
NF-κB	nuclear factor κ-light chain enhancer of activated B-cells
NP-40	Nonidet-P40
O.D.	optical density
$p21^{WAF1}$/CDKN1A	cyclin-dependent kinase inhibitor 1A
$p27^{KIP}$/CDKN1B	cyclin-dependent kinase inhibitor 1B
$p16^{INK4a}$/CDKN2A	cyclin-dependent kinase inhibitor 2A
p53	tumour protein p53
PAR	protease-activated receptors
PIAS-3	protein inhibitor of activated STAT
PP2A	protein phosphatase 2A
pAb	phosphorylated antibody
PIM	proviral integration site for Moloney murine leukaemia virus
Pim1	gene encoding mouse Pim1 kinase
PIM1	gene encoding human PIM1 kinase
PKR	protein kinase RNA regulated
pl-grade	prostate lesion grade
poly (A)	poly adenylated
PTEN	phosphatase and tensin homologue deleted in chromosome 10
RAF	rat fibrosarcoma homologue

RAS	rat sarcoma virus homolog
Rb	Retinoblastome
RNasin	RNase inhibitor
SCF	stem cell factor
s-grade	senescence grade
SMAD	small mothers against decapentaplegic
SRC	v-Src-avian sarcoma - viral oncogene homologue
TB buffer	Tris-borate buffer
TEMED	N,N,N,N`-Tetramethylethylendiamide
Tg	transgen
TGFβ	tumour growth factor beta
TKO	triple knock-out
TRAIL	TNF-related apoptosis inducing ligand
WHO	world health organization
Ø	diameter

Introduction

1. Introduction

1.1. General introduction to cancer

Cancer is the uncontrolled growth and spread of cells that may affect almost any body tissue. Among men, prostate and lung cancer are the most common cancers worldwide. For women, the most common cancers are breast and cervical cancer. More than 12 million people are diagnosed with cancer every year. It is estimated that there will be 16 million new cases every year by 2020. Cancer causes 7.6 million deaths every year—or 12.5% of deaths worldwide (data WHO/ www.who.int./en). In 2008 alone in the European Union 2.5 million people were diagnosed with cancer and 1.23 million died of cancer that year (European cancer commission/ www.eu-cancer.iarc.fr). Although 5-year survival rates increase every year, there is still an urgent need for molecular characterisation of the signalling pathways that lead to the development of cancer, in order to find better therapies.

1.2. What is it cancer? And how does it evolve?

The terms neoplasia and tumour are often used as synonymous. The term cancer stands for malignant tumours, which differ from benign tumours by their infiltrative and destructive growth as well as by their ability to form metastases. In a tissue carrying a tumour the number of cells is higher than in its normal counterpart, indicating that an alteration either in the cell cycle regulation or in the apoptosis control mechanisms is responsible for the mass change. Despite the fact that cell proliferation, differentiation and apoptosis underlie exact homeostatic control mechanisms, a change in these homeostatic balances, leaning towards either cell proliferation, to the disadvantage of cell differentiation, or inhibiting cell death (apoptosis), will result in an elevated overall cell number.

Through initial events (DNA damage and mutation, viral infections, etc.), which may represent a growth advantage for the cell, a clone of identical cells may form. This can subsequently lead to a tumour if other genetic or epigenetic events accumulate where the clone no longer underlies the host's homeostasis control mechanisms. The malignant characteristics are inheritable from mother to daughter cells and by that genetically fixed (Fearon and Vogelstein 1990), thus, if a tumour has a clonal origin, all the malignant cells share the same malignant characteristics. Malignant tumours have also been shown to become invasive and have metastatic properties. Indeed, malignantly transformed cells acquire the ability to form tumours in immunodeficient mice, but also to form foci in culture of immortalized cells. This surrogated property has been used for over 20 years to identify

oncogenes by the ability of immortal mouse cells to form foci when transfected with human tumour cell DNA (Pulciani, Santos et al. 1982).

1.3. Tumourigenesis

It is well established that defective processes of cellular homeostasis, such as functions involved in DNA repair and stability, result in a predisposition towards malignant transformation (Hanahan and Weinberg 2000). However, tumourigenesis is a multi-step process in which accumulation of genetic alterations drives the progressive transformation of normal cells into tumour cells. These alterations involve (i) signal-independent proliferation, (ii) escape from negative cell cycle control, (iii) constitutive protection from apoptosis, (iv) escape from cellular senescence, (v) angiogenesis induction, and (vi) local tissue invasion and metastasis. Each of these “abnormal” processes corresponds to a normal event either during development, tissue remodelling, stress, inflammation, or immune responses. The major difference is that while normal events need to be exogenously triggered by various combinations of growth factors, cytokines and hormones, pathological processes can proceed cell-autonomously. Certain combinations of normal events may then become transformation-specific due to their aberrant “constitutive” execution due to (I) mutated components of signalling pathways, (ii) improper interpretation of exogenous clues as a result of mutations in the recipient cell, (iii) failure of feedback mechanisms, or (iv) modulation of a non-mutated pathway by aberrant cross-talk with other mutated pathways. Thus, a number of tumour-related processes most likely correspond to de-regulated normal events (Hanahan and Weinberg 2000). Over the last decades, enormous advances have taken place defining basic molecular events central to many of the above processes. These include the characterisation of growth factors, their receptors and signal transducers, which have been biochemically, molecularly, or genetically (i.e. in model organisms such as yeast, flies, worms and mice) characterised to determine their functions. Central to malignant transformation are the inactivation of tumour suppressor genes (such as *p53, Rb*, or CDK inhibitors) and the activation of proto-oncogenes (e.g. *SRC, RAS, MYC*) by mutation or chromosomal rearrangements, invariably leading to broad changes of gene expression regulation. This type of analysis also allowed the unravelling of the tumourigenic function of key regulators of normal embryonic development (e.g. the TGFß/Smad, Delta/Notch or Hedgehog/Patched pathways), of components of the apoptotic machinery (de-regulation of pro-apoptotic proteins such as BAX or BAD, caspases, or inactivation of anti-apoptotic genes such as *BCL-2, FLIP* or members of the IAP family of caspase inhibitors); or the role of adhesion molecules (E- and N-cadherins, N-CAM, ß-

catenin) in late stages of cancer progression (local invasion and metastasis) (Hanahan and Weinberg 2000). Over the last decade beside these “old” hallmarks of cancer new ones have emerged and their contribution to the tumour microenvironment and tumourigenesis has to be considered. Nowadays “enabling characteristics” and hallmarks of cancer are differentiated (Hanahan and Weinberg 2011). Hallmarks are usually acquired over time through enabling characteristics such as inflammation and genomic instability (Hanahan and Weinberg 2011). Genomic instability generates random mutations, among which some can induce hallmarks of cancer. Through the complicated inflammation network in cancer (see 1.7.2.), hallmark-facilitating programmes are activated by sustained proliferative signalling, limited cell death, activated extracellular matrix-modifying enzymes facilitating angiogenesis, invasion, and metastasis (Hanahan and Weinberg 2011). Among the new emerging cancer hallmarks it has been established that reprogramming energy metabolism and evading immune destruction contribute to tumourigenesis (Hanahan and Weinberg 2011).

This impressive progress has been obtained, mainly, by the analysis of individual oncogenes and/or tumour suppressors, identifying key players involved in isolated basic mechanisms. As apoptosis is the end point for a range of tumour-suppressive mechanisms, evolved to prevent the emergence of autonomous cells, understanding its pathways is crucial to provide valuable insight into unknown aspects of tumour biology, with consequent prognostic and therapeutic implications. It has been shown that apoptosis can be controlled by a number of survival pathways, involving different kinases. Among these, are the AKT, MEK/ ERK and PIM kinases (Blanco-Aparicio, Renner et al. 2007; McCubrey, Steelman et al. 2007; Zhao, Hamza et al. 2008).

1.4. Tumour cell senescence

Cell senescence is the proliferative arrest in normal cells after a number of cell divisions. Today it is thought of as “terminal growth arrest”. Senescent cells cannot divide even after mitogen stimulation but they remain metabolically active. Cells undergoing senescence show characteristic morphological changes such as enlarged and flattened shape and increased granularity (Campisi, Kim et al. 2001). Senescence can be the normal process of “growing old”, resulting from telomere shortening (replicative senescence) or can be induced (accelerated senescence) by several factors like oxidative stress, DNA-damage or oncogene activation (oncogene-induced senescence – OIS). In both senescence types, growth arrest is induced by p53 activation which induced $p21^{WAF1}$ (p21) increase and cell cycle arrest (Noda, Ning et al. 1994; Alcorta, Xiong et al. 1996). Subsequently, $p16^{INK4A}$

(p16) is constitutively upregulated involved in maintaining the terminal arrested state in senescent cells. So, on first glance senescence must have a tumour-suppressive function: therefore, it is not surprising that tumour cells display not only senescence-promoting changes (RAS mutations) but senescence-inhibiting adaptions (p53 inhibition) (Roninson 2003). A good example for that is prostate cancer (PC). Within these tumours senescent cells appear due to anticancer treatment or external stress. These cells resistant to apoptosis are reservoirs for secreted factors that inhibit tumour growth but can also secrete mitogenic, antiapoptotic and angiogenic factors (Campisi 2001; Roninson 2003) mostly promoted due to the increased expression of p21 and p16. This concept could mean that increase of p21 and p16 suppose a bad prognosis as they upregulate tumour-promoting factors (Fig. 1).

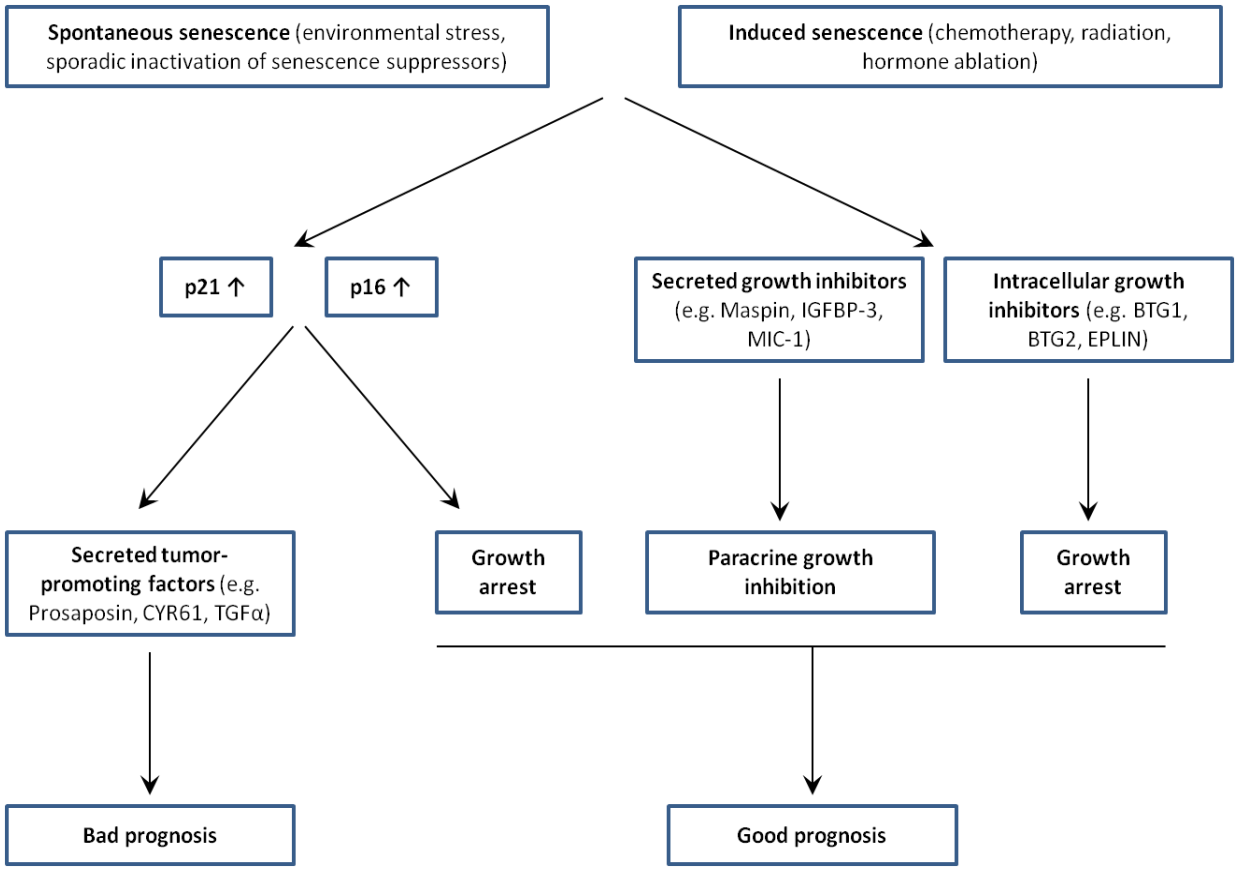

Figure 1. Tumour cell senescence and its implication for disease prognosis.

This concept is undermined by the fact that p16 is not expressed in normal prostate tissue but can be found in 50 % of prostate carcinoma (Lee, Capodieci et al. 1999). It is also an indicator of early relapse in prostate cancer – PC (Halvorsen, Hostmark et al. 2000). p21 is also increased in prostate cancer tissues independently of p53 (Osman, Drobnjak et al.

1999) and is associated with early relapse. p21 is also a significant marker of progression from androgen-dependent to androgen-independent PC (Fizazi, Martinez et al. 2002). It has to be mentioned that these correlations of p21 strongly depend on the genetic patient background (worse prognosis for Caucasian than for African American men). On the other hand, other senescence-associated tumour suppressors such as Maspin and IGFBP do not have the same effect in tumour cell senescence and correlate with a good prognosis (Roninson 2003).

1.5. The PIM kinase family

The PIM proteins are a family of short-lived protein serine/threonine kinases that are expressed at low levels in many tissues but mainly in haematopoietic cells and are highly conserved through evolution in multicellular organisms. This family of kinases is composed of three different members (PIM1, PIM2 and PIM3) that are highly homologous at the amino acid level, (Brault, Gasser et al. 2010) yet differ partially in their tissue distribution (Eichmann, Yuan et al. 2000). Functional redundancy of the three PIM kinases has been shown *in vitro* (Bullock, Debreczeni et al. 2005; Mukaida, Wang et al. 2011) and *in vivo* (Mikkers, Nawijn et al. 2004). They were originally identified in the 1980s as oncogenes in murine leukaemia virus (MuLV-induced lymphoma (Cuypers, Selten et al. 1984). PIM kinases are overexpressed in many haematopoietic malignancies and solid tumours. PIM kinases were originally implicated in cell survival by their ability to suppress Myc-induced apoptosis in a mouse model of lymphoma (Dautry, Weil et al. 1988; Borg, Zhang et al. 1999).

1.5.1. PIM kinase activity and regulation

PIM kinases are not regulated by membrane recruitment or phosphorylation like other kinases and are unusually regulated primarily by transcription. PIM kinases do not have a regulatory domain and are likely to be constitutively active when expressed (Laird, van der Lugt et al. 1993; Qian, Wang et al. 2005). Thus, their regulation appears to occur at the level of transcription, translation and proteosomal degradation (Amaravadi and Thompson 2005).

1.5.1.1. *PIM* kinase gene expression and translation

PIM kinases are single copy genes located: *PIM1* – chr. 17 in humans/ chr. 6 in mice; *PIM2* – mouse and human on the X chromosome; *PIM3* – chr. 15 in humans / chr. 22. in mice (Mikkers, Nawijn et al. 2004). For example, the *PIM1*-promoter is highly GC-rich and does not contain a TATA or CAAT box (Wang, Bhattacharya et al. 2001). *PIM* mRNA transcripts are encoded by 6 exons, giving rise to different PIM protein isoforms of different molecular masses which all maintain their serine/threonine kinase activity (Fig. 2); (Xie, Xu et al. 2006). The PIM kinases show high homology between each other, for example PIM1 and PIM3 are 71% identical at the amino acid level, whereas PIM1 and PIM2 depict 61% homology (Mikkers, Nawijn et al. 2004).

PIM genes are primary response genes, whose transcriptions are rapidly upregulated upon mitogenic stumuli and are transiently induced in response to a wide range of growth factors (Wang, Bhattacharya et al. 2001; White 2003; Hogan, Hutchison et al. 2008): interleukin-2 (IL-2), IL-3 and others, granulocyte- macrophage colony-stimulating factor (GM-CSF) and GCSF, alpha and gamma interferon (IFN) and many more. The majority of these factors transduce their primary signal through the JAK/STAT pathway, indicating that this cascade is probably instrumental in regulating the expression of the *PIM* genes (Mikkers, Nawijn et al. 2004).

.

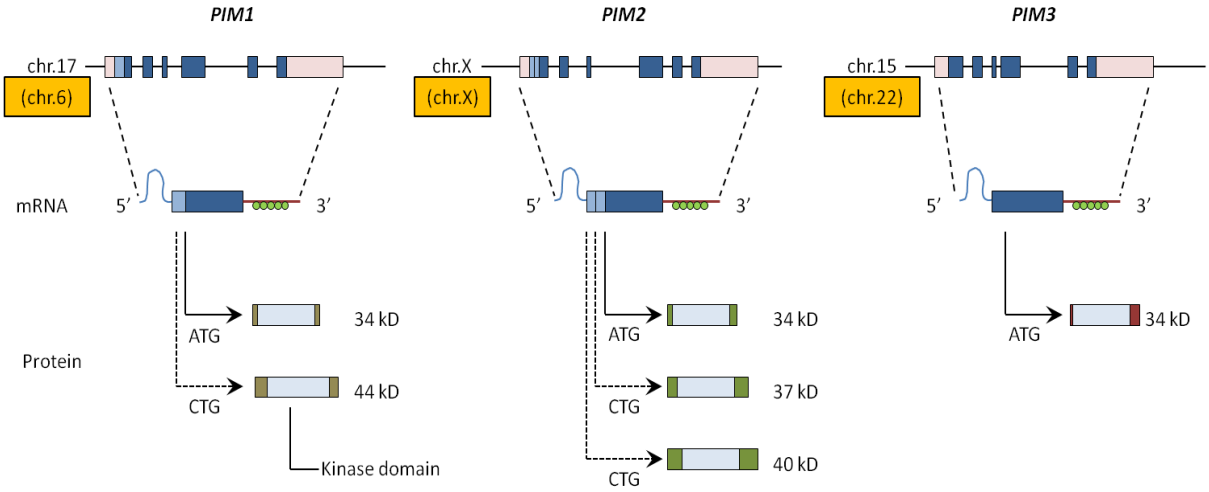

Figure 2. Different PIM genes, their transcripts and resulting proteins. *PIM* genes are located differently on mouse and human (orange boxes) chromosomes. *PIM* mRNA transcripts are encoded by 6 exons (dark blue boxes) with large 5' and 3' UTRs (rose boxes) with G/C-rich regions (light blue boxes) and 5 copies of AUUUA destabilising motifs (green circles). By using alternative translation initiation sites (solid and dashed arrows) and additional codons at the 5' end of these mRNAs (light blue boxes), different protein isoforms are synthesised.

The JAK/STAT pathway is activated by cytokine binding to cell surface receptors (Isaac, Siu et al.). JAK kinase subsequently phosphorylates the cytoplasmic receptor domain, thus creating recruitment sites for STATs and other signalling proteins. Activation of STATs by phosphorylation through JAK leads to their dimerisation and nuclear translocation. In the nucleus they regulate target gene expression by binding to specific promoter regions of the corresponding target genes (Fig.3).

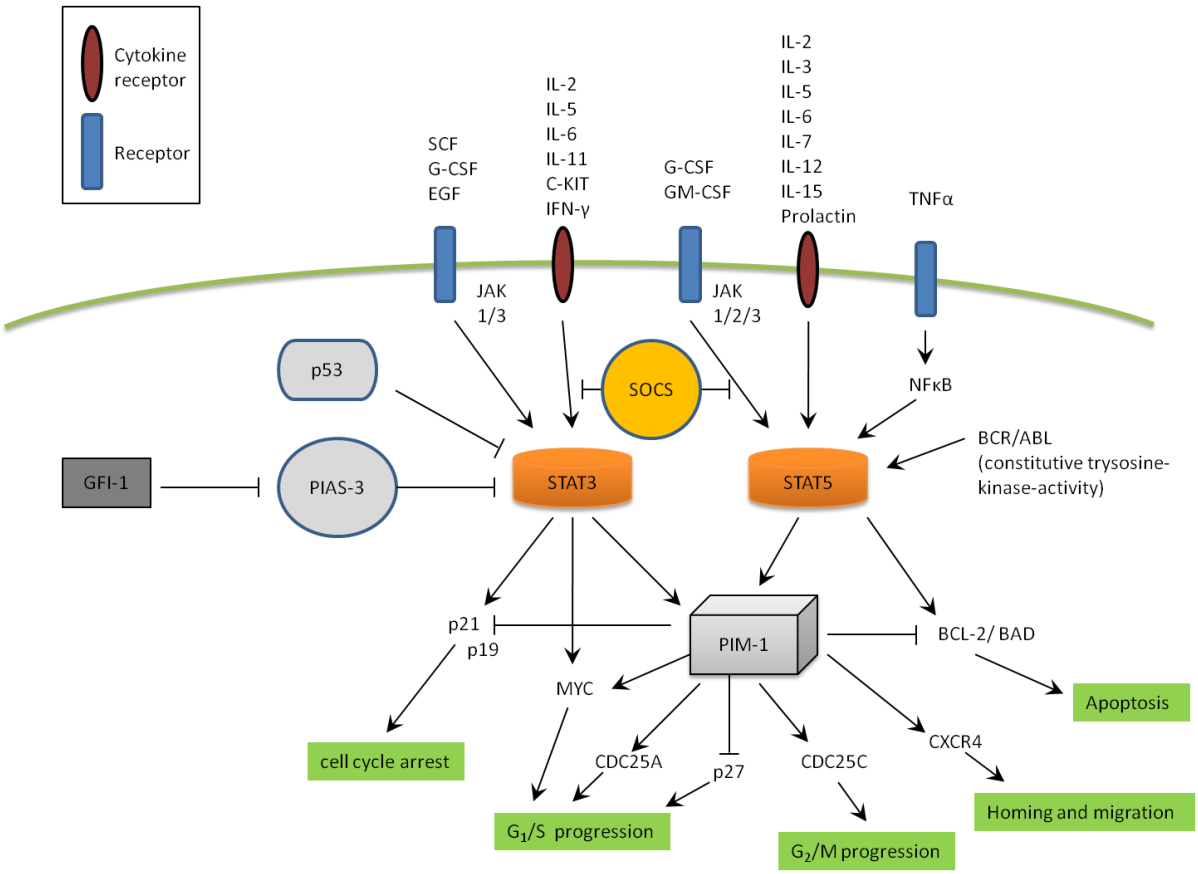

Figure 3. The JAK/STAT signalling pathway and PIM1 activation. Cytokine receptor stimulation by interleukin and growth factors activate STAT proteins via JAKs. STAT3 and STAT5 then directly regulate PIM1 expression. PIM1 itself phosphorylates several target proteins and thereby inactivates or activates proteins involved in cell cycle progression or apoptosis

For example, STAT3 and STAT5 bind directly to the *PIM1* promoter at the ISFR/GAS-sequence (IFN-γ activation sequence), thus upregulating *PIM1* gene expression. Additionally PIM1 is able to negatively regulate the JAK/STAT pathway by binding to SOCS proteins (suppressor of cytokine signalling), a group of negative regulators of the JAK/STAT pathway (Bachmann and Moroy 2005).

Gene expression of either one of the 3 PIM kinases is also induced by activation of transcription factors downstream of growth factor signalling pathways such as NF-κB and PIM1 expression can be induced by hypoxia in solid tumours independently of HIF1α (Chen, Kobayashi et al. 2009/A) and upon DNA damage by Krüppel-like factor 5 (KFL5), thereby protecting cells from apoptosis (Zhao, Hamza et al. 2008).

At the translation level it has been shown that mRNA transcripts of *PIM* are short lived due to multiple copies of destabilising AUUU(A) sequences in the 3´UTR regions, and on the other hand are "weak" transcripts due to GC-rich regions in the 5`UTR sequence. This is underlined by the fact that overexpression of eIF4E leads to an increase of PIM1 protein level, confirming cap-dependent translation of *PIM1* (Hoover, Wingett et al. 1997).

In addition, it was determined that the 3`UTR region of *PIM1* mRNA contains a stem-loop-pair sequence that specifically binds to eIF4E and thereby allows nuclear export and translation of the *PIM1* transcript (Culjkovic, Topisirovic et al. 2006).

1.5.1.2. Posttranslational regulation

PIM kinases do not require post-translational modifications to induce kinase activity. Their activity is largely regulated at the protein stability level; for example, by ubiquitylation and proteasomal degradation. For example PIM1 and PIM3 bind to PP2A, resulting in dephosphorylation, ubiquitylation and proteasomal degradation of PIM. It has also been shown that binding of PIM1 to HSP90 stabilises PIM1 protein levels and that binding of PIM1 to HSP70 results in its ubiquitylation and proteasomal degradation. Interestingly, hypoxia prevents ubiquitin-mediated proteasomal degradation of PIM1 in a HSP90-dependent manner. (Mizuno, Shirogane et al. 2001; Fox, Hammerman et al. 2003; Shay, Wang et al. 2005).

1.5.1.3. Regulation of MYC transcriptional activity by PIM kinases

Although the PIM kinases have been identified as oncogenes in transgenic models, by themselves they are only weakly transforming. However, they have been shown to greatly enhance the ability of c-Myc to induce lymphomas (Breuer, Slebos et al. 1989; van Lohuizen, Verbeek et al. 1989; Allen and Berns 1996; Allen, Verhoeven et al. 1997). It is understood that mere overexpression of MYC induces an apoptotic response, which has to be overcome to permit oncogenesis (Cuypers, Selten et al. 1986; Allen, Verhoeven et al. 1997; Wang, Bhattacharya et al. 2001). PIM kinases (PIM1 and PIM2) have been shown to

counteract this MYC-induced apoptosis (Nawijn, Alendar et al. 2011). This has also been proved for prostate cancer, where PIM1 is most likely to cooperate with MYC in cellular transformation as it is the most consistently expressed gene between MYC-positive and MYC-negative prostate cancer tumour samples (Zippo, De Robertis et al. 2007; van der Poel, Zevenhoven et al. 2010).

1.5.2. PIM kinases promote cell cycle progression and survival signalling

PIM kinases mediate their physiological activities through phosphorylation of a wide range of cellular substrates which, due to the functional redundancy of the PIM kinase family, greatly overlap. Previously described phosphorylation targets include SOCS-1 (Paukku and Silvennoinen 2004), runt-related transcription factor 1 (RuNX1) and RuNX3 (Aho, Sandholm et al. 2006); cell cycle regulators such as $p21^{WAF1}$ and $p27^{Kip1}$ (Wang, Bhattacharya et al. 2002; Morishita, Katayama et al. 2008), CDC25A phosphatase (Mochizuki, Kitanaka et al. 1999) and the kinase cTAK/MARK3/Par1A, and transcriptional repressors (HP1), activators (NFATc1 and c-MYB) and coactivators (p100) (Koike, Maita et al. 2000; Ishibashi, Maita et al. 2001; Rainio, Sandholm et al. 2002; Winn, Lei et al. 2003; Evans and Fox 2007). More recently, PIM2 has been shown to phosphorylate the ribosomal protein 4E-BP1, causing its dissociation from eIF4E, which may affect protein synthesis as eIF4E is a rate-limiting factor (Paukku and Silvennoinen 2004). Interestingly, several of the mentioned substrates are shared with AKT kinases, and PIM and AKT often phosphorylate the same residues (Amaravadi and Thompson 2005; Nawijn, Alendar et al. 2011). Therefore, PIM kinases are strongly implicated in cell cycle progression and cell growth. PIM kinases are also implicated in apoptosis (for example, through BAD phosphorylation) and have been shown to induce genomic instability. This last effect is mainly mediated through interaction between PIM1 and NUMA (nuclear mitotic apparatus protein) (Bhattacharya, Wang et al. 2002). It has been shown that checkpoint control is lost under PIM1 overexpression, and as a consequence cells with spindle abnormalities are not arrested in mitosis and are also not able to efficiently complete the cell cycle, resulting in polyploidy and multinucleation (Roh, Gary et al. 2003). As all these are mechanisms used by tumours to override mitotic spindled checkpoint (Shah, Pang et al. 2008), *PIM1* overexpression might play an important role in early tumourigenesis driving genomic instability.

1.5.3. PIM kinases in cancer

The PIM kinase family members are considered oncogenes and have been implicated in tumourigenesis either alone or functioning synergistically with c-MYC (Allen and Berns 1996; Allen, Verhoeven et al. 1997). Initially, elevated levels of PIM1 kinase were discovered in leukaemia and lymphoma tumours (Cuypers, Selten et al. 1986; Selten, Cuypers et al. 1986; Wang, Bhattacharya et al. 2001). However, more recently, PIM1 was found to be increased in solid tumours, including pancreatic and prostate cancer, squamous cell carcinoma, gastric carcinoma, colorectal carcinoma, liver carcinoma (Bachmann and Moroy 2005; Shah, Pang et al. 2008), and recently liposarcoma (Nga, Swe et al. 2010) and bladder cancer (Guo, Mao et al. 2010). Increased levels of PIM2 kinase have been detected in various lymphomas as well as in prostate cancer. Several *in vitro* studies also connected PIM2 kinase with liver cancer (Brault, Gasser et al. 2010). PIM3 kinase has been found aberrantly expressed in malignant lesions of endoderm-derived organs, like liver and pancreas, and also in Ewing's sarcoma (Brault, Gasser et al. 2010).

Table 1: List of human cancers with reported expression increase of any of the three PIM kinases.

Tumour Subtype	**Gene**	**Prognosis**	**References**
Haematological malignancies*			
B-CLL	*PIM2*	ND	(Chen, Redkar et al. 2009)
Mantle cell lymphoma	*PIM1;PIM2*	poor	(Hsi, Jung et al. 2008)
DLBCL	*PIM1; PIM2*	poor	(Poulsen, Borup et al. 2005)
Primary mediastinal large B cell lymphoma	*PIM1*	ND	(Dave, Fu et al. 2006)
Acute myeloid leukaemia	*PIM2*	ND	(Tamburini, Green et al. 2009)
Malignancies of epithelial origin			
Bladder Cancer	*PIM1*	ND	(Guo, Mao et al. 2010)
Prostate cancer	*PIM1; PIM2*	good	(Dhanasekaran, Barrette et al. 2001)
Perineural invasion in prostate cancer	*PIM2*	poor	(Li, Szabolcs et al. 2006)
Pancreatic cancer	*PIM1; PIM3*	good (*PIM1*)	(Reiser-Erkan, Erkan et al. 2008)
Gastric carcinoma	*PIM1; PIM3*	poor (*PIM3*)	(Warnecke-Eberz, Bollschweiler et al. 2009)
Squamous cell carcinoma of head and neck	*PIM1*	poor	(Shah, Pang et al. 2008)
Oral squamous carcinoma	*PIM1*	ND	(Chiang, Yen et al. 2006)
Colorectal carcinoma	*PIM1;PIM3*	ND	(Popivanova, Li et al. 2007)
Liver cancer	*PIM1;2;3*	ND	(Gong, Wang et al. 2009)
Liposarcoma	*PIM1*	ND	(Nga, Swe et al. 2010)
Ewings sarcoma	*PIM3*	ND	(Brault, Gasser et al.)

B-CLL: B-cell chronic lymphocytic leukaemia; DLBCL: diffuse large B-cell lymphoma;

According to World Health Organization (WHO) classification 2008 (Jaffe, Harris et al. 2008)

Recent studies have correlated PIM1 kinase with chemoresistance in prostate cancer cells, which is a common occurrence in more aggressive, hormone-refractory prostate cancers (Chen, Kobayashi et al. 2009/B; Mumenthaler, Ng et al. 2009). PIM1 kinase has also been linked to hypoxia-promoted genetic instability in solid tumours facilitating cell survival, resulting in tumours with a more aggressive phenotype (Chen, Kobayashi et al. 2009/A). It has also been shown that *Pim1* overexpression induces senescence in mouse fibroblasts (Zemskova, Lilly et al. 2010).

1.5.4. PIM kinases as a therapeutic target

PIM kinases are interesting targets for new drug development, since they are overexpressed in many cancers and involved in cancer-specific pathways such as survival, cell cycle progression and migration/homing. Developing effective PIM inhibitors is also important to overcome PIM-promoted chemoresistance of cancer cells through BAD inactivation and hypoxia-induced drug resistance (Reiser-Erkan, Erkan et al. 2008; Chen, Kobayashi et al. 2009/B; Lopez-Ramos, Prudent et al. 2010), as well as PIM-induced rapamycin resistance (Swords, Kelly et al. 2011). PIM is also activated by docetaxel, thus promoting survival of docetaxel treated PC cells (Zemskova, Sahakian et al. 2008). The emerging importance of PIM kinases in human tumourigenesis has raised growing interest in developing small molecule inhibitors for them. Several different classes of PIM inhibitors have recently been reported - reviewed in (Magnuson, Wang et al. 2010) -, but only a few of them have been tested in cell-based assays or animal models to demonstrate anticancer activity (Morishita, Katayama et al. 2008; Chen, Redkar et al. 2009; Lin, Beharry et al. 2010; Santio, Vahakoski et al. 2010) efficiently blocking several cellular functions of PIM kinases and chemoresistance induced by PIM (Mumenthaler, Ng et al. 2009).

In addition, only a few of them are effective against all PIM family kinases (Chen, Redkar et al. 2009; Swords, Kelly et al. 2011), since most of them have been focused on PIM1. Due to functional redundancy (Mikkers, Nawijn et al. 2004), simultaneous targeting of all PIM kinases can be of advantage in treating cancer patients. Yet no severe side effects are expected, since mice lacking all three Pim family members are just slightly deficient in their growth responses, but otherwise viable with a normal life span (Mikkers, Nawijn et al. 2004). It has also been shown, that PIM inhibitors synergise with rapamycin, gefitinib, sunitinib and BCL-2 inhibitor ABT-737 (Beharry, Zemskova et al. 2009; Blanco-Aparicio, Collazo et al. 2011; Siu, Virtanen et al. 2011; Song, Kandasamy et al. 2011).

1.6. Mouse models in cancer

Mice have been used as cancer models for nearly 30 years for many reasons – they are small, require little food and housing space, they are easy to handle, have a reasonable offspring size and an acceptably short generation span. But the main reasons are the wide genetic knowledge about this species, the similarity between human and mice genetics and the ease of manipulating their genome. However, mouse models are not “perfect” and may never be because although they are more sophisticated nowadays and despite high genetic similarity between humans and mice there are still specific differences not only in the genome but also in other aspects such as metabolism and immune system, etc. That is why mouse models have to be seen as a complementary tool that enables the scientist to determine a cancer phenotype within the tumour microenvironment and intact immune system; they enable drug development/testing for specifically targeted pathways, facilitate pharmacodynamic and pharmacokinetic studies and they permit monitoring of drug delivery and thus assessment of drug action on tumour development by *in vivo* imaging.

1.6.1. PIM kinase mouse models

To date, there are several mouse models for Pim kinases which have shown that overexpression of Pim kinases alone is not sufficient for tumourigenesis but rather requires the concomitant overexpression of a cooperating gene such as *c-myc, N-myc,* or *bcl-2* (van Lohuizen, Verbeek et al. 1989; Breuer, Wientjens et al. 1991; Acton, Domen et al. 1992; Hoover, Wingett et al. 1997). Because experimental overexpression of Pim1 induces tumours at a relatively low incidence and with a long latency, it has been classified as a weak oncogene (transgenic mice in which Pim1 was expressed specifically in lymphoid tissue, developed T-cell lymphoma with a 5–10% incidence before 7 months of age (Moroy, Verbeek et al. 1991). However, a very strong synergism with regards to tumourigenicity occurs between Pim1 and 2 and c-Myc, which could be observed in bi-transgenic mice overexpressing *c-Myc* and *Pim1* in lymphoid tissue with the result that such mice died in utero of pre-B cell lymphoma (Zhang, Wang et al. 2008). Interestingly, animals deficient in Pim1 are viable and show only a minor defect in haematopoiesis (Domen, van der Lugt et al. 1993; Laird, van der Lugt et al. 1993), suggesting that Pim1 contributes to haematopoietic cell growth and survival, although its role is probably secondary to other signalling pathways. More importantly, mice lacking expression of *Pim1, Pim2* and *Pim3* are viable and fertile, although they show a profound reduction in body size at birth and throughout postnatal life (Mikkers, Nawijn et al. 2004). In addition, the *in vitro* response of

distinct haematopoietic cell populations to growth factors is severely impaired. These results indicate that members of the PIM protein family are important but dispensable factors for growth factor signalling (Mikkers, Nawijn et al. 2004). Together, these studies suggest that PIM kinases may play a distinct role in tumour formation *in vivo*, implying that they may be novel targets for cancer therapy (Magnuson, Wang et al. 2010).

1.7. Prostate cancer

Prostate Cancer (PC) is the most common malignancy in men in the Western world. In 2008 over 910.000 men were diagnosed with prostate cancer, with the highest incidence lying in Western Europe, Northern America and Australia/New Zealand, and the lowest being in Asia. Incidence has increased constantly over the last decade, mainly due to availability of prostate-specific-antigen (PSA) screening in symptom-free men. Prostate cancer usually develops slowly, passing through a series of defined states such as prostate intraepithelial neoplasia (PIN), prostate carcinoma *in situ*, invasive and metastatic carcinoma (Wang, Gao et al. 2003). PIN, generally known as a likely primary precursor for human prostate cancer, can be determined as low-grade or high-grade. The latter are believed to be a primary state of prostate adenocarcinoma (Roy-Burman, Wu et al. 2004). But as not all PIN lesions progress to invasive prostate cancer it is hard to predict which ones will. The molecular pathways that will contribute to the progression of high-grade PIN lesions to prostate adenocarcinoma are still being widely investigated. Today we know that aberrations in specific signalling molecules such as extracellular growth factors, protein tyrosine kinase cell surface receptors, intracellular anti-apoptotic or transcription factors, nuclear receptors and their ligands, growth suppressors, cell cycle regulators and others are implicated in the process of disease progression (Roy-Burman, Wu et al. 2004). Prostate cancer is a very heterogeneous disease with many pathways involved, so understanding where malignant cells arise from is of the utmost importance for the development of effective therapies. The main reason for that the most common therapy is androgen deprivation therapy as tumours are androgen-dependent, but over time, most cancers become androgen-independent, developing into hormone refractory prostate cancer (HRPC) (Denis and Murphy 1993). To that end, mouse models provide valuable insight to that question. To date, there have been several PC mouse models established. In view of this work, the most important ones have been the *Pten* mouse models that showed that inactivation of one *Pten* allele is enough to induce PC in mice as early as ten months of age (Wang, Gao et al. 2003), and a *Myc/Pim1* mouse model that showed that coexpression

of *c-Myc/Pim1* after lentiviral-mediated gene transfer induced PC within 6 weeks (Wang, Kim et al. 2010).

In view of this work it should also be mentioned that sole overexpression of PIM1 has been implicated in prostate cancer development. It has been shown that PIM1 is overexpressed in high-grade prostate intraepithelial neoplasia (HGPIN), which might be a sign that PIM kinases are involved in the early development of prostate malignancy (Valdman, Fang et al. 2004). PIM1 expression is also increased under androgen ablation therapy (van der Poel, Zevenhoven et al. 2010) and its expression is associated with hormone refractory PC (HRPC). And although PIM1 might not be sufficient to initiate expression of androgen-dependent genes like PSA which requires transcriptional activity through androgen receptor (AR), it might be involved in the step from an androgen-dependent to an androgen-independent state in prostate carcinoma.

1.7.1. Mouse vs. human prostate

As there are nearly no naturally occurring PCs in mice there are pros and cons of using mouse models for PC research. There are significant similarities and differences in the anatomy of the mouse and human prostate, which needs to be considered when evaluating mouse models of human prostatic disease. Therefore, a big challenge has been to establish mouse models that develop PCs that accurately mimic the human disease.

Table 2: Differences between mouse and human prostate cells.

	human	mouse
secretory cells	- columnar form - secrete prostatic proteins and fluids from apical cell surface into lumen	- columnar form - secrete prostatic proteins and fluids from apical cell surface into lumen
basal cells	- continuous layer between secretory cells and basement membrane	- fewer basal cells - discontinuous layer
neuroendocrine cells	- scattered and rare	- even more rare
stroma	- robust fibromuscular stroma	- modest stroma

In both species prostates and accessory glands derive from Wolffian ducts and urogenital sinuses and are androgen-sensitive (Roy-Burman, Wu et al. 2004). In both, prostates are composed of glands and ducts showing similar epithelial cell types (secretory, basal and

neuroendocrine) which presumably carry out the same physiological function, although the ratio varies between species {Table 2; (Roy-Burman, Wu et al. 2004) }.

One main difference between the human and mouse prostate lies in the structure of the prostate. The mouse prostate consists of four lobes: anterior (coagulating gland), ventral, dorsal and lateral (the latter are commonly known as dorsolateral), {(Abate-Shen and Shen 2002); Fig. 4}. The human prostate, on the other hand, has one "lobe", divided into three zones: central, transitional and peripheral. The peripheral zone covers 75% of the human prostate and is the "hot spot" for malignancies, as most human PCs are found in this area (Powell, Cardiff et al. 2003). And although the dorsolateral lobe in mice has been described as most similar to the peripheral zone in human prostate tissue (Powell, Cardiff et al. 2003) the consensus today is that there is no direct relationship between the zones of the human prostate and any lobe of the mouse prostate (Shappell, Thomas et al. 2004).

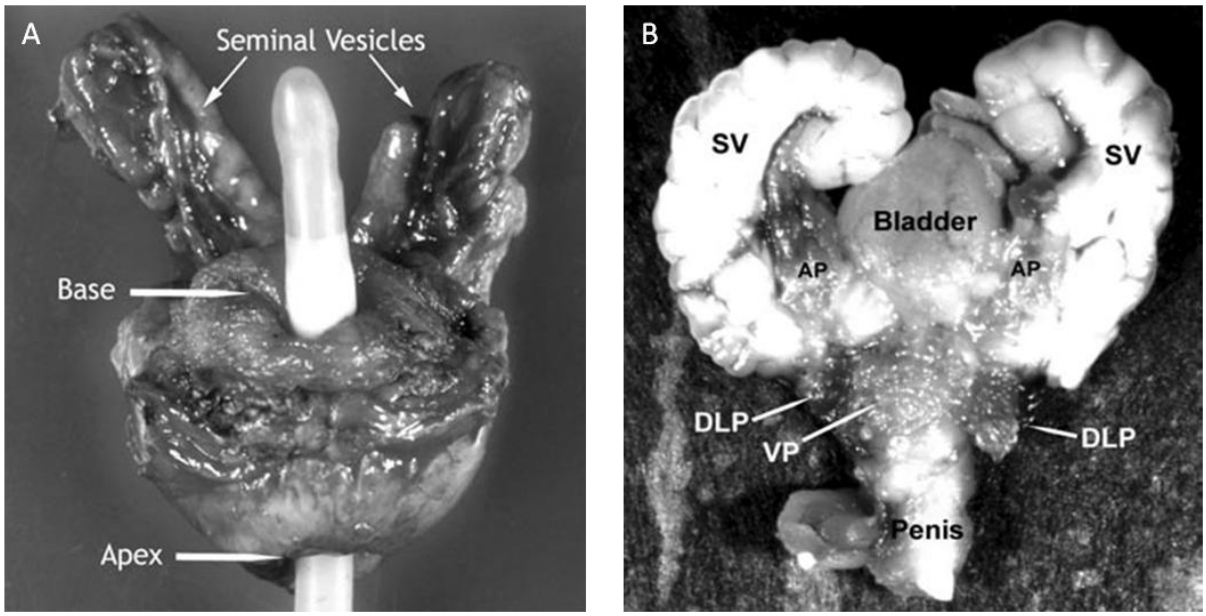

Figure 4. Anatomical comparison of human and mouse prostate glands. **A: Ventral view of fresh human prostate.** Tubing demonstrates the path of the urethra. The urinary bladder would sit on top (base) of the prostate, and the bottom of the prostate (the apex) would rest on the urogenital diaphragm. **B: Ventral view of formalin-fixed mouse prostate.** The mouse prostate consists of four paired lobes, namely, ventral (VP), dorsal (DP) and lateral (LP), which are referred to together as DLP, and anterior (AP) prostate; (SV, seminal vesicle). (figure copied from Roy-Burman et al.; Endocr.-Relat. Canc. (2004) 11, 225-54; 1351-0088/04/011–225 © 2004 Society for Endocrinology Printed in Great Britain; http://www.endocrinology-journals.org)

Another difference between mice and human PC to bear in mind when comparing mouse models with human PC is that cancer metastasis in mice often originates from mesenchymal cells, whereas in humans it tends to evolve from epithelial cells (Valkenburg

and Williams 2011). It has also been shown to be difficult to induce bone metastasis in mice, which is the most common metastasis in human PCs.

So, to recapitulate, the ideal prostate cancer mouse model would show epithelial hyperproliferation and hyperplasia leading to mPIN. The mice would then develop non-invasive carcinoma in situ which should evolve into locally invasive adenocarcinoma followed by a metastatic stage and/or castration resistance, which would be of utmost interest as androgen-independent tumours are currently untreatable (Valkenburg and Williams 2011).

1.7.2. Prostate cancer and inflammation

Another discussed link towards prostate cancer development is the implication of inflammation, which has been linked to cancer since the 19th century. It is known that chronic inflammation predisposes to different cancers such as gastric, colon and prostate cancer. In fact, an inflammatory component can be found in the microenvironment of many neoplasic tissues (Colotta, Allavena et al. 2009). Cancer-related inflammation (CRI) is characterised by prominently tumour-associated macrophages, infiltration of white blood cells, presence of polypeptide messengers of inflammation (IL-1, IL-6, TNF, etc.) and the occurrence of tissue remodelling and angiogenesis (Colotta, Allavena et al. 2009). Schematically, two pathways have been implicated in CRI. On one hand, an intrinsic pathway, which suggests that genetic events cause neoplasia and initiate inflammation-related programmes that lead to the development of an inflammatory microenvironment (Borrello, Alberti et al. 2005; Mantovani, Allavena et al. 2008; Mantovani 2009). Up untill now several oncogenes (e.g. RAS/RAF) and tumour suppressors have been shown to be able to juggle the proinflammatory circuits. On the other hand, an extrinsic pathway has been mapped out where inflammatory conditions facilitate cancer development. For example, infections (e.g. *Heliobacter pylori* – gastric cancer; papilloma virus – cervical cancer), autoimmune diseases (e.g. chronic inflammatory bowel disease – colon cancer) and inflammatory conditions such as prostatitis in prostate cancer have been shown to increase the risk for progression (Colotta, Allavena et al. 2009). Cytokines and transcription factors are key players where both pathways meet. NF-κB, STAT3 and IL-6 have been identified as such key players. NF-κB induces inflammatory cytokines, adhesion molecules and many more. It is also known to induce anti-apoptotic genes such as PIM kinases, thus promoting survival in tumour cells. STAT3 is constitutively activated in tumour and immune cells and has been shown to be involved in carcinogenesis and tumour immune invasion (Kortylewski, Kujawski et al. 2005; Yu, Kortylewski et al. 2007). STAT3 controls cell

proliferation and survival by regulating *c-MYC*, *PIM1, CYCLIN D1* and *BCL-2* expression (Becker, Fantini et al. 2004). IL-6, on the other hand, is a multifunctional cytokine that promotes cell growth and anti-apoptotic activity (Lin and Karin 2007; Naugler and Karin 2008). The NF-κB/IL-6/STAT3 cascade has already been linked to colon cancer, multiple myeloma and prostate cancer (Kortylewski, Xin et al. 2009). Also, in AR-negative PC cells, IL-6 is known to inhibit apoptosis mediated through increased AKT phosphorylation (Culig and Puhr 2011). Other cytokines regulated by NF-κB implicated in prostate cancer are, for example, IL-4 and IL8. IL-4 activates androgen receptors (AR) in LN-CAP cells (Culig and Puhr 2011) and is considered to be an antiaopototic cytokine as it stimulates the AKT pathway (Culig and Puhr 2011). IL-8 induces angiogenesis and metastasis, mediating its angiogenic effect through MMP9 on the formation of new blood vessels. IL-8 also inhibits TRAIL-based apoptosis through c-Flip regulation and upregulates AR activity (Culig and Puhr 2011). All these results suggest an involvement of the PIM kinase family in CRI.

Aims

2. Aims

- Validate PIM kinases as drug targets. To that end, we will study the effect of depleting specific Pim isoforms in a model of 3 methylcholanthrene carcinogenic-induced sarcoma

- Study the effect of *PIM1* overexpression in prostate on hormone treatment- and aging-induced neoplasia.

- Study a possible cooperation between loss of one *Pten* allele and *PIM1* overexpression in prostate under hormone treatment as well as in aging.

Methods

3. Methods

3.1. Biological reagents used

Antibiotics: Puromycin (Calbiochem) 50 µg/ml; Ampicilin (Sigma) 1mg/l; Penicillin/Streptomycin (Gibco) 40 U/ml; Fungizone (Gibco) 1 µg/ml.

Treatments: 3-Methycholanthrene (Sigma) 10mg/ml; Testosterone (Sigma) 12.5.mg/cycle; Estradiol (Sigma) 1.25 mg/cycle.

Vectors: pGEM-Teasy (Invitrogen); p-VL-1(A. Nebreda, CNIO)**;** pBabepuro, pBabepuro-H-RAS^{V12}, pBabepuro-PIM1, pBabepuro-PIM2, pBabepuro-PIM3.

Bacterial strains: All used plasmid were propagated by bacterial strains *E.coli* TOP10 (Invitrogen) or Max Efficiency (Invitrogen). The bacteria were grown under agitation in LB medium (10 g/l tripton, 5 g/l yeast extract, 10 g/l NaCl; pH 7.0) at 37°C for 16h.

3.2. Basic techniques of molecular biology

All basic techniques of molecular biology procedures were carried out using standard protocols (e.g. from Maniatis: "Molecular cloning – a laboratory manual"; 2^{nd} edition) or following the protocol provided by the manufacturer when using commercial kits. Other specific protocols used here that were developed in the laboratory where this work was carried out are specified.

3.2.1. Polymerase chain reaction (PCR)

The PCR-standard mix contained 0.2 mM of each of the four dNTPs (dATP, dCTP, dGTP, dTTP; Fermentas), 10 pmol of each primer (Sigma), 2 mM of $MgCl_2$ (CNIO), 1U of Taq polymerase (CNIO), 10x reaction buffer - 100 mM Tris-HCl, pH 8.3, 500 mM KCl (CNIO) and the appropriate amount of DNA diluted in dH_2O. The reactions were done in the T3 thermocycler (Biometra). The conditions were specified in each case using specifically designed primers (Tables 5,6,8). The PCR products were separated in a 1,5% agarose gel (Seakem), samples were diluted in 10x loading buffer (Fermentas) and run at 100 – 120V in either TAE or TBE buffer for 60 min. Amplified fragments were visualized with ethidium bromide (Promega).

3.2.2. Construction of the transgenic DNA

The sequence of the *PIM1* was amplified by PCR using specifically designed primers (Fig. 5) and cDNA of human IMR90 cells as a template and a Myc-tag was added.

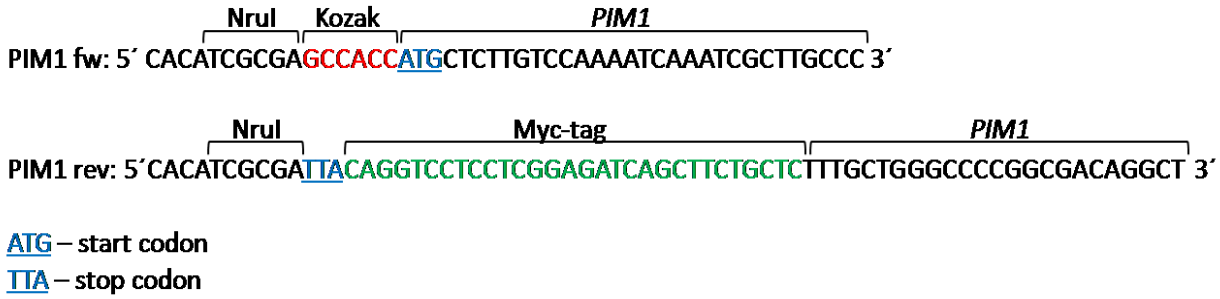

Figure 5. Specific primer construct to amplify PIM1 and Myc-tag. Specific primers for amplification of *PIM1* include a NruI restriction site, the Kozak sequence to assure translation initiation, start and stop codon of *PIM1* and a Myc-tag at the 3´end of the *PIM1* sequence.

To verify the sequence, the PCR fragment was cloned into the pGEM-Teasy vector system, the sequence was verified by sequencing at the Genomics Unit of the CNIO following their protocols. After verification of the sequence and when coding sequence and frame were intact, human *PIM1*–Myc tag were cloned into the pVL-1 vector using NotI restriction enzyme. The constructs carrying the transgene were generated inserting the *PIM1* sequence into the pVL-1 vector, which carries all the additional genetic elements necessary for the inducibility of the transgene (Fig. 19), such as a CMV-enhancer, a β-actin promoter, the LoxP/STOP cassette and a polyA tail. The right insertion was verified by sequencing. Primers designed specifically for the sequence of human *PIM1*, which do not amplify mouse *Pim* genes were used for all PCRs and subsequent genotyping of mice (Tables 5,6,8). The DNA construct was linearized using PvuII enzyme and injected into embryonic stem cells, where it was inserted by random recombination. The embryonic stem cells carrying the transgenes were selected by southern blot and injected into pseudo pregnant mice. Embryonic stem cell injection, selection and transfer were carried out by the Transgenic Mice Unit of the CNIO according to their standard protocols.

3.3. Cell Culture

3.3.1. Cell lines

The following table shows all cell lines used in this work, including culture medium, cell type and origin.

Table 3: Description of cell lines used in this study. All cell lines were grown under conditions as described in 3.3.2. MEFs were established as described in 3.3.6.

Cell line	specie	Cell type	origin
MEFs wild type (WT)	mouse	embryonic fibroblasts	This study
MEFs WT_ H-RAS^{V12}	mouse	embryonic fibroblasts	This study
MEFs DKO (*Pim1 (+/+), 2,3*KO)	mouse	embryonic fibroblasts	This study
MEFs DKO_H-RAS^{V12}	mouse	embryonic fibroblasts	This study
MEFs TKO (*Pim1,2,3*KO)	mouse	embryonic fibroblasts	This study
MEFs TKO_H-RAS^{V12}	mouse	embryonic fibroblasts	This study
Linx-E	human	HEK293T; expresses retroviral genes *gag-pol* and *env* (ecotropic)	D. Beach

3.3.2. Culture Conditions and cell line conservation

All cell lines were grown in DMEM culture medium supplemented with glutamine (Sigma/Gibco), 10 % FBS (Sigma/Genycell), 40 U/ml penicillin, 40 U/ml streptomycin and 1 µg/ml fungizone (all Gibco/Invitrogen); further referred to as complete medium. Cells were grown on 10 cm ø plates and splitted when a confluent monolayer of cells was observed under the inverted microscope. As mouse fibroblasts and Linx-E are adherent cells it was necessary to detach them by using Trypsin-EDTA 1x (0.05 % Trypsin, 0.53 mM EDTA•4Na; GIBCO) before splitting them; usually 1:4 – 1:6. After passing the cells to a new culture dish, they were maintained in an incubator at 37°C with a 5 % (v/v) CO_2-atmosphere for 3-4 days until the plate was confluent again. All work was done in a biosafety flow-hood class II Bio-II-A (Telstar). Cells that were not needed in culture were stored in liquid nitrogen (using 2ml cryotubes) to conserve the cell line. The cells were detached from the plate, transferred to a 15 ml conical tube and centrifuged for 5 min at 1200 rpm. The pellet was diluted in 90 % FCS / 10 % DMSO (Sigma). 200 µl of that suspension were added to each vial for freezing. Usually, two or three vials were frozen from a 10 cm ø plate, depending on confluence and cell line. The tubes were sealed and immediately placed into a polystyrene box at -80°C for at least 24 hours before they were transferred to the liquid nitrogen tank.

Cells were frozen in such a small volume (200 µl) since this small volume reduces the critical step in the thawing process (the time required for the cells to go from –40ºC to +4ºC, i.e. the time in which ice crystals can be formed). To thaw the stored cells, the cryotube with the frozen cells was taken from the liquid nitrogen tank and warmed immediately in a 37°C water bath until the cells were thawed. Before opening the tube, it had to be cleaned with 70% ethanol to prevent contamination. Subsequently, 100 µl of pre-warmed media were added stepwise several times to the thawed cells. Then the diluted cells were transferred into a 15 ml conical tube and 10 ml of pre-warmed medium were added drop wise. Afterwards the cells were centrifuged for 5 minutes at 1200 rpm (300x g) at room temperature. The supernatant was then aspirated carefully and the cells were plated in their usual growth medium.

3.3.3. Transfection of cells using calcium phosphate

One day prior to transfection the cells were seeded at appropriate concentrations, on either a 10 cm ø (3 x 10^5 cells) or a six well plate (6 x 10^4cells/well), to reach 70-80% confluence the day of transfection. 2-4h prior to transfection the medium was changed adding 10 ml fresh complete medium to a plate of 10 cm ø. To transfect, 20-30 µg of the DNA to be transfected was added to a 15 ml conical tube and mixed with 80 µl $CaCl_2$, added up to 500 µl with sterile Water (Milli-Q). While making air bubbles with a pipette 500 µl HBS 2X buffer (NaCl 270 mM, HEPES 55mM, Na_2HPO_4 1.5 mM, pH 7.0) were added drop by drop. In order to allow the formation of calcium phosphate crystals the mixture was incubated at room temperature for 30 min and then added to the cell culture drop by drop. The cells were left for 8-16h at 37°C before the medium was changed with fresh complete medium and the cells left for another 48h at 37°C before further use.

3.3.4. Retroviral infection of cells

Linx-E cells were seeded and transfected with the desired retroviral vector with calcium phosphate (as described in 3.3.3.) and incubated for 8-16h at 37°C. After that time the medium was changed, 10 ml of fresh complete medium was added and the cells were incubated at 32°C for 48h. Then the supernatant containing the virus was filtered through a cellulose acetate filter (0.45 µm, Millipore) and final volume of 8 µg/ml polybrene (Sigma) – a polycation, which reduces the electrostatic repulsion between the virus and the cell membrane, thus supporting cell infection – and an equal volume of complete medium was added. To infect the desired cells the receptor cells were seeded the day prior to infection in

order to reach 50-70% confluence for the infection. To infect the receptor cells the medium was replaced with medium mixed with the viral supernatant and the plates were centrifuged for 1h at 1500 rpm and later incubated at 32°C for 6-8h. Afterwards the viral carrying medium was aspirated and fresh complete medium was added. The cells were maintained at 37°C for 48h until the corresponding selection was started.

3.3.5. Selection of transfected or infected cells

48h after infection or transfection the cells were splitted 1:2 and selection using the corresponding (i.e. antibiotic puromycin at 2 µg/ml; Calbiochem) was started and maintained until the control cells (not infected/transfected cells) were dead. Afterwards individual clones or cell populations were isolated for further use. The concentration of the antibiotic was lowered to half or less (e.g. 0,5 µg/ml of puromycin) for maintenance of the selected cells.

3.3.6. Generation of MEFs

Mouse embryonic fibroblasts (MEFs) were generated from mouse embryos (day 12.5 of gestation) of FVB wild type mice (from here on referred to as WT) and genetically modified mice for *Pim1, 2* and *3* which will be from here on referred to as DKO (double knock out - expressing *Pim1*, but not *Pim2* or *3*) and TKO (triple knock out – totally depleted of all three *Pim* kinases). After eliminating head and liver (which were lysed and used for genotyping), the embryo was mechanically disaggregated and trypsinized for 10 min at 37ºC. The adherent cells were grown in DMEM (Sigma) supplemented with 10% fetal bovine serum (FBS) from Sigma and 1% penicillin G sulphate/ streptomycin (Gibco) on Ø 10 cm culture plates. When the plate was full, a part of the cells of each clone were frozen and the rest were kept in culture until they overcame the crisis of senescence. Once immortalized, one clone of each genotype was selected for further analysis.

3.3.7. Cellular assays

3.3.7.1. Proliferation assay

2x 10^4 cells were sown per well of 35mm in triple trial for each point of the growth curve (day 0, 2, 4, 6, 8, 10). At 24h the first cells (day 0) were fixed in glutaraldehyde (Sigma) at 0.5%, and every 48h the next point was taken and the culture medium of the remaining

cells was changed. After all cells were fixed they were dyed with crystal violet solution (Merck) at 1% and the plates were washed in water several times. After resuspending in acetic acid (Merck) at 15%, the relative cell number was quantified measuring the absorbance at 595nm. The values are represented referring to day 0.

3.3.7.2. Growth under low serum conditions

Similar to the proliferation assay only that at day 0 the medium was changed to the corresponding serum concentration. The results are expressed as a percentage of the cell growth referring to the growth at day 0. Culture medium: 2% (DMEM + 2% FBS), 0.5% (DMEM + 0.5% FBS).

3.3.7.3. Clonability

1x 10^4 cells were sown on a 10cm plate in triple trial and cultured under standard conditions for 10 days, changing the medium twice a week. After 10 days the cells were fixed and dyed with crystal violet at 1 %. After washing the plates the colonies that have been formed were counted.

3.3.7.4. Loss of growth contact inhibition

4x 10^4 cells were sown per well of 35 mm in triple trial. The medium was changed every 48h during 14 days. On day 14 the cell were fixed with gluteraldehyde 0.5% and later dyed with methylene blue (Sigma) to visualize the formed foci.

3.3.7.5. Activation of p53 by 3-Methylcholanthrene (3MC)

1x 10^6 pre-senescent MEFs (passage 3) were sown on a 10cm plate the day before the experiment. The day of the experiment (cells 70% confluent) the medium was changed to medium containing 10 µM 3MC (Sigma). Cells samples for Western Blot analysis (see 3.6.2.) were taken at different time points (0, 2, 4, 6, 8, 12, 24, 48h).

3.4. Assays with mice

3.4.1. Mouse lines used in this study

Table 4: Mouse lines used in this study. Mouse lines used for this work have been either generated in the lab at the CNIO or have been provided by other groups.

Colony	Genotype	Description	Genetic backround	Origin
PSA61-Cre	*PSA61-Cre* (+/T)	Transgenic, expressing Cre-recombinase in prostate	FVB	J. Trapman
FVB	Wild type	Wild type	FVB	CNIO
Pten-Wu	*Pten*(lox/lox)	Uninduced conditional knock-out	C57/BL6	Wu
PIM1	*PIM1* (+/T)	Carrying, not expressing *PIM1* transgene	C57/Bl6	CNIO
PIM1/ PSA61-Cre	*PIM1* (+/T); *PSA61-Cre* (+/T)	Transgenic, expressing Cre-recombinase and *PIM1* in prostate	Mixed FVB-C57/Bl6;	CNIO
PIM1/ PSA-Cre/ Pten	*PIM1* (+/T); *PSA61-Cre* (+/T); *Pten* (+/lox)	Heterozygously expressing transgenes Cre-recombinase and *PIM1* in prostate, 1 allele of *Pten* deleted in prostate	Mixed FVB-C57/Bl6;	CNIO
Pim-DKO	*Pim1* (+/+), *Pim2,3* (-/-)	Expressing both wt alleles of *Pim1*; depleted of *Pim2* and *Pim3*	FVB	M Narwijn
Pim-TKO	*Pim1* (-/-), *Pim2,3* (-/-)	depleted of all *Pim* kinases	FVB	

A summary of abbreviated names and corresponding genotypes of the mouse lines mainly used in this study follows:

- WT
- tgPIM1: *PIM1*(+/T);*PSA-CRE* (+/T)
- Pten-Het: *Pten*(+/lox);*PSA-CRE* (+/T)
- tgPIM1/ Pten-Het: *PIM1*(+/T); *Pten*(+/lox);*PSA-CRE* (+/T)
- DKO: *Pim1* (+/+)*; 2,3* (-/-)
- TKO: *Pim1,2,3* (-/-)

3.4.2. Genotyping of used mouse lines

3.4.2.1. Lysis of mouse tails

Four weeks after birth the mice were weaned and 2-3 mm of the tail was cut, placed into a 1.5 ml Eppendorf tube and stored at -80°C. To lyse the tail tissue, 400 µl lysis buffer (KCl 50 mM, MgCl2 1.5 mM, Tris-HCl 10 mM (pH 8.3; all from Merck), IGEPAL CA 630 (NP40, Sigma) 0.45%, Tween20 (Sigma) 0.45%; Proteinase K (Promega) 10 mg/ml) were added and the tubes were incubated at 55°C over night shaking at 220 rpm. After 16h the lysates were incubated at 95 -100°C for 30 min to inactivate the Proteinase K, the tubes were centrifuged at full speed for 10 sec and 2 µl of the lysates were used for the genotyping PCR.

3.4.2.2. Tail genotyping by PCR analysis

Transgenic *PIM1* as well as *Pim1, 2, 3* KO-mice were genotyped by PCR using PCR protocols provided in tables 5 and 6.

Table 5: Primers used for genotyping of Pim-KO mice: Primer sequences and PCR programmes were used as published by Mikkers et al. PCR fragments were seperated on a 1,5% agarose gel.

Gene	Primer sequence (5´- 3´)	Thermocycler programme	Expected band (bp)		
			(+/+)	(+/-)	(-/-)
Pim1	Pim1fw: AAGCACGTGGAGAAGGACCG Pim1rev: GACTGTGTCCTTGAGCAGCG Neo: CGTCCTGCAGTTCATTCAGG	1. 95°C 2 min 2. 95°C 30 sec 3. 64°C 45 sec 4. 72°C 90 sec to # 2 x 34 cycl. 5. 72°C 7 min 6. 4°C pause	500	500/400	400
Pim2	Pim2fw: CACCGCGTCACGGATAGACG Pim2rev: CCACCTTCCACAGCAGCG Hygrofw: AGCACTCGTCCGAGGGCAAAG Hygrorev: CACGGTGGACCAGCCTAGC	1. 95°C 2 min 2. 95°C 30 sec 3. 64°C 45 sec 4. 72°C 90 sec to # 2 x 34 cycl. 5. 72°C 7 min 6. 4°C pause	900	900/600	600
Pim3	Pim3fw: CTGGACCAAATTGCTGCCCAC Pim3rev: GGATCTCTGGTTCAAGTATCC LacZ1: CGTCACACTACGTCTGAACG LacZ2: CAGCCAGATGATCACACTCG	1. 95°C 2 min 2. 95°C 30 sec 3. 58°C 45 sec 4. 72°C 90 sec to # 2 x 34 cycl. 5. 72°C 7 min 6. 4°C pause	390	390/500	500

Table 6: Primers used for genotyping transgenic mouse lines used in this study: Primer sequences and PCR programmes were specifically designed for genotyping of mice. PCR fragments were seperated on a 1,5% agarose gel.

Gene	Primer sequence (5´- 3´)	Thermocycler programme	Expected band (bp)			
			(+/+)	(+/-)	(-/-)	(-/T)
PIM1	Fw: CGAGATCGCCATATTTGGTGT CCCCGAG Rev: CCAGCTTGGTGGCGTGCAGG TCGTTGCA	1. 95°C 5 min 2. 95°C 45 sec 3. 65°C 30 sec 4. 72°C 45 sec to # 2 x 34 cycl. 5. 72°C 5 min 6. 4°C pause				350
Pten	Fw: GTCATCTTCACTTAGCCATTG Rev: ACTCAAGGCAGGGATGAG	1. 94°C 4 min 2. 94°C 1 min 3. 57°C 1 min 4. 72°C 2 min to # 2 x 39 cycl. 5. 72°C 10 min 6. 4°C pause	900	900/1000	1000	
PSA61	Fw: CTTGTAGGGTGACCAGAGCAG Rev: GCAGGCATCCTTGCAAGATG	1. 95°C 5 min 2. 95°C 1 min 3. 59°C 1 min 4. 72°C 1 min to # 2 x 34 cycl. 5. 72°C 7 min 6. 4°C pause				330

3.4.3. Maintenance of mouse colonies

Colonies of 15 to 30 mice of each genotype were established and sperm of each mouse line was frozen. All animals were kept in the CNIO animal facility according to the norms of this facility based on the Real Decreto 1201/2005 and sacrificed by CO2 inhalation either within a programmed procedure or as humane endpoint to avoid suffering, when the animal showed any sign of an important sickness.

3.4.4. Carcinogenic treatments

3.4.4.1. Carcinogenesis induced by 3-Methylcholanthrene

The carcinogen 3-Methylcholanthrene (3MC, Sigma) was dissolved in sesame oil (Sigma) at a final concentration of 10 mg/ml. The solution was heated up to 100 °C for 1 h and mixed vigorously in order to completely dissolve the 3MC. Mice of 3-5 month of age were injected with 1 mg (100 µl) of 3MC once into the right hind leg and later examined once a week (twice a week after tumour growth onset in the first mouse had been detected). The mice were sacrificed when the tumour reached a volume of approx. 1,7 cm^3.

3.4.4.2. Carcinogenesis induced by Testosterone and Estradiol

The hormones testosterone (Sigma) and β-Estradiol (Sigma) were mixed with colourless silicone (Soudal) and dried for 48 h. Then pellets were stamped out using an 8 mm biopsy punch (Stieffel) resulting in a 30 mg hormone/silicone pellet. We used male mice with an average age of 8 weeks. The mice were anesthetized using 2% isofluorane. The lower back of the animal was cleaned with iodine to avoid infection later on. A 5 mm incision was made at the lower back and the pellets were inserted under the fur. The wound was then closed using 7 mm stainless steel wound clips (Stoelting).

Table 7: Total dose of implanted hormones

	Implanted total dose at 8 weeks of age	Implanted total dose at 16 weeks of age
testosterone	12,5 mg	18,75 mg
β-Estradiol	1,25 mg	1,87 mg

After 10 days the wound clips were removed. The procedure was repeated after 8 weeks as the hormone pellets lose effectivity. The total doses of the implanted hormones are shown in table 7. To ensure the health of the animals the mice were monitored every 24–48 h (depending of the health status of each animal) for signs of urinary problems to avoid pyelonephritis.

3.4.5. Necropsy and histopathological studies

Once sacrificed, necropsy of each animal was done in the animal facility of the CNIO according to the established norms. Tissues for histopathological and molecular analysis were taken as fast as possible to avoid degradation. Tissues meant for molecular analysis were immediately put in carbonic ice and later stored at -80 ºC. Tissues for histopathological studies were fixed in 10% formalin for 24h, dehydrated at different ethanol concentration and xylol and embedded in paraffin at 65 ºC thus obtaining tissue blocks. Tissue fixation and paraffin embedding was carried out at the Comparative Pathology Unit at the CNIO.

3.4.6. Grading of mPIN

16 week old male mice were sacrificed and prostate tissue was taken and prepared for immunohistochemistry (see 3.4.5.). H&E staining of prostate tissue was used for mPIN grading.

3.4.7. Statistical data analysis

The computer programme GraphPad Prism was used for all statistical analysis. To determine statistical significance of tumour growth and bone invasion, one-way ANOVA analysis was used. To determine statistical significance of survival curves Mantel-Cox test was used. To determine the statistical significance of the quantifications of lesions in prostate and the statistical significance of the differences in the grades of hyperplasia in bladder and urethra as well as the differences in inflammation and pyelonephritis incidence a one-way ANOVA (first round of treatment) or a one tailed student´s t-test (second round of treatment) was used.

3.5. Analysis of transgene expression on the RNA level

3.5.1. Extraction of total RNA

Total RNA of cells and tissue was extracted and purified using TRI-Reagent (Molecular Research Center, Ohio) according to the manufacturer's manual. Cells growing in a monolayer were washed with 1x PBS (Lonza) and stored at -80ºC on the plate. Tissue samples were frozen in an Eppendorf tube on dry ice and weighed with the tube. 1 ml TRI-Reagent was used per Ø 10 cell culture dish and 50-100 mg of tissue. A sterile RNAse free plastic pistol was used to homogenize the tissue. Cells were lysed by pouring the TRI reagent on the plate and scraping the monolayer of the plate, transferring the sample to a 1.5 ml Eppendorf tube. After homogenization of the sample the tube was left on ice for 5 minutes and afterward 200 µl Chloroform (Merck) were added to separate the phases. The tube is left at 4ºC for 2-15 min, then centrifuged at 12000x g for 15 min at 4 ºC and the aqueous phase is transferred to a new tube containing 500 µl Isopropanol (Merck) to precipitate the RNA. Then the sample is incubated on ice for 5-10 min and centrifuged at 4 ºC for 8 min at 12000x g. Last the RNA is washed 3 times with 1 ml 70 % EtOH (Merck) by centrifuging it at 12000x g for 5 min. The RNA pellet is then left to air dry for 5-10 min at room temperature and dissolved in 50 µl 0.1 % DEPC water (CNIO) and stored at -80 ºC.

3.5.2. Reverse transcription and PCR

We analyzed the expression of different transcripts in tissues by reverse transcription-PCR (RT-PCR). For this, total RNA was isolated from tissues as described in 3.5.1. using TRI-Reagent, treated with DNase, and reverse transcribed with random hexamer primers (Promega) and avian myeloblastosis virus-reverse transcriptase (Roche). The cDNA was amplified in a single PCR, using specific primer combinations as described in table 8.

Table 8: Primers and protocols for PIM cDNA amplification. Specifically designed primers were used to amplify cDNA obtained through reverse transcription-PCR after total RNA extraction from tissues. Fragment length was controlled on 1.5% agarose gels.

Gene	Primer sequence (5´- 3´)	Thermocycler programme	Expected band (bp)			
			(+/+)	(+/-)	(-/-)	(+/T)
Pim1	Fw: ATGCTCCTGTCCAAGATCAACTC Rev: CTCCAGGATCAGCACGAAACTA	1. 95°C 5 min 2. 95°C 1 min 3. 60°C 2 min 4. 72°C 2 min to # 2 x 36 cycl. 5. 72°C 5 min 6. 4°C pause	330	330		
Pim2	Fw: ATGTTGACCAAGCCTCTGCAGG Rev: GCTCAAGGACCAGCATGAAGC	1. 95°C 5 min 2. 95°C 1 min 3. 60°C 2 min 4. 72°C 2 min to # 2 x 36 cycl. 5. 72°C 5 min 6. 4°C pause	330	330		
Pim3	Fw: ATGCTGCTGTCCAAGTTCGGCT Rev: GCTCGAACCAGTCCAGCAAGC	1. 94°C 5 min 2. 94°C 1 min 3. 66°C 2 min 4. 72°C 2 min to # 2 x 37 cycl. 5. 72°C 5 min 6. 4°C pause	330	330		
PIM1	Fw: CAAGGACGAAAACATCCTTATC Rev: GATGGGACCCGAGTGTATAGCC	1. 95°C 5 min 2. 95°C 45 sec 3. 66°C 30 sec 4. 72°C 45 sec to # 2 x 37 cycl. 5. 72°C 5 min 6. 4°C pause				500
Gapdh	Fw: AAGGTCGGTGTGAACGGATT Rev: TTGCTGGGGTGGGTGGTC	1. 95°C 5 min 2. 95°C 1 min 3. 59°C 1 min 4. 72°C 1 min to # 2 x 34 cycl. 5. 72°C 7 min 6. 4°C pause	1000			

3.6. Analysis of protein expression

3.6.1. Extraction of total protein

The cells were trypsinized and washed twice in 1x PBS (Lonza), then pelleted for 30 seconds at 14000x g and the pellet was broken and 4 pellet-volumes of lysis buffer (Tris-Hcl pH 7.5 50 mM, NP40 1 %, glycerol 10 %, NaCl 150mM, protease inhibitor cocktail complete 2 mM Roche) were added. The samples were then kept on ice for 30 min, vortexing the tube once in a while, followed by a 15 min centrifugation at 14000x g at 4 ºC. Then, carefully avoiding the pellet, the supernatant containing the protein extract was transferred to a new eppendorf tube and the sample was stored at -80 °C until use. Total protein of mouse tissues frozen and maintained at -80 °C was extracted after mechanical disintegration of the tissue using a sterile plastic piston. For protein extraction, 1ml lysis buffer was added into the 1.5 ml eppendorf tube containing the disintegrated tissue and after 10 min of centrifugation at max speed (15000 x g) at 4 °C the supernatant was transferred to a new tube and centrifuged several times until all tissue artifacts or fat was eliminated. The protein extracts were aliquoted and stored at -80 °C until use.

3.6.2. Western Blot

The amount of protein was determined by Bradford assay (Bio-Rad) using BSA (bovine serum albumin; Fermentas) as a standard. The appropriate protein quantity was dissolved in Laemli buffer (Tris-HCL pH 6.8 62.5 mM, glycerol 10 %, SDS 1 %, 2-mercapto ethanol 5 %, bromphenol blue 0.0025 %) and the proteins were separated in SDS-PAGE gels (12 %) before they were blotted onto Nitrocellulose Transfer membrane (Whatman - Protrans). The proteins were visualized via the Odyssey LI-COR system (Odyssey). Tables 9 and 10 show all used antibodies.

3.6.3. Immunohistochemistry

Of prepared paraffin tissue blocks, using an automated microtome, 2 µm cuts were taken of and dyed with haematoxylin and eosin or different antibodies (Tables 9 and 10). All staining were carried out at the Comparative Pathology Unit at the CNIO according to established protocols. The slides were then scanned using Mirax Scan (Zeiss®) and digitalized with the AxioVision programme (Zeiss®). Pictures were taken using the Panoramic Viewer software (Zeiss ®).

Table 9: Used primary antibodies for immunohistochemistry and Western Blot.

Primary Antibody	Manufacturer	Cat. number	WB	IHQ
Ki-67 /MKI67	Master Diagnostica	0003110QD		Predil.
Caspase 3	R & D Systems	AF835		1 : 400
Cyclin D1	DAKO	M3635		1 : 75
p53(CM5p)	Leica	NCL-p53-CM5p		1 : 200
p21	Santa Cruz	sc-397-G		1 : 300
$p19^{ARF}$	Santa Cruz	sc-32748		1 : 50
$p16^{INK4a}$	Santa Cruz	sc-1207		1 : 50
AR	Santa Cruz	sc-816		1 : 50
ER	Santa Cruz	sc-542		Predil.
Cytokeratin 14	Thermo Scientific	RB-9020-P0		1 : 4500
Smooth muscle actin	Thermo Scientific	090309F		1 : 250
p53	Cell Signaling	2524	1 : 1000	
4E-BP	Cell Signaling	9644	1 : 1000	
p4E-BP $^{Thr37/46}$	Cell Signaling	9459	1 : 1000	
GSK3β	BD Transduction	610202	1 : 1000	
$pGSK3\beta^{Ser9}$	Cell Signaling	9336L	1 : 1000	
$p27^{KIP}$	BD Pharmingen	610241	1 : 1000	
AKT	Cell Signaling	9272	1 : 2000	
$pAKT^{Ser473}$	Cell Signaling	4051L	1 : 1000	
ERK1/2	Cell Signaling	9102L	1 : 1000	
$pERK1/2^{Thr202/Tyr204}$	Cell Signaling	9101L	1 : 1000	
Actin	Sigma	A5441	1 : 5000	
Tubulin	Sigma	T6557	1 : 10000	

Table 10: Used secondary antibodies for immunohistochemistry and Western Blot.

Secondary Antibody	Manufacturer	Cat. number	WB	IHQ
Alexa Fluor 680 (goat anti-rabbit)	Invitrogen	A21057	1 : 5000	
IRDye 800CW (donkey anti-mouse)	Rockland-Inc	605-731-002	1 : 5000	
Omnimap (anti-rabbit)	Ventana	760-4311		Predil.
Horse raddish peroxidase (goat anti-rabbit)	Dako	P0448		1 : 50
Biotinylated-IgG (rabbit anti-goat)	Dako	E0446		1 : 200
Rat-HRP on mouse	Biocare	RT517L		Predil.
IgG (rabbit anti-mouse)	Epitomics	3024-I		1 : 500

Results

4. Results

4.1. Examining tumourigenic properties of *Pim* kinase depletion

4.1.1. Establishment of *Pim*-KO mouse line at the CNIO

Pim1(+/-),2,3KO mice (kindly provided by M. Narwijn, NKI–Netherlands) were crossed with each other to maintain the colony and generate the different cohorts of each genotype (*Pim1*(+/+),*2,3*KO; *Pim1*(+/-),*2,3*KO; *Pim1,2,3*KO). This mouse strain was previously analyzed and described by M. Mikkers et al (Mikkers, Nawijn et al. 2004). As described, *Pim1,2,3*KO (TKO) mice had notably less body fat and less muscle mass (Fig. 6C) showing smaller size and weight. Although *Pim1,2,3*KO mice were described as normally fertile in mendelian proportions, in our hands merely 7% of all born mice of this strain were TKO mice (Fig. 6B) and we were not able to obtain offspring from TKO mice.

A

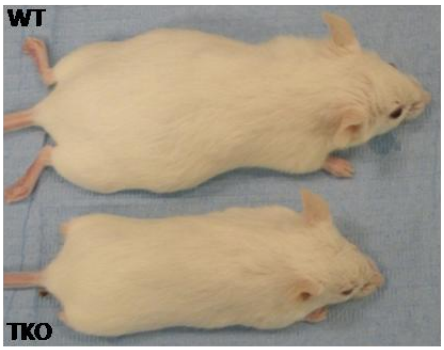

B **113 matings resulting in 257 born animals**

genotype	no. animals	% of total	expected %
*Pim1(+/+);2,3*KO	85	33.07 %	25%
*Pim1(+/-);2,3*KO	155	60.31 %	50%
*Pim1,2,3*KO	16	6.62 %	25%

C

	Weight at 10 weeks (reduction %)		**Size at 10 weeks (reduction %)**	
	male	**female**	**male**	**female**
WT (n = 13)	29 g ± 0,7 (100%)	23 g ± 0,5 (100%)	10 cm ± 0,6 (100%)	9.5 cm ± 0,5 (100%)
DKO (n = 19)	22,8 g ± 0,5 (-21%)	18,7 g ± 0,6 (-19%)	9.5 cm ± 0,5 (-5%)	8.5 cm ± 0,4 (-10%)
TKO (n= 7)	17,5 g ± 0,4 (-40%)	13,5 g ± 0,7 (-40%)	8.5 cm ± 0,4 (-15%)	7.6 cm ± 0,3 (-20%)

Figure 6. Characteristics of Pim kinase KO mice. **A: Comparative picture**. Comparision of wild type versus *Pim1,2,3*KO (TKO) mice at 10 weeks of age. **B: Comparision of mating results.** Numbers of overall matings, animals born alive and subsequent proportions of resulting genotypes. **C: Comparison of weight and length reduction**. Weight and length reduction of *Pim1 (+/+),2,3*KO (DKO) and *Pim1,2,3*KO (TKO) mice to wild type mice at 10 weeks of age.

Pim1(+/+),*2,3*KO (DKO) and *Pim1*(+/-),*2,3*KO mice were phenotypically normal.

4.1.2. Generation of MEFs depleted of *Pim* kinases

In order to characterize the role of Pim kinases in cell proliferation, first, we measured how the absence of Pim isoforms alters the growth properties of cells. We generated MEFs from double *Pim2/3* knockout mice (DKO) or from mice lacking all three isoforms (TKO), in parallel with isogenic wild-type MEFs. To that end, we first immortalised MEFs from all genotypes. MEFs followed similar senescence kinetics and were immortalised with similar frequency irrespective of the genotype (not shown).

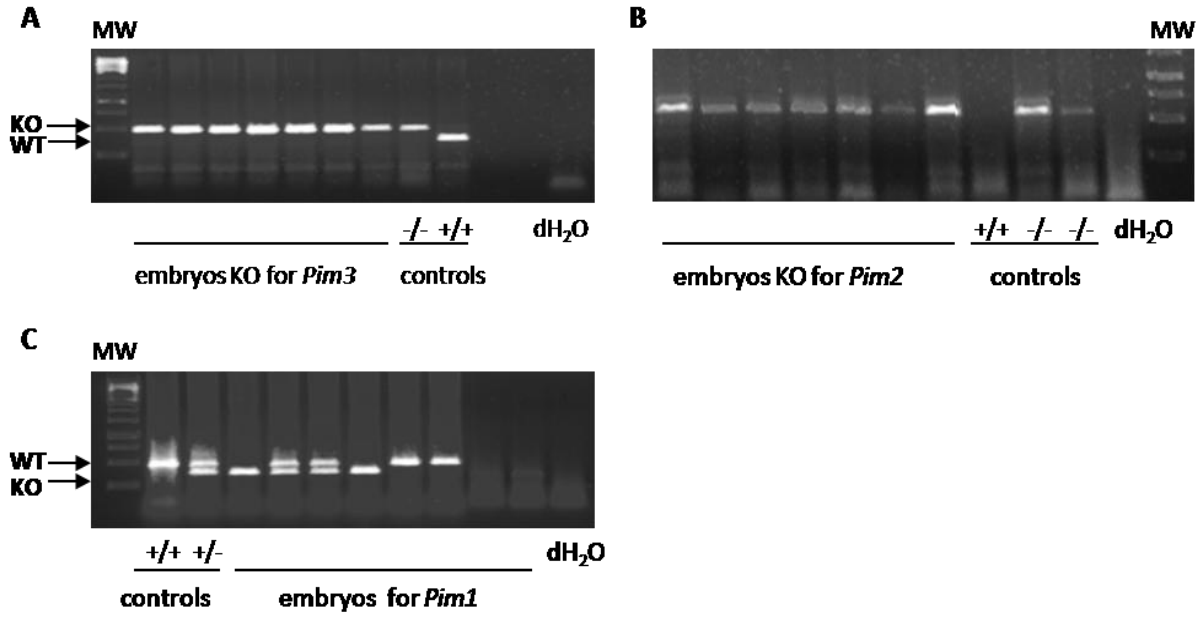

Figure 7. Genotyping of MEFs. Heads of extracted embryos were lysed according to protocol and PCR was performed using DNA from those lysates as well as primers specified in Mikkers et al. **A: Genotyping for *Pim3*KO and WT** (exp. bands 390 bp for WT allele and 500 bp for KO allele); **B: Genotyping for *Pim2*KO** (exp. bands 550 bp for KO allele), **C: Genotyping for *Pim1*KO and WT** (exp. bands 500 bp for WT allele and 400 bp for KO allele).

Once immortalised, MEFs were grown in media with optimal (10%) or suboptimal (0.5% and 2%) concentrations of serum (Fig. 8). At 0,5%, all MEFs showed very slow growth but no apoptosis, irrespective of the Pim isoforms that were expressed. At 2% of serum we observed clear differences in the growth of MEFs depending on the genotype. TKO MEFs showed poor growth compared with wild-type MEFs, while DKO MEFs showed intermediate proliferation. The differences between DKO and TKO increase in respect to wild-type MEFs at 10% serum concentration (Fig. 8).

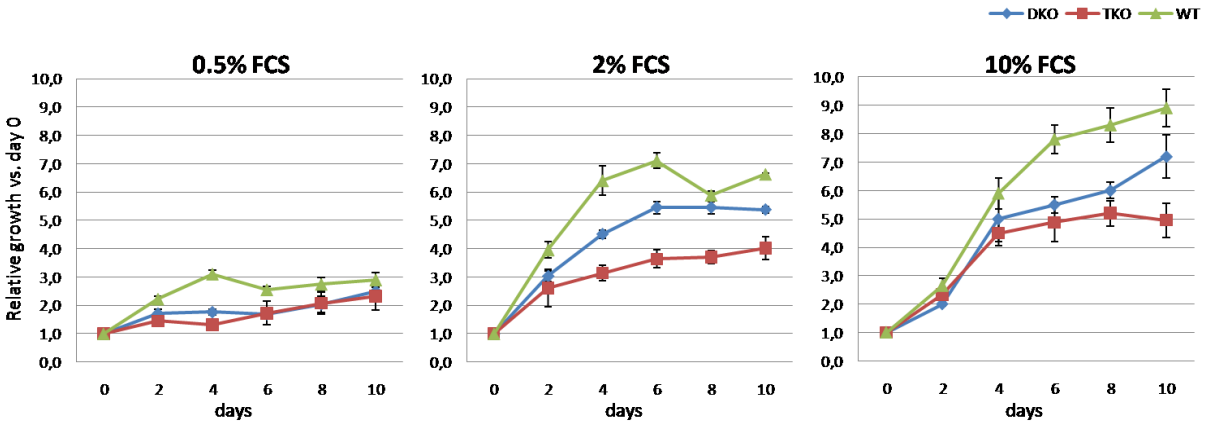

Figure 8. Proliferation of immortalized MEFs under different serum conditions. 5x10^3 Cells of each genotype were grown under different serum conditions (10 %, 2 % and 0.5 % respectively). Every 48 hrs for 10 days a time point was taken. Cells were fixed, stained with crystal violet and after resuspension in 15 % acetic acid; absorbance was measured at 595 nm. The number of cells counted as relative measure of absorbance.

However, these differences were more dramatic in MEFs expressing oncogenic H-RAS^{V12} (Fig. 9). MEFs were infected with viruses carrying oncogenic H-RAS^{V12} or empty vectors and selected for provirus integration. MEFs carrying H-RAS^{V12} were seeded as before in optimal or suboptimal growth conditions. At low serum doses, all MEFs, irrespective of their genotype, were unable to grow, showing high apoptosis.

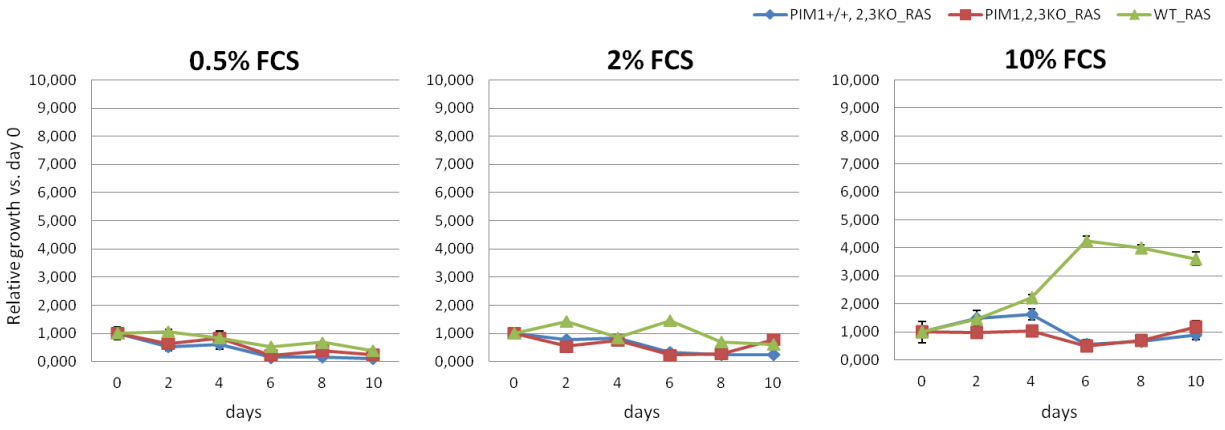

Figure 9. Proliferation of immortalized MEFs expressing H-RAS^{V12}. Cells of each genotype were infected with viruses carrying H-RAS^{V12} and resistance for puromycin (pBabepuro-H-RAS^{V12} plasmid). After antibiotic selection (puromycin) for 5 days, 5x10^3 cells were seeded and grown under different serum conditions (10 %, 2 % and 0.5 % respectively). Every 48 hrs for 10 days a time point was taken. Cells were fixed, stained with crystal violet and after resuspension in 15 % acetic acid; absorbance was measured at 595 nm. The number of cells counted as relative measure of absorbance.

However, at 10 % serum, WT MEFs expressing H-RAS^{V12} grew fast, while TKO and DKO MEFs grew initially but stopped growth with high apoptosis after the initial rounds of duplication (Fig. 9). These data suggest that loss of Pim kinases might render cells resistant to oncogenic transformation.

To examine this hypothesis we transfected WT, TKO and DKO MEFs with oncogenic H-RAS^{V12} and measured the number of foci formed. In this assay, combined loss of *Pim2* and *Pim3* is sufficient to block the foci formation induced by H-RAS^{V12} (Fig. 10A). TKO MEFs grew forming a non-homogeneous layer of cells, making it difficult to assess the foci formation.

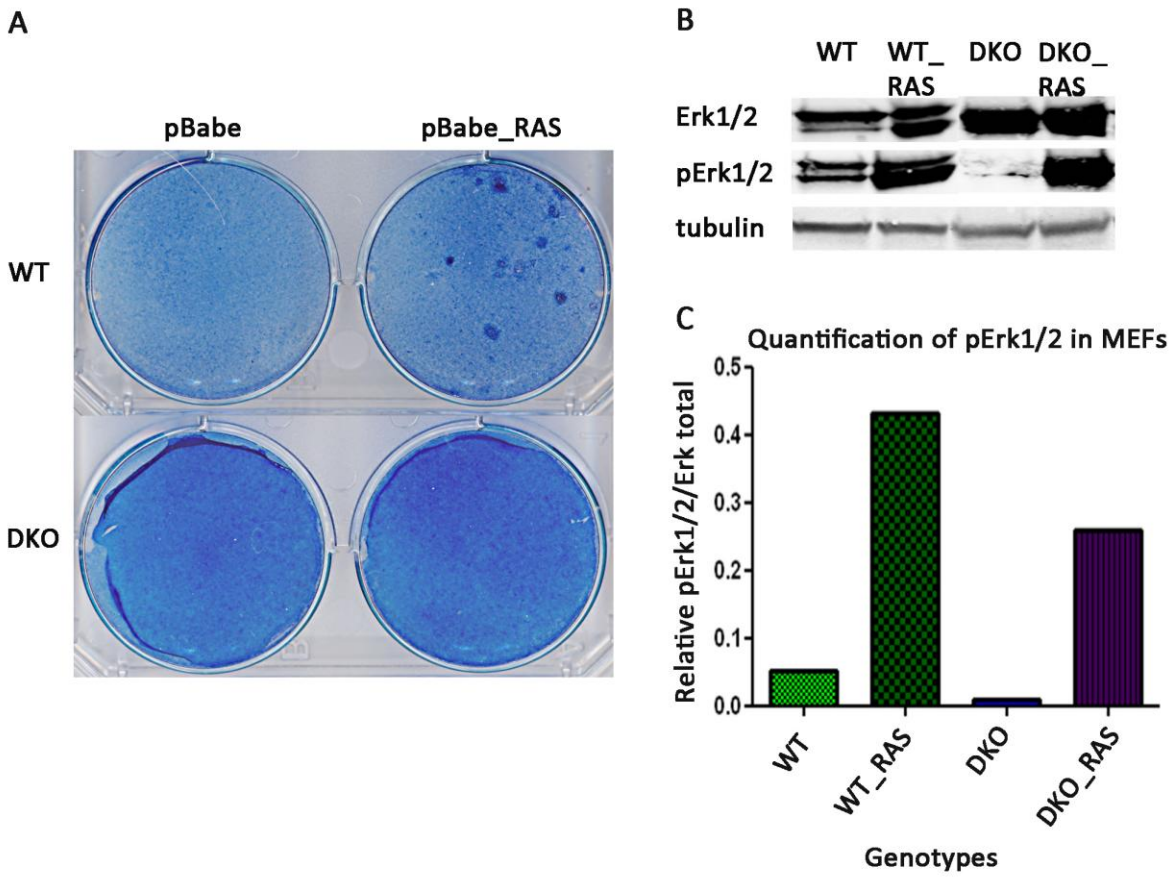

Figure 10. Growth characteristics of MEFs in culture. **A: Loss of growth contact inhibition.** Cells were transfected with the plasmid pBabepuro- H-RAS^{V12} carrying the H-RAS^{V12} oncogene and grown for 2 weeks changing the medium every 2 days. Cells were then stained with methylene blue to visualize the foci and photographed. **B: Western blot analysis of infected MEFs to evaluate pErk/Erk expression as a downstream target of RAS.** Protein levels of Erk1/2 and pErk1/2 were determined using 100 µg protein extract for each genotype. **C: Quantification of pErk1/2 levels in MEFs.**

To verify that H-RAS^{V12} expression in infected cells is upregulated we determined expression levels of Erk1/2 by Western blot (Fig. 10B), as it is a downstream target of Ras.

Quantification of relative pErk1/2 levels to total Erk1/2 levels showed that infected wild type and DKO cells have higher pErk1/2 levels than uninfected cells of the same genotype (Fig. 10C).

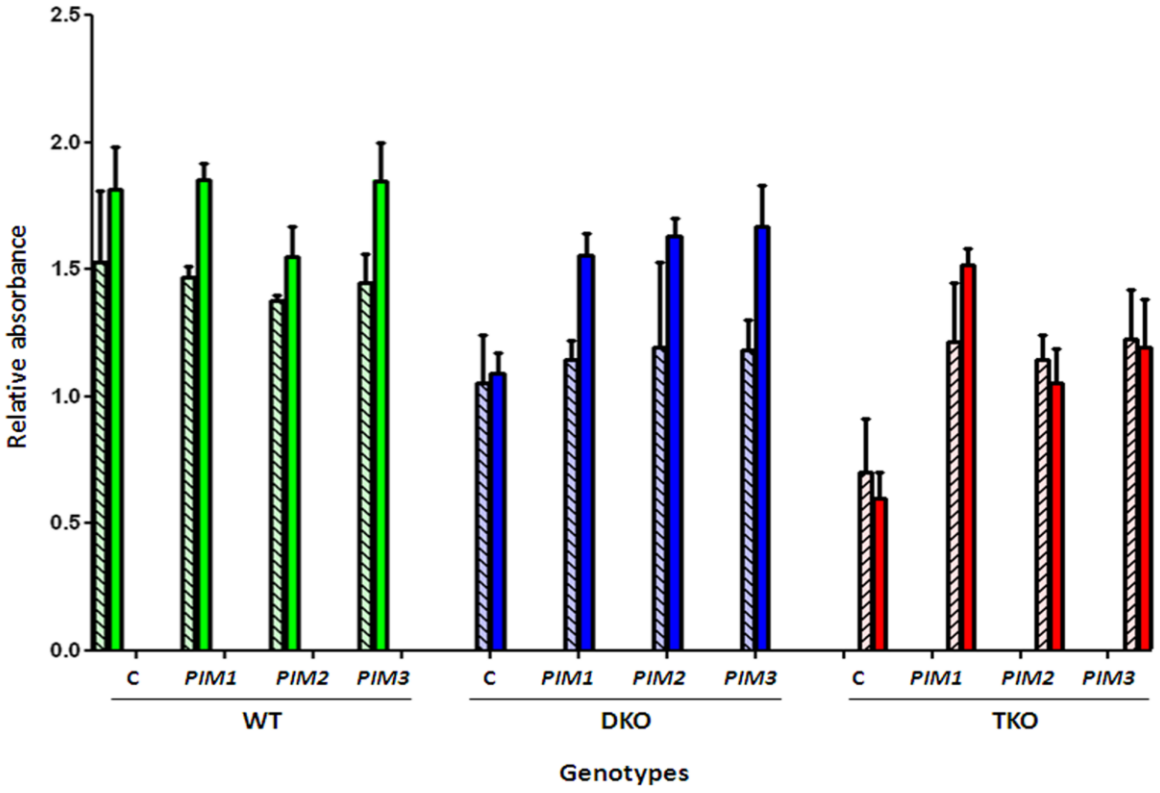

Figure 11. Relative role of PIM isoforms in MEFs saturation density. Cells of each genotype (WT, DKO, TKO) were transfected with the different *PIM* isoform as indicated, under the same constitutive promoter. After selection the different mass cultures were transfected with a plasmid carrying H-RAS^{V12}. After selection, the different mass cultures were seeded and grown under 10 % serum conditions until they reach confluence. Then, the cells were cultured in the same plate for one more week, changing media every 2 days. After this time, cells were fixed, stained and the number of cells counted as a relative measure of absorbance

To compare the data among the three genotypes and to explore the functional relevance of each Pim kinase *in vitro* individually, we decided to perform saturation density analysis. Immortal non transformed MEFs have growth contact inhibition, stopping growth once a monolayer is formed. However, oncogenically transformed MEFs continue growth after the monolayer is formed increasing the density of cells. We observed that the growth of DKO and specially TKO MEFs is lower than the growth of WT cells (Fig. 11, lanes C). To compare the individual role of each kinase isoform in this assay we expressed ectopically *PIM1, PIM2* or *PIM3* into wild type MEFs, or MEFs lacking *Pim2* and *3* (DKO) or lacking all three *Pim* isoforms (TKO). We observed that the increased expression of one isoform of PIM kinases into Pim containing MEFs (WT or DKO) does not alter significantly the saturation density of control cells (Fig. 11, hatched bars). However, in TKO MEFs, the

recovery of PIM activity is sufficient to alter growth forming monolayer (data not shown) and increase the saturation density to levels similar to DKO cells (Fig. 11, hatched bars). Furthermore, we measured the response of these cells to oncogenic transformation with H-RAS^{v12}. Oncogenic transformation with H-RAS, as expected, increases saturation density in WT MEFs, and the increase in one of the PIM isoforms does not seem to provide any advantage (Fig 11, solid bars). In DKO cells expressing only *Pim1*, H-RAS^{V12} does not increases saturation density, correlating with the results observed in Fig. 10A. However, expressing H-RAS^{V12} in MEFs, that recovered the expression of 2 isoforms, increased the saturation density to levels similar to WT cells (Fig. 11, solid bars). Finally, in TKO MEFs, the expression of H-RAS^{V12} does no increase the saturation density in any of the cultures expressing only one isoform (Fig.11, solid bars). Our data indicate that at least the expression of 2 isoforms is necessary to provide ability to support oncogenic transformation. Only overexpression of *PIM1*, in the absence of *Pim2* and *3* seems to provide some benefit in the presence of oncogenic H-RAS.

The reduced proliferation rate together with the inability to form foci after transfection with oncogenic H-RAS^{V12} shows that the depletion of Pim kinases renders cells resistant to oncogenic transformation. This is also underlined by the fact that, MEFs also showed different abilities to form colonies (Fig. 12) according to the expression of Pim kinases. As can be seen in figure 12, cells wild type for all Pim kinases showed an increased ability to form colonies. An ability, which is slightly reduced in DKO MEFs and nearly absent in TKO MEFs.

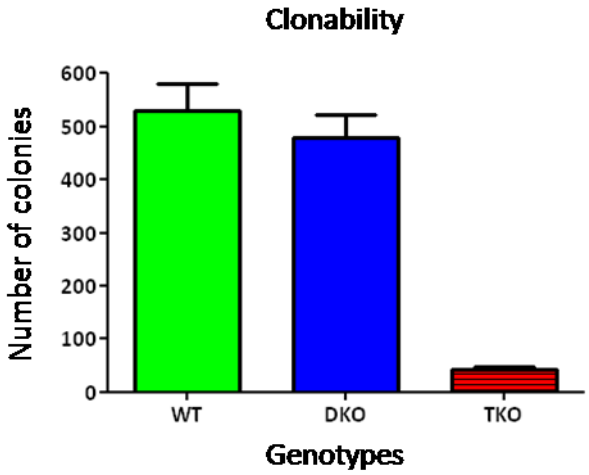

Figure 12. Clonability of untransfected MEFs. Cells were sown at low concentrations (1 x 10^4 cell per 10 cm plate) and grown for 2 weeks. Cells were then stained with crystal violet, and after washing, the colonies were counted.

4.1.3. 3-Methylcholanthrene induced Sarcoma in mice depleted of Pim kinases

3-Methylcholanthrene is a carcinogen known to induce primary sarcoma in mice by DNA damage leading to genomic instability. To evaluate whether Pim kinases play a relevant role in the process of sarcomagenesis induced by the carcinogen 3-Methylcholantrene (3MC), we performed intramuscular injection of 3MC (see 3.4.4.1.) which produced sarcoma tumours with an onset of tumour growth at approximately 98 days after inoculation. An in deep account of the time to first tumour observation, showed that wild type tumours appear in average around 12-20 days earlier than DKO or TKO tumours respectively.

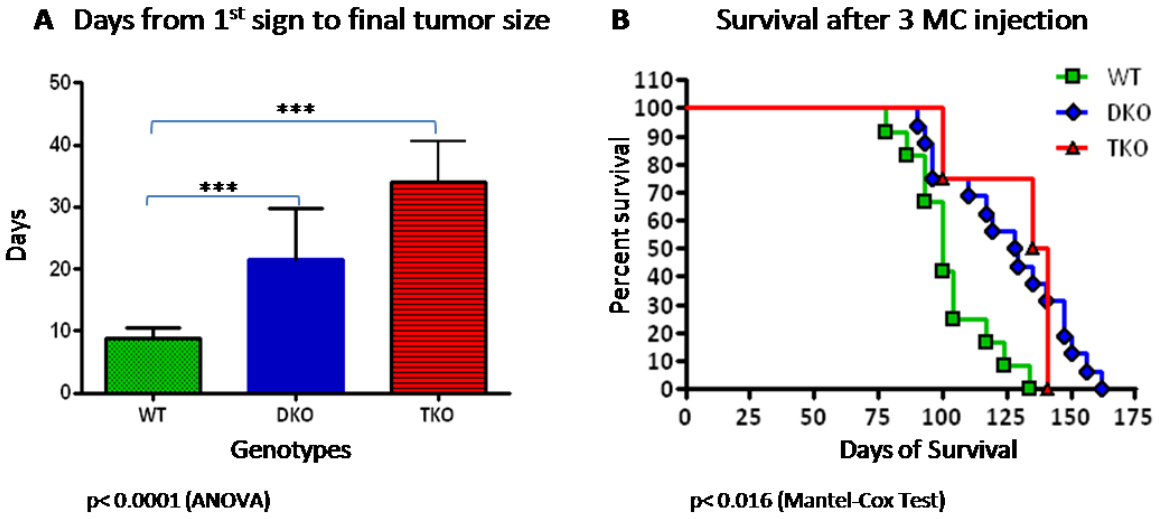

Figure 13. Sarcomagenesis in Pim-KO mice after 3-Methylcholanthrene injection. Mice were injected with 3-Methylcholanthrene (3MC) as described in 3.4.4.1.. Animals were monitored weekly and twice per week after onset of tumour growth in the first animal was observed. When tumours reached final volume size (1,7cm^3), animals were sacrificed for humane end point. **A: Days of tumour growth from first sign of growth onset to final tumour size of 1,7cm^3. B: Survival time of the animals from injection of 3MC until humane endpoint.**

Tumours took an average of 9 days in wild type mice to reach the final volume of 1.7cm^3, indicating the rapid growth of these tumours (Fig. 13A). However, in DKO mice it took an average of 21 days to reach the same size while in TKO mice the tumours reached this size in 33 days (Fig. 13A).This significant time increase indicated that lack of Pim2 and Pim3 kinases was sufficient to produce a significant delay in the growth of the sarcoma. Additional loss of Pim1 produced an additional delay. This slow sarcoma growth rate was reflected in the survival of the mice (Fig. 13B). DKO and TKO mice treated with 3MC died significantly later than wild type mice. This was due to the lower growth rate of the tumour, since in all three genotypes the sarcomas appeared approximately at the same time (Fig. 13B).

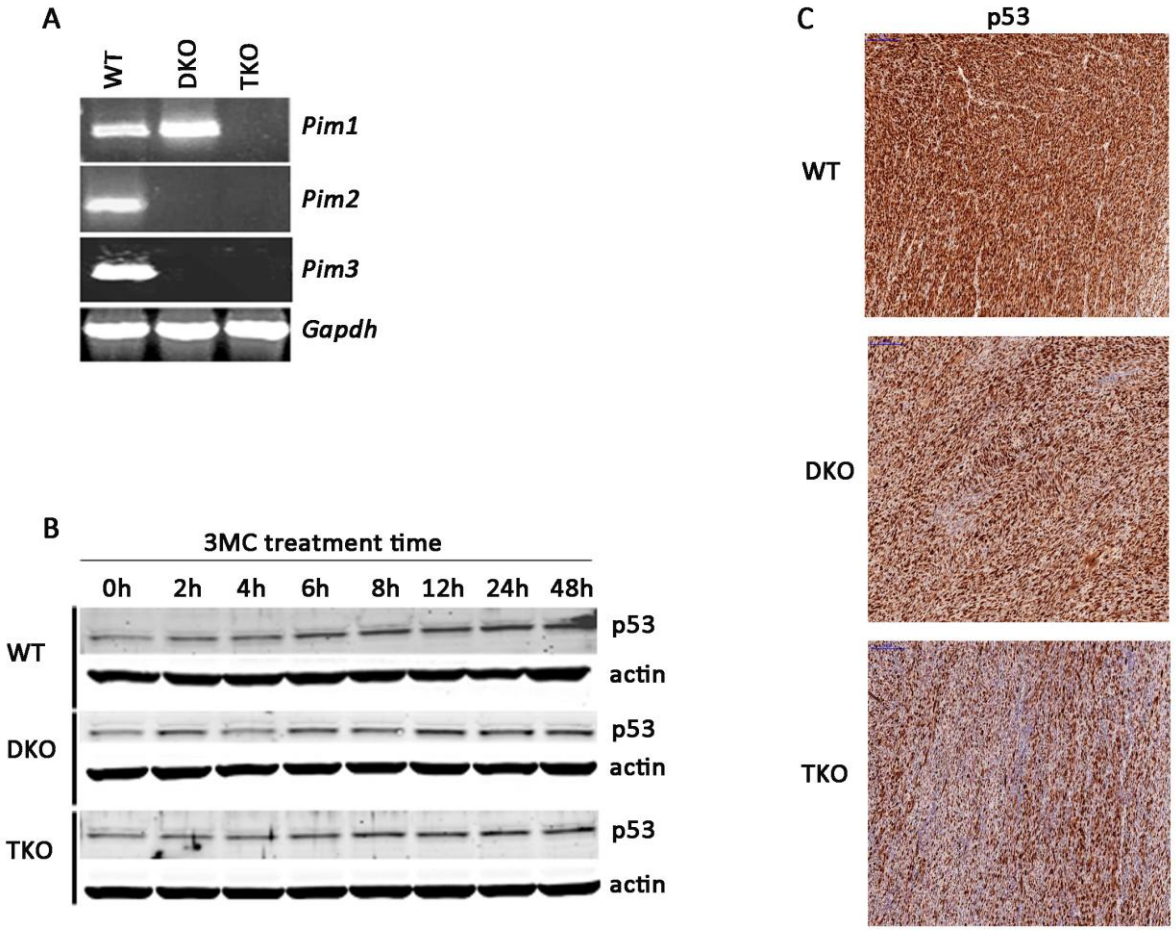

Figure 14. DNA damaging effect of 3-Methycholanthrene. **A: Relative expression of the *Pim* isoforms in tumours of mice treated with 3MC.** RNA was extracted of tumours and a reverse transcriptase PCR was performed to obtain cDNA which was amplified using specifically designed primers. PCR fragment length was checked on 1,5 % agarose gels. **B: Activation of p53 by 3-Methylcholanthrene (3MC).** Pre-immortalized MEFs were treated with 10 µM 3MC. Total protein was extracted at each time point indicated in hrs and p53 expression was determined by Western blot**. C**: **Immunohistochemistry of tumours for p53.** All tumours were hybridized with antibodies against p53. Mutant p53 is recognized by strong nuclear staining indicating stabilization of the p53 protein

To confirm the relative contribution of each isoform to sarcomagenesis we analyzed whether the tumour generated by the carcinogenic treatment in each mouse derives from true KO cells, or whether they maintain the relative expression of the Pim isoforms. We collected mRNA form all the tumours and evaluated the presence of individual *Pim* isoform RNA expression (Fig. 14A). We observed that the sarcoma originated in wild type mice maintained expression of all 3 *Pim* isoforms, while DKO tumours expressed only *Pim1*. Tumours originated in TKO mice did not express any *Pim* isoform. The analysis of sarcomas and treated pre-immortalized MEFs from all 3 genotypes showed that 3MC activated p53 in DKO and TKO MEFs (Fig. 14B) and tumours (Fig. 14C) to a similar extent

as in WT cells and tumours, which was expected from the DNA-damage activity of 3MC. As a consequence, all tumours carried mutated p53 (Fig. 14C). Subsequently we analyzed the proliferation marker KI67 and the apoptosis marker Caspase-3 (Fig. 15) in sarcomas of all genotypes.

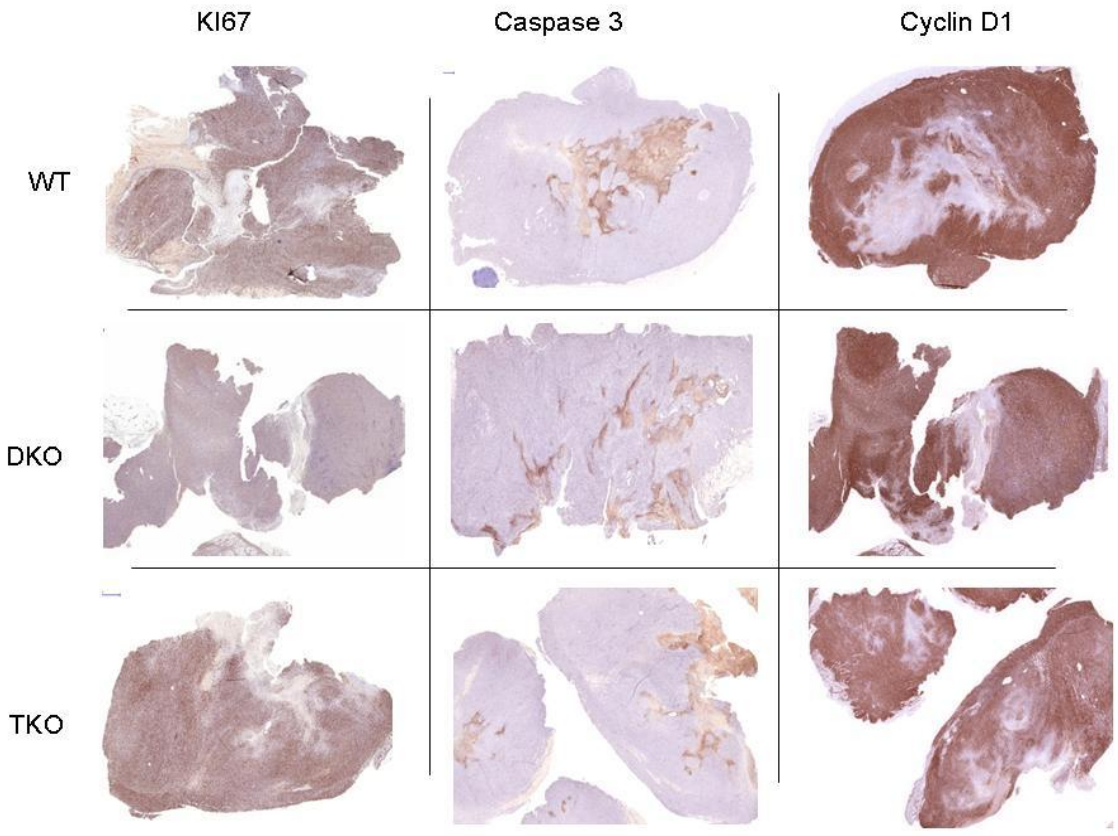

Figure 15. Characterization of 3MC induced sarcoma. Immunohistochemistry of KI67, Caspase 3 and Cyclin D1 in 3MC induced sarcoma. Several different fields for each tumour were immunostained with antibodies against the proliferation markers KI67 and Cyclin D1 and apoptotic marker Caspase 3. Proliferation markers KI67 and Cyclin D1 show similar high staining in every genotype with a high intra- and intertumoural variability. Apoptosis marker Caspase 3 shows low activation regardless of the tumour's genotype but also a high variability within each tumour and among different tumours.

All tumours, independently of the genotype showed similar levels of Caspase-3 activation. All tumours contained high KI67 staining as corresponds to fast growing tumours. Differences between genotypes for both markers were not statistically significant due to the variability among tumours and precluded any conclusion regarding increased apoptosis or proliferation. Similar observation was made when Cyclin D1 was quantified (data not shown). DKO and TKO tumours showed lower number of Cyclin D1 stained cells, and although the variability among tumours was too high to assign statistical significance, it

showed a clear trend that tumours of DKO and TKO mice were less proliferative. The reduced levels in Cyclin D1 might explain reduced rate of proliferation in the tumour, as Cyclin D1 is a target of Pim kinases.

To study the mechanism implicated in the reduction of growth rate in Pim-deficient tumours, we analysed the relative levels of proteins that are direct or indirect targets of Pim kinases and might be involved in slowing the cell cycle. Pim kinases phosphorylate $p27^{Kip1}$, inducing its degradation (Morishita, Katayama et al. 2008), and might alter the protein translation through 4EBP-1 (Beharry, Zemskova et al. 2009; Blanco-Aparicio, Collazo et al. 2011). On the other hand, Pim3-induced tumours show increased levels of Cyclin D1 (Wu, Wang et al. 2010) and active Gsk3β alters Cyclin D1 stability by enhancing its degradation (Carnero 2010). Furthermore, since AKT has been reported to be situated downstream of PIM in some models (Hu, Li et al. 2009), we also measured the phosphorylation status of this protein (Fig. 16).

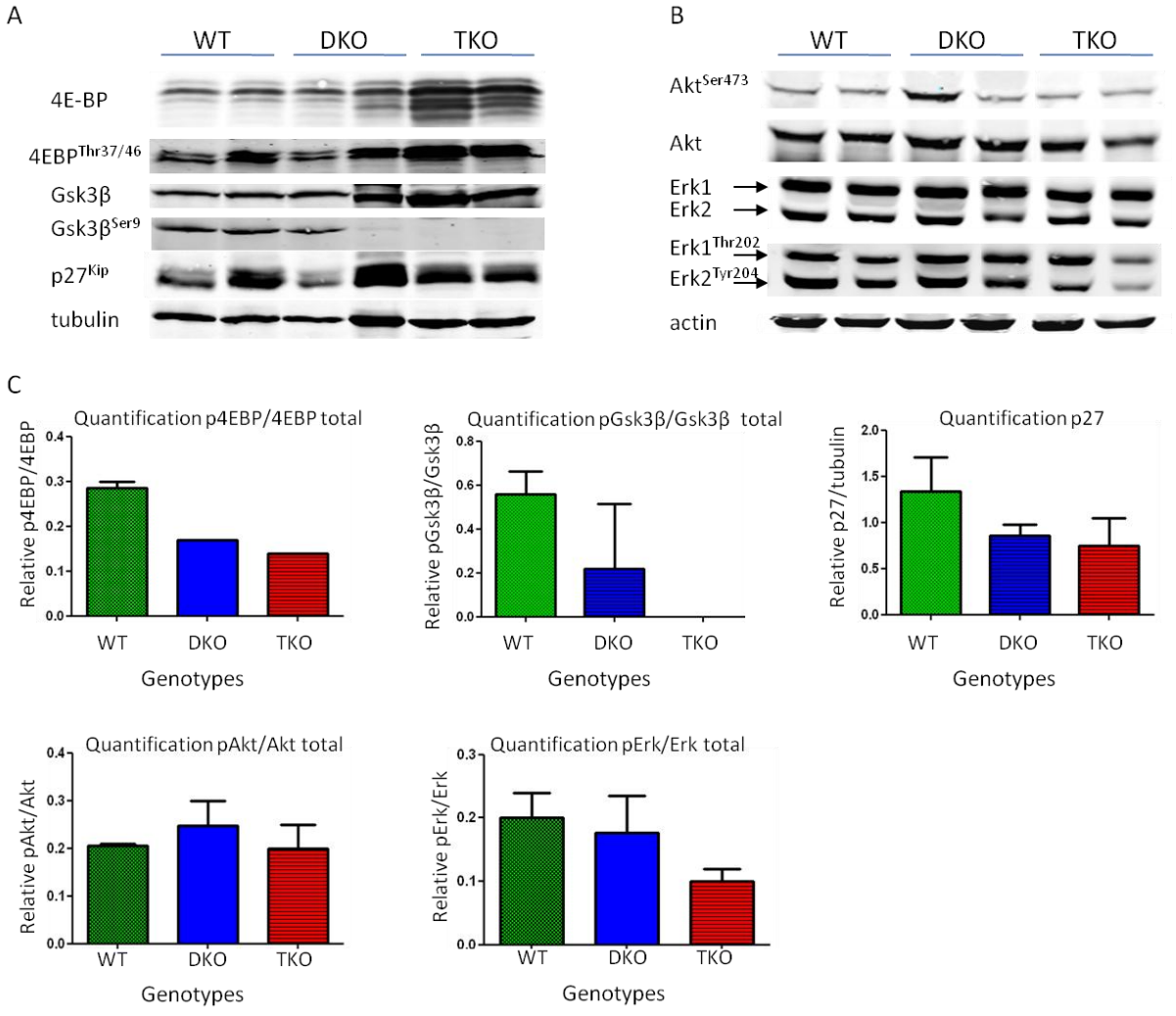

Figure 16. Western blot analysis of Pim kinase targets. **A and B: Western Blot analysis of direct or indirect Pim kinase targets.** For Western bot analysis, whole cell protein was extracted from 2 tumours of each genotype and levels of different proteins were determined by Western blot. **C: Quantification of relative protein levels.**

We did see differences in 4E-BP1 phosphorylation among the tumours of the different genotypes, with reductions around 40% in the DKO and TKO tumours (Fig. 16A and 16B). We observed also lower levels of pErk and $p27^{Kip1}$ (although both decreases were not significant) in most DKO and all TKO tumours we analysed (Fig. 16A and B). But in all cases there was an important amount of active protein remaining. However, the analysis of Gsk3β phosphorylation at ser9 (inactive form) by Western blot showed that this residue is not phosphorylated in most DKO and all TKO tumours (Fig. 16A and C). Only one DKO tumours showed phosphorylated Gsk3β at ser9, while none of the analysed TKO tumours showed ser9 Gsk3β phosphorylation (to assure results, we analysed Gsk3β phsophorylation in a total of 5 tumours per genotype – data not shown). By contrast, Akt phosphorylation did not show significant variations among tumours (Fig. 16B and C), indicating that the effect on Gsk3β is not due to inactive Akt in Pim-null tumours. To explore whether that effect on ser9 Gsk3β phosphorylation was a general effect due to Pim absence we analyzed Gsk3β in MEFs from all three genotypes (Fig. 17). All MEFs showed similar content on Gsk3β and Gsk3β phosphorylated at Ser9, indicating that loss of Gsk3β phosphorylation at Ser9 occurs during the tumourigenic process.

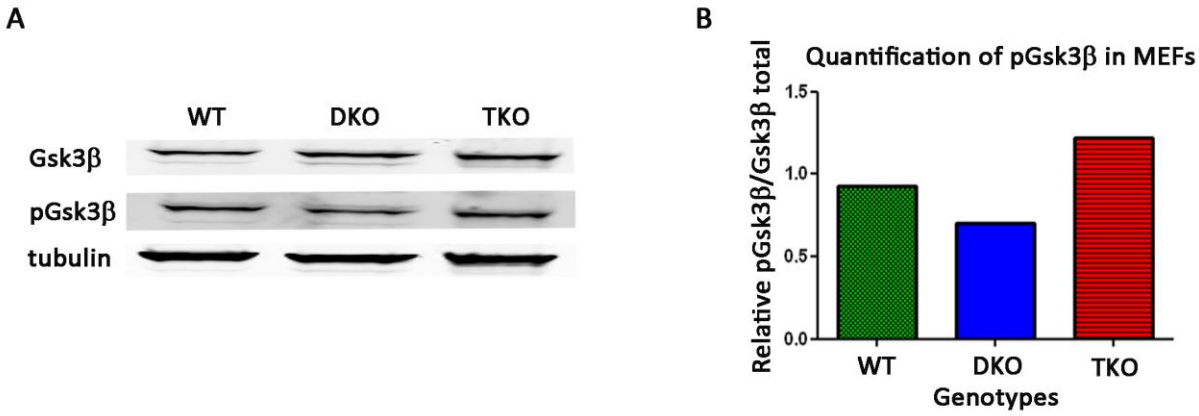

Figure 17. Western blot analysis of Gsk3β levels in MEFs. Whole cell protein was extracted from MEFs of each genotype and levels of Gsk3β were determined by Western blot using 100 µg of protein and later quantified.

4.1.4. Loss of Pim kinases reduces bone invasion by sarcoma

One interesting property in our 3MC-induced sarcomas was the microscopically observed bone invasion (Fig. 18A). Sarcoma cells degrade bone and invade bone marrow. In over 80% of tumours induced in wild type animals we detected bone invasion by these sarcomas

(Fig. 18B). However, the microscopic analysis showed that lack of Pim2 and 3 reduced the percentage of sarcomas invading bone to 31%. Lack of all three isoforms reduced bone invasion to 17% (Fig. 18A) confirming the relevance of these kinases in the process.

To determine further into the mechanisms of decreased bone invasion we looked at changes in another important factor for bone invasion, such as MMP9. MMP9 is a gelatinase or type IV collagenase that degrades native collagen type IV, a major component of the basement membrane and belongs to a subgroup of the MMP family. MMPs participate in normal physiologigal processes but have been associated with tumour progression, invasion and metastasis. (MacDougall and Matrisian 1995; Coussens, Tinkle et al. 2000; Vande Broek, Asosingh et al. 2004). To determine Mmp9 expression in 3MC sarcoma we extracted protein from the tumour of each genotype and analysed protein expression by Western blot (Fig. 18 C and D). Quantification of Mmp9 protein levels showed a decrease in Mmp9 levels in DKO mice and near absence of Mmp9 in TKO mice, which could explain the decrease in bone invasion in these genotypes.

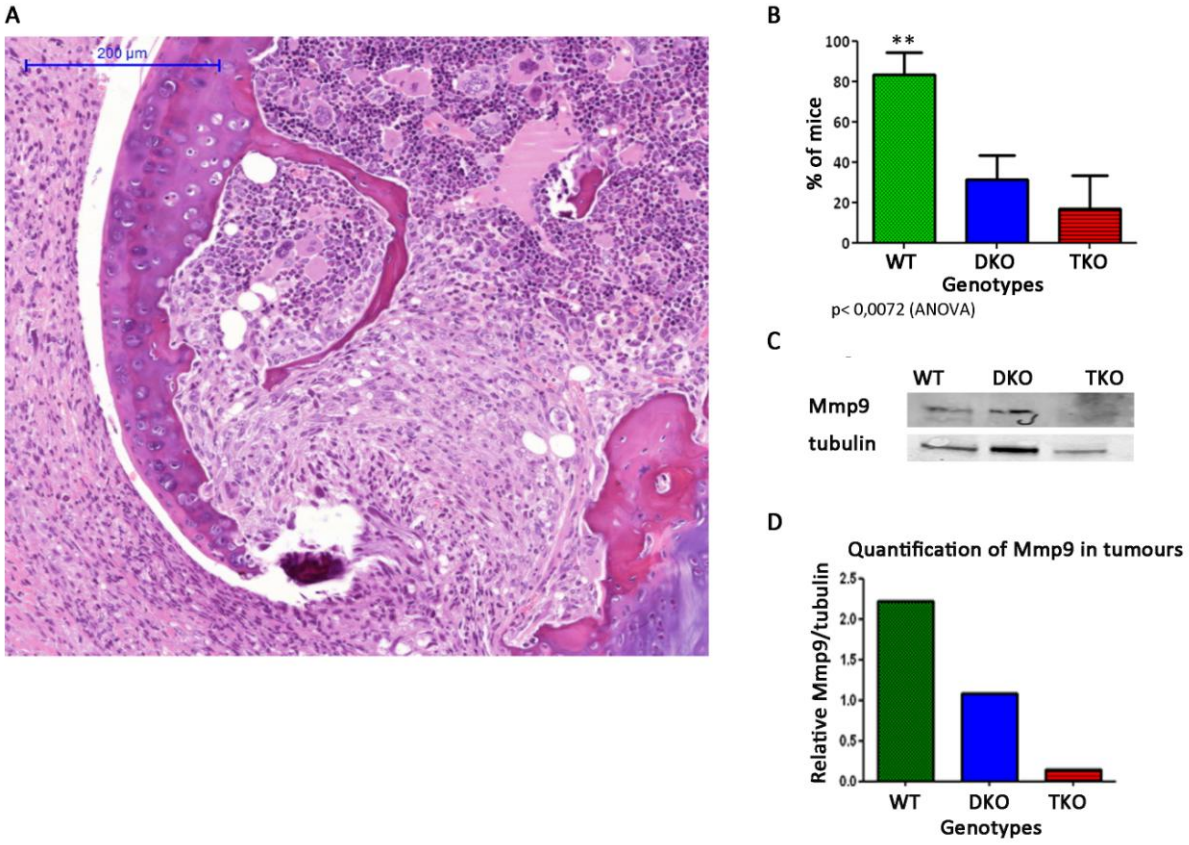

Figure 18. Depletion of Pim kinases reduces bone invasion by 3MC induced sarcoma. **A: H&E staining of sarcoma with bone invasion.** Tumour shown was extracted from wild-type mice. **B: Percentage of mice that showed bone invasion of sarcoma.** Significantly more wild-type mice show bone invasion of sarcoma compared with mice depleted of Pim kinases. **C: Western blots analysis of Mmp9 in tumors.** Whole cell protein was extracted from MEFs and levels of different proteins were determined by Western blot. One representative MEF clone per each genotype is shown. **D: Quantification of the levels of Mmp9 in tumours.** The graph shows the relative levels of the Mmp9 protein related to tubulin.

4.2. Generation of transgenic mice carrying *PIM1* transgene

4.2.1. Plasmid generation

The sequence of the human *PIM1* was amplified and verified as described in 3.2.2. The construct carrying the transgene was generated inserting the *PIM1* sequence into the pVL-1 vector, which carries all the additional genetic elements necessary for the inducibility of the transgene (Fig. 19), such as a CMV-enhancer, a β-actin promoter, the LoxP/STOP cassette and a polyA tail.

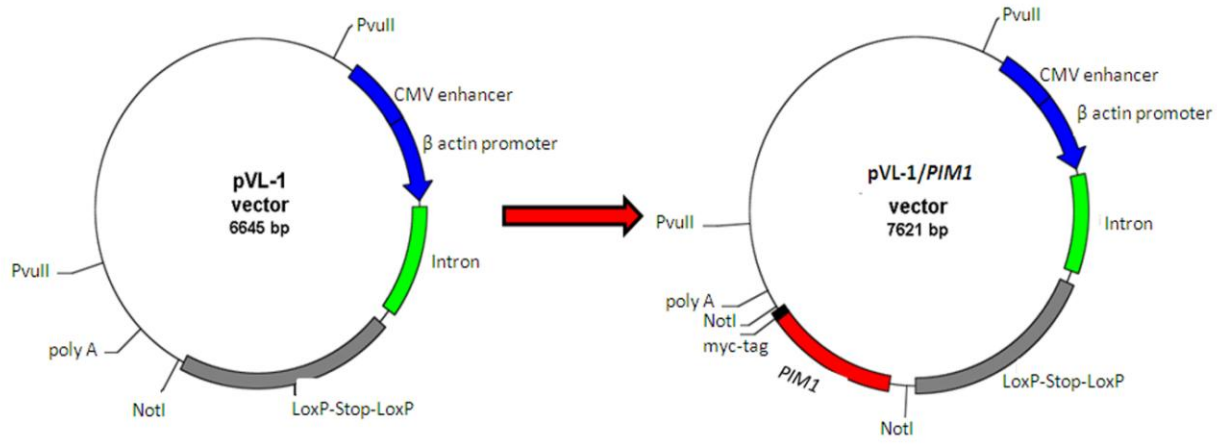

Figure 19. Generation of the plasmid carrying the transgenic PIM1 construct. PIM1 sequence was amplified as described in 3.2.2. and verified by sequencing analysis. The transgenic sequences were inserted in to the pVL-1 vector via the NotI restriction site.

The DNA construct was subsequently linearized using PvuII enzyme and injected into embryonic stem cells, where it was inserted by random recombination. Embryonic stem cell injection, verification and transfer of the blastocyst into foster mice were carried out by the Transgenic Mice Unit of the CNIO.

4.2.2. Mouse line generation

Mice born after embryonic stem cell injection were genotyped using specifically designed primers (Table 6). From those mice we identified several possible founder mice which were crossed with wild type C57/Bl6 mice and resulting pups were genotyped to verify germ line transmission. Founder mice that showed germ line transmission were then bred to verify conditional transgene expression by RT-PCR. To that end we generated mouse lines that express the transgenene and Cre-recombinase by crossing the founder mice with mice expressing Cre-recombinase tissue specifically (Table 4).

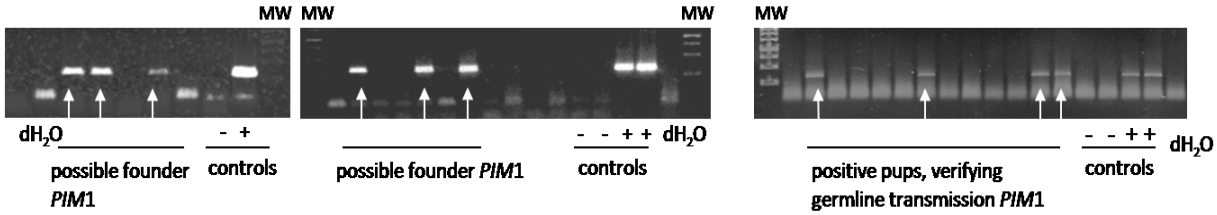

Figure 20. Identification of possible founder mice carrying the PIM transgene. Tail tips of possible founder mice and their offspring were lysed according to protocol and genotyping PCR was performed using DNA from those lysates as well as specifically designed primers (Table 6). PCR fragment length of expected 330 bp was checked on a 1.5% agarose gel.

This resulted in pups expressing *PIM1* tissue specifically (Fig. 21) since the Lox/Stop/Lox cassette will be excised by the Cre-recombinase thus allowing transgene expression.

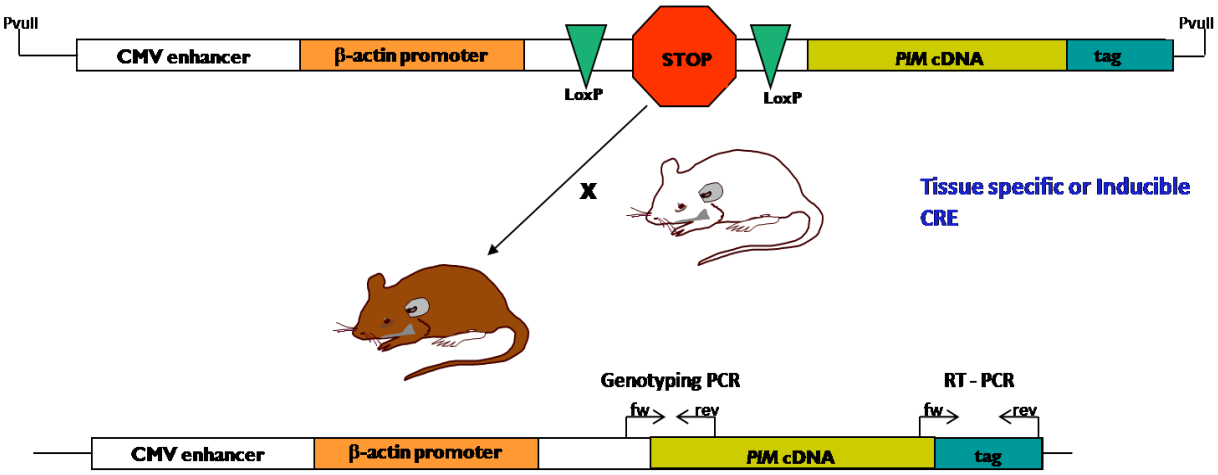

Figure 21. Generation of transgenic mice expressing PIM1 tissue specifically. Animals carrying the respective transgene were crossed with mice expressing Cre-recombinase in a tissue specific manner, thus resulting in a mouse line that expresses the transgene tissue specifically depending on tissue specific Cre-recombinase expression, as the Lox/Stop/Lox cassette will be excised.

4.2.3. Expression of *PIM1* transgene

We identified two founder mice for *PIM1* transgenic mice of which only one had good breeding results. To check transgene expression by reverse transcriptase PCR (RT-PCR), we extracted total RNA (3.5.1.) of several tissues of 10 weeks old mice expressing the transgene in prostate (*PIM1/PSA61*-Cre mice) and did the RT-PCR as described in 3.5.2. Subsequent single PCR using cDNA revealed that the *PIM1* transgene was only expressed in prostate but not in any other tissues (Fig. 22). Surprisingly after two rounds of hormone treatment the same PCR revealed that the transgene was now also expressed in bladder (see 4.3.5.).

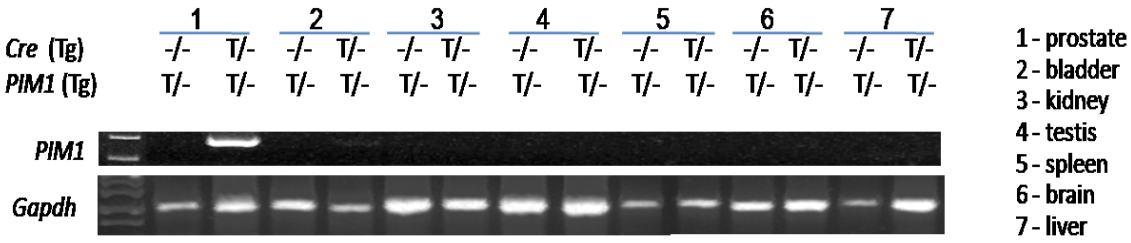

Figure 22. Relative expression of PIM1 in tgPIM1 mice. RNA was extracted of different tissues of 10 weeks old mice and a reverse transcriptase PCR was performed to obtain cDNA which was amplified using specifically designed primers. PCR fragment length was checked on 1, 5% agarose gels.

4.3. *PIM1* transgenic expression in prostate

4.3.1. Grading mPIN lesions

To grade the lesions of mouse prostate intraepithelial neoplasia (mPIN) we used the consensus grading system established at the Bar Harbor Meeting; October 2001 (Cardiff, Rosner et al. 2004) using mPIN grades from mPIN I to mPIN IV followed by carcinoma. For fine tuning we decided to use a numeric categorization system for prostatic epithelia lesions that subdived the mPIN grades into prostate lesion grades (pl-grade) 0 to 13 (Fig. 23); whereas pl-grade 0 represents a prostate free of lesions and pl-grade 13 represents carcinoma (see table 11). A normal epithelium only has one cell layer of luminal cells (pl-grade 0) but when intraepithelial neoplasia begins to appear, more cell layers can be seen. Lesions start to grow in one gland (focal); if there are more than 3 affected glands within the same lesion grade in one lobe it is called multifocal. If more than 30% of one lobe is affected, mPIN lesions are diffuse.

mPIN I lesions (pl-grade 1-3) are small lesions with up to one or two layers and are divided into focal (pl-grade1), multifocal (pl-grade 2) and diffuse (pl-grade 3) as are also mPIN II - IV . When the lesions grow and become mPIN II (pl-grade 4-6) they start to fill up the gland with increasing but not severe atypia. mPIN III lesions (pl-grade 7-9) fill up more than 50% of the lumen of the gland, extending along the duct to involve adjacent ones with atypical cells, poorly orientated with increasingly severe nuclear pleomorphism and hyperchromasia. Mitosis are present.

Table 11: Characterization and classification of mPIN. All data from (Shappell, Thomas et al. 2004)

"mPIN is the neoplastic proliferation of epithelial cells within preexisitng or normal basement membrane confined gland spaces with or without documented progression to invasive carcinoma. These epithelial cells demonstrate nuclear atypia and stratification. The foci can acquire a tufting, micropapillary, or cribiform growth." Shappell et al, Bar Harbor meeting report; Cancer Research 64, 2004			
mPIN grade	**prostate lesion grade (pl-grade)**	**localization**	**characterization**
normal	0		- 1 luminal cell layer of normal cells
mPIN I	1	focal	- small foci - 1 or 2 layers of atypical cells - cells larger and taller than normal cells - fibromuscular stroma intact
	2	multifocal	
	3	diffuse	
mPIN II	4	focal	- ≥ 2 layers of atypical cells - cells larger and taller than normal cells - increasing but not severe nuclear pleomorphism and hyperchromasia - larger nuclei and vesicular chromatin pattern - fibromuscular stroma intact
	5	multifocal	
	6	diffuse	
mPIN III	7	focal	- foci almost fill lumen of ducts - atypical cells poorly orientated - increasingly severe nuclear pleomorphism and hyperchromasia - mitosis present - fibromuscular stroma intact - gland outline smooth
	8	multifocal	
	9	diffuse	
mPIN IV	10	focal	- foci fill lumen of ducts - duct profiles are distorted and irregular - fibromuscular sheat irregular or absent - epithelium still surrounded by laminin layer - lesions exted along duct to involve adjacent ducts - increased severe pleomorphism and hypercromasia - central necrosis may be present
	11	multifocal	
	12	diffuse	
carcinoma	13		- epithelium loses surrounding laminin layer

mPIN IV (pl-grade 11-12) fill up the whole gland distorting it, but the lesion is still confined to the gland. The epithelial cells exhibit severe nuclear pleomorphism and hyperchromasia with mitotic figures. Central necrosis may be present. When mPIN IV lesions turn to carcinoma the lesion is not confined to the gland anymore, in fact the fibromuscular layer loses its integrity with penetration of malignant cells into the surrounding stroma.

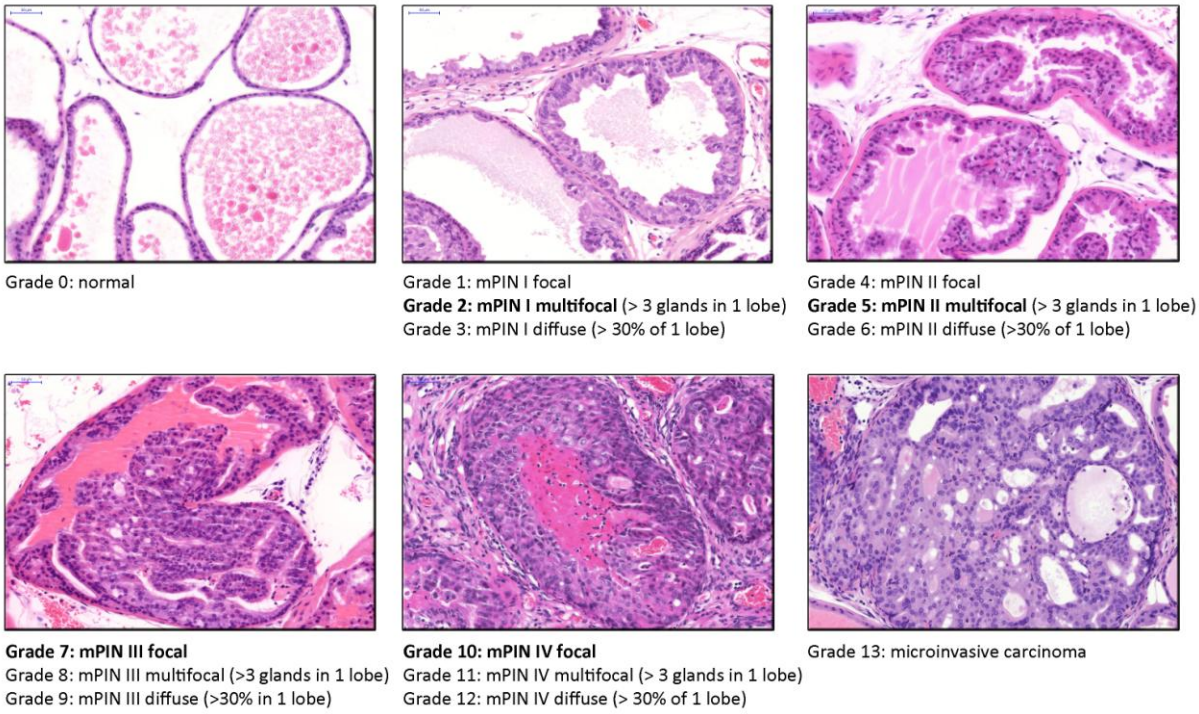

Figure 23. Grading example for prostate intraepithelial neoplasia (mPIN) in genetically engineered mice. 16 week old male mice were sacrificed and prostate tissue was taken and prepared for immunohistochemistry. H&E staining of prostate tissue was used for mPIN grading. mPIN grades were transferred to a numeric system subdividing each mPIN grade into subgrades depending on the quantity of affected glands. Subgrades are: focal, multifocal (more than 3 glands of 1 lobe affected) or diffuse (more than 30 % of 1 lobe affected) as explained above. (Grades depicted in pictures are indicated with bold letters).

As mPIN IV lesions and carcinoma in early state look much alike in a H&E staining, it is helpful to use ancillary techniques such as immunohistochemistry staining for smooth muscle actin (SMA) and cytokeratin 14 (CK14) to differentiate mPIN IV from carcinoma. In a mPIN IV lesion CK14 and SMA can be detected as a continuous staining at the basal epithelial cell layer of the prostate gland, where as early invasion in prostate carcinoma is characterised by disruption of the basal layer where staining is not continuous or fully lost (Fig.24).

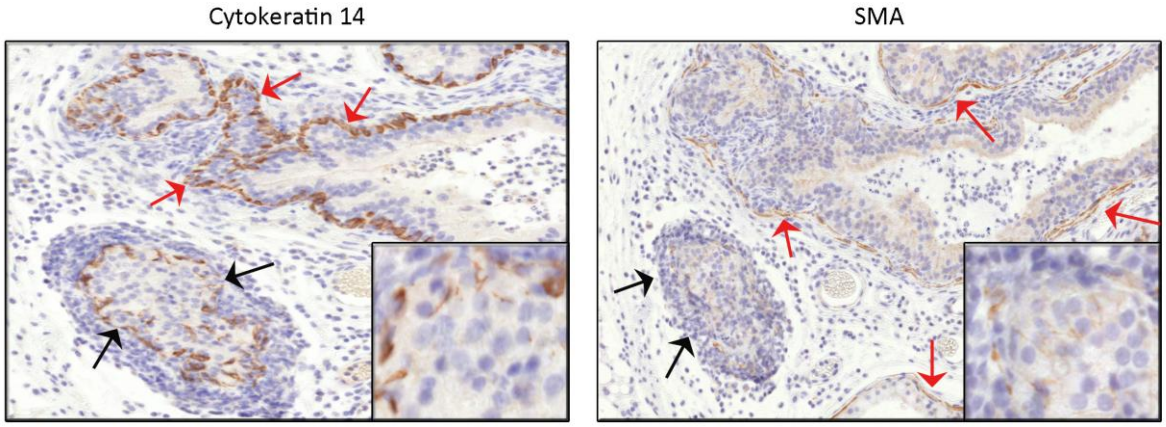

Figure 24. Differentiation of mPIN IV lesions and microinvasive carcinoma. 16 week old male mice were sacrificed and prostate tissue was taken and prepared for immunohistochemistry. To differentiate mPIN IV lesions (red arrows) from microinvasive carcinoma (black arrows) immunohistochemistry for Cytokeratin 14 (CK14) and Smooth muscle actin (SMA) were done. To be count as a microcarinoma continuous staining of both CK14 and SMA has to be lost at the basal epithelial layer of the prostate gland in question (black arrows and insert).

4.3.2. PIM1 cooperates with Pten loss in hormone-induced mouse prostatic intraepithelial neoplasia, mPIN.

PIM1 has been implicated in prostate cancer as a prognostic factor (Dhanasekaran, Barrette et al. 2001). But as *PIM1* is supposedly a "weak" oncogene we decided not only to study mouse prostate intraepithelial neoplasia (mPIN) solely induced by PIM1 overexpression but we also wanted to determine if PIM1 overexpression had an effect in hormone-induced mPIN. The hormone treatment used in this work was adapted from a protocol to induce hyperplasia in prostate used since the 1970ies (DeKlerk, Coffey et al. 1979). This treatment protocol is known to induce prostate hyperplasia at the ratio of testosterone / estradiol (10:1).

Loss of one *Pten* allele is known to induce high-grade prostate lesions within 10 month of age (Wang, Gao et al. 2003) So to explore whether simultaneous overexpression of PIM1 and loss of one *Pten* allele has an additive or synergistic effect in prostate carcinogenesis we also induced mPIN in mice with only one *Pten* allele (from here on named Pten-Het mice) and mice overexpressing our transgene and only carrying one *Pten* allele (from here on named tgPIM1/Pten-Het mice).

Before starting the hormone treatment we assessed the lesions in non treated animals at 8 weeks of age. Whereas nearly 70 % of untreated wild type and tgPIM1 mice showed no lesions (Fig. 26), 80 % of PTEN-Het mice displayed type mPIN II lesions (pl-grade 4). The

difference was even greater in tgPIM1/Pten-Het mice, here 50 % showed mPIN II lesions (pl-grade 5) lesions and 30 % reached a maximum of mPIN III (pl-grade 7) (Fig. 25).

Whereas the percentage of mPIN lesion grades in wild type mice after one round of hormone treatment roughly stayed the same (60 % normal, 40 % mPIN I), hormone treatment aggravated mPIN lesions in all other genotypes. Over 50 % of tgPIM1 mice showed mPIN I lesions after one treatment round, compared to 25 % without treatment; reaching a maximum of mPIN II lesions in 18 % of this group (Fig. 25). Pten-Het and tgPIM1/Pten-Het mice displayed a more drastic change. Both genotypes reached significantly higher mPIN grades compared to WT and tgPIM1 mice after 1 round of hormone treatment ($p<0.0006$); (Fig. 26). After 1 treatment round 55 % of Pten-Het mice showed mPIN II lesions (pl-grade 6), 40 % mPIN III lesions (pl-grade 8) and 1 animal reached mPIN IV (pl-grade 10). The severity of induced mPIN lesions in tgPIM1/Pten-Het mice was even greater. 65 % of tgPIM1/Pten-Het mice showed mPIN III lesions (pl-grade 8), 2 animals (11 %) reached mPIN IV (pl-grades 10 and 11) and only 24 % of mice with this genotype still only showed mPIN II lesions (Fig. 26).

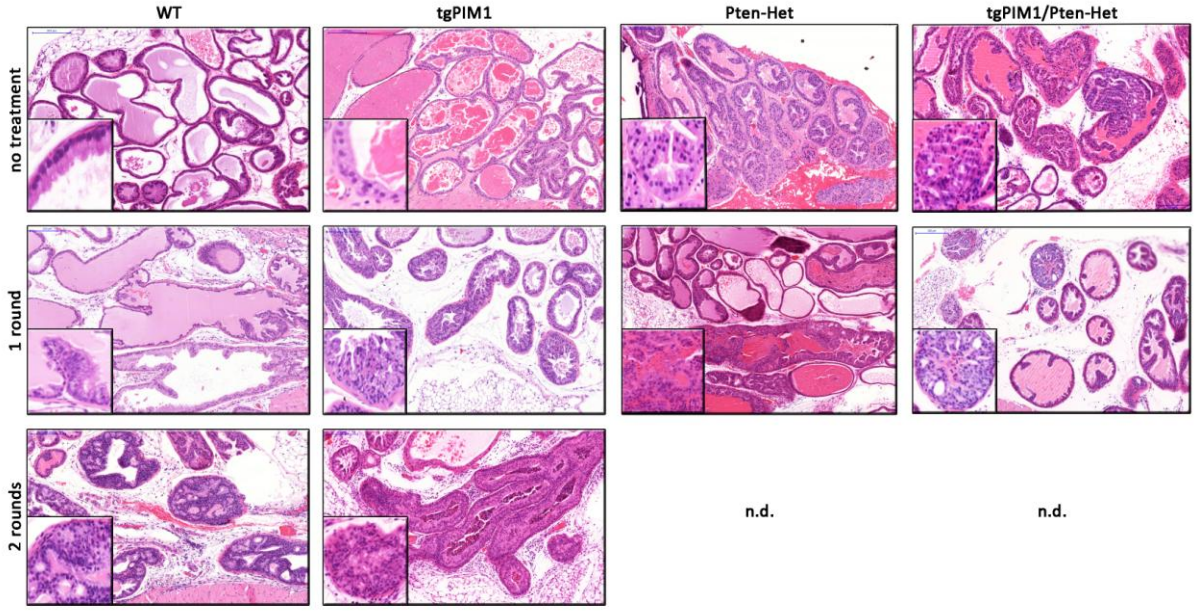

Figure 25. Representative pictures of higher grade mPIN lesions developed after hormone treatment. To determine the development of mPIN lesions due to hormone treatment 8 week old untreated mice of each genotype, and mice of corresponding genotypes that were hormone treated for 1 or 2 rounds, were sacrificed and prostate tissue was taken. H&E staining of prostate tissue was used for mPIN grading. mPIN grades I – IV were then subdivided as described in table11. **No treatment:** WT) pl-grade 0; tgPIM1) pl-grade 1; Pten-Het) pl-grade 5; tgPIM1/Pten-Het) pl-grade 8; **1 round of hormone treatment:** WT) pl-grade 2; tgPIM1) pl-grade 4; Pten-Het) pl-grade 10; tgPIM1/Pten-Het) pl-grade 11; **2 rounds of hormone treatment:** WT) pl-grade 6; tgPIM1) p-grade 13;

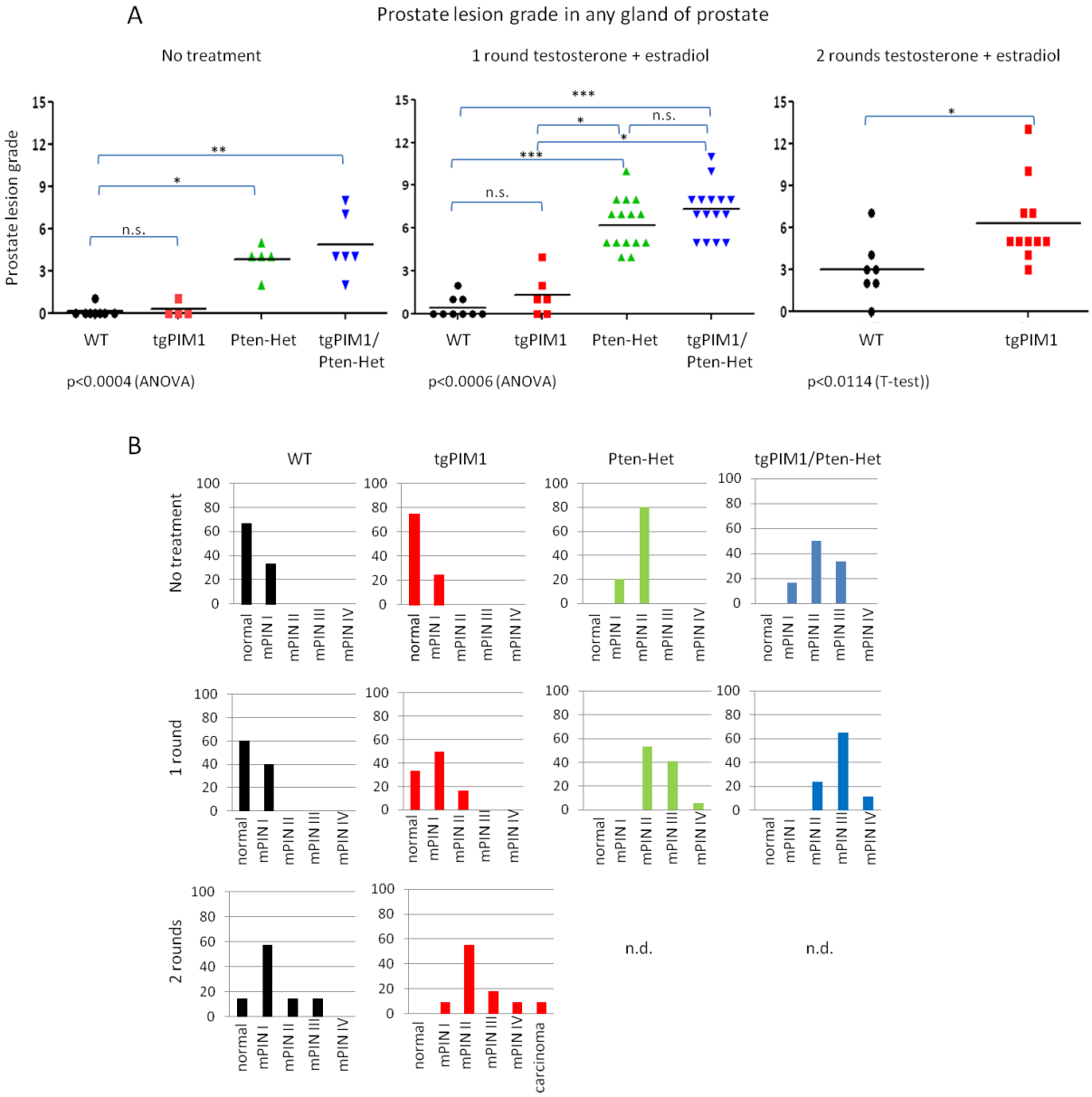

Figure 26. Incidence of mPIN lesions after hormone treatment. 8 week old male mice of each genotype were implanted with testosterone- and estradiol – silicone pellets for 8 weeks (1 round), wild type mice and transgenic PIM1 mice were treated with the same pellets for another 8 weeks (2 rounds). To determine the development of prostate lesions due to hormone treatment, 8 week old untreated mice of each genotype, and mice of corresponding genotypes that were hormone treated for 1 or 2 rounds, were sacrificed and prostate tissue was taken. **A: Grade of prostate lesions reached in each treatment round.** H&E staining of prostate tissue was used for prostate lesion grading applying Bar Harbor grading system and subdividing mPIN I-IV as described in table 11 (grading example). **B: Incidence (in %) of mPIN lesions per genotypes and rounds of hormone treatment.** Percentage of developed mPIN lesions (mPIN I - IV and carcinoma) was determined for each genotype /treatment group using H&E staining of prostate tissue.

Although differences in mPIN grades between Pten-Het and tgPIM1/PTEN-KO mice were not significant, there seemed to be a trend to a higher severity of mPIN in tgPIM1/Pten-Het mice, indicating a possible cooperation of *PIM1* and the loss of one *Pten* allele in the

severity of hormone-induced mPIN (Fig. 26). Due to significantly increased inflammation and subsequent pyelonephritis rate in tgPIM1/Pten-Het mice during the first round of hormone treatment, leading to the necessity of humane endpoint for these mice, a second round of treatment was not done (n.d.). This point will be discussed later under 4.3.4. However we were able to apply a second round of treatment to wild type and tgPIM1 mice. After the second treatment round, 58 % of WT mice showed mPIN I lesions (mainly pl-grade 3), and 1 animal (13 %) reached pl-grade 7. Compared to WT mice, mPIN grades increased significantly in tgPIM1 mice after the second round ($p<0,0114$). 60 % of tgPIM1 mice showed mPIN II lesions (pl-grade 5), 20 % reached mPIN III (pl-grades 6-9) and 1 animal mPIN IV (pl-grade 11) and 1 animal displayed a carcinoma grade (Fig. 26).

4.3.3. *PIM1* does not cooperates with *Pten* loss in aging induced mPIN

It has been published by (Park, Walls et al. 2002; Wang, Gao et al. 2003) that the loss of one *Pten* allele in prostate induces high-grade mPIN lesions in nearly 100% of the tested cohort by the age of 10 month. So to determine the effect of sole PIM1 overexpression after 10 month and to detect a possible cooperation of PIM1 overexpression and the loss of one *Pten* allele we sacrificed wild type, tgPIM1, Pten-Het and tgPIM1/Pten-Het mice at the age of 10 month and screened the prostate for mPIN lesions, using H&E staining. It showed that 100% of wild type mice did not develop mPIN lesions, whereas 89 % of tgPIM1 mice showed mPIN I (pl-grade 2) and 11 % reached mPIN II (pl- grade 5) (Fig. 27 and 28). Nevertheless, 80 % of Pten-Het developed high-grade prostate hyperplasia mPIN III-IV or carcinoma, but differently from what we expected, the carcinoma rate was only 20 %. Opposed to the initial hypothesis of a possible cooperation between PIM1 overexpression and *Pten* loss of one allele, tgPIM1/Pten-Het mice showed less (although not significantly less) severe prostate hyperplasia than Pten-Het alone. Only 66 % of tgPIM1/Pten-Het mice showed mPIN III-IV lesions not reaching carcinoma, whilwe 60 % of Pten-Het mice showed mPIN III and IV, reaching carcinoma in two mice – 20 % of cohort (Fig. 28A and B. To differentiate mPIN IV grade lesions from carcinoma in these 10 month old mice, staining for Smooth muscle actin (SMA) and Cytokeratin 14 (CK14) were done for all high-grade mPIN (mPIN IV and possible carcinoma) verifying the grading of prostate lesions (Fig. 29).

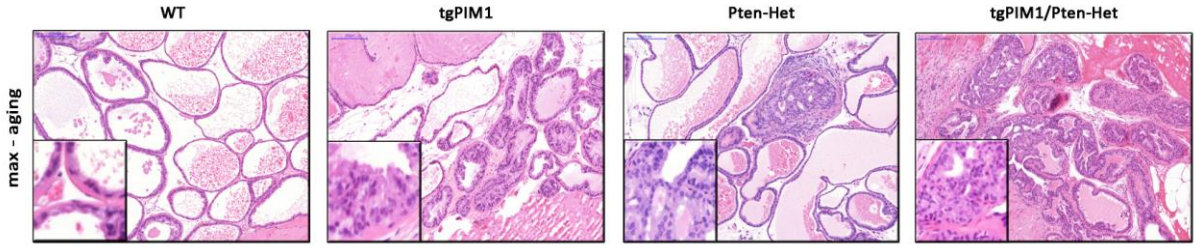

Figure 27. Representative pictures of maximal mPIN lesions in 10 month old untreated mice. To determine the development of mPIN lesions over time without hormone treatment, 10 month old untreated mice of each genotype were sacrificed and prostate tissue was taken. H&E staining of prostate tissue was used for mPIN grading applying Bar Harbor grading system and subdividing mPIN I-IV as described in table 11. **Maximal pl-grade reached:** WT) pl-grade 0; tgPIM1) pl-grade 5; Pten-Het) pl-grade 13; tgPIM1/Pten-Het) pl-grade 11.

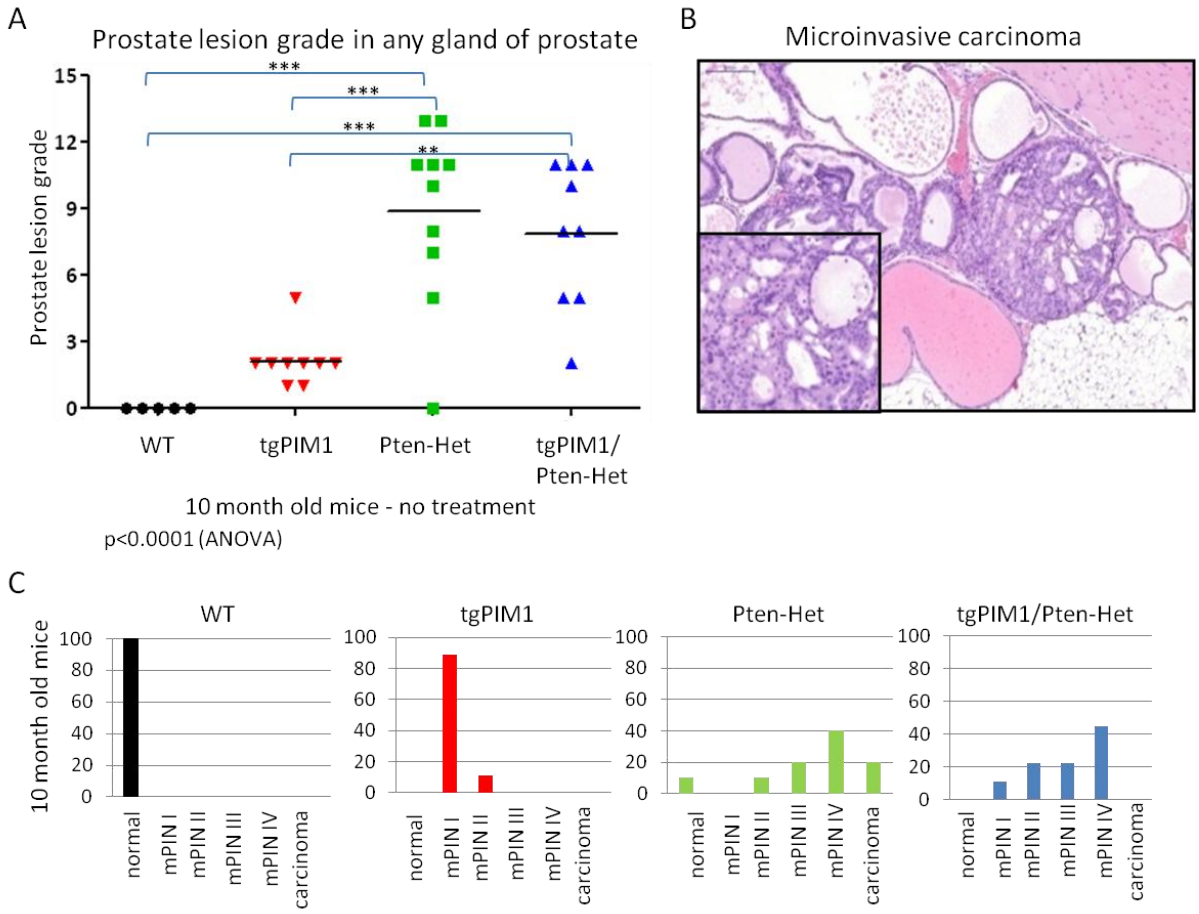

Figure 28. Incidence of mPIN lesions in 10 month old untreated mice. To determine the development of mPIN lesions over time without hormone treatment, 10 month old untreated mice of each genotype were sacrificed and prostate tissue was taken. H&E staining of prostate tissue was used for mPIN grading applying Bar Harbor grading system and subdividing mPIN I-IV as described in figure. **A: Prostate lesion grade in any gland of prostate. B: H&E staining of a microcarcinoma.** Microcarcinoma in a 10-month old Pten-Het mouse. **C: Incidence (in %) of mPIN lesions per genotype in 10 month old mice.** Percentage of developed mPIN grade (mPIN I-IV and microinvasive carcinoma) was determined for each genotype using H&E staining of prostate tissue.

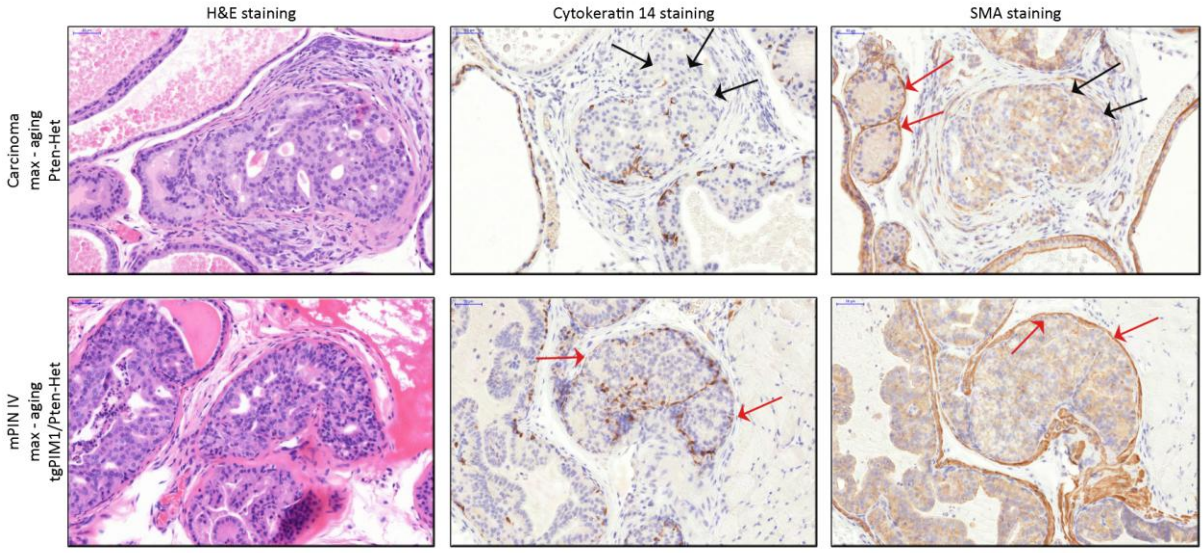

Figure 29. Differentiation of mPIN IV grade lesions and carcinoma in 10 month old untreated mice. H&E staining of prostate tissue of 10 month old mice was used for mPIN grading. CK14 and SMA staining were done to differentiate mPIN IV lesions (as in tgPIM1/Pten-Het mice) from microinvasive carcinoma in (as in Pten-Het mice). Red arrows indicate intact SMA staining- mPIN IV lesion, black arrows indicate where SMA and CK14 immunostaining were negative – carcinoma.

4.3.4. Expression of *PIM1* transgene leads to impaired immune response in hormone treated mice

Hormone treatment with testosterone and estradiol (ratio 10:1) induces low levels of prostate inflammation in treated animals, mostly due to the estradiol (Yatkin, Bernoulli et al. 2009). Usually animals with a normal immune response seem to be able to handle this, as high levels of inflammation have not been reported to this date when using the same protocol, even at higher dosis. However, in this study tgPIM1/Pten-Het mice showed a significantly increased inflammation rate (55 %) during the first round of treatment compared to all other genotypes (approx. 10-20 %; Fig. 30). tgPIM1 animals, although they did only show slightly increased inflammation levels during the first round of treatment (20 %), have a significantly increased inflammation incidence during the 2nd round of treatment (66 %, Fig. 30). Due to this increased inflammatory response, 50 % of tgPIM1/Pten-Het developed pyelonephritis during the first treatment round and 45 % of tgPIM1 mice did so during the second round (Fig. 31).

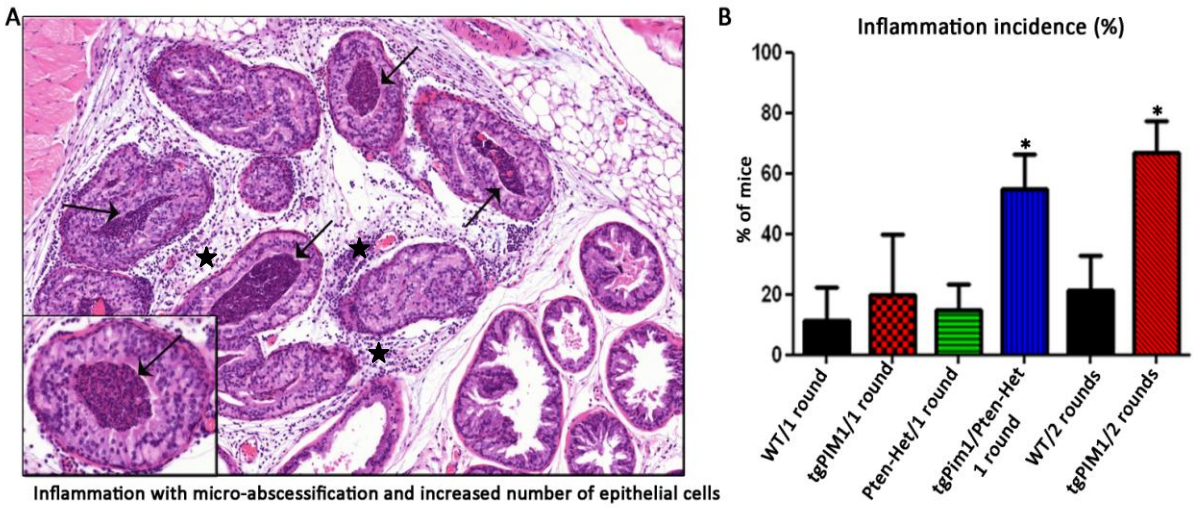

Figure 30. Inflammation incidence in hormone treated mice. **A: H&E staining of a prostate with micro-abscessification**. Prostate of a 16 week old tgPim1/PTEN-KO mouse after one round of hormone treatment showing stromal edema and inflammation (stars) with micro-abscessification (black arrows). **B: Percentage of inflammation incidence of every genotype after one or 2 rounds of hormone treatment respectively.**

As pyelonephritis is very painful and leads to the death of the animal within 12-24 hrs, so animals were sacrificed at the minimal sign of kidney problems and we decided not to carry on with additional rounds of hormone treatment due to the very high rate of affected animals.

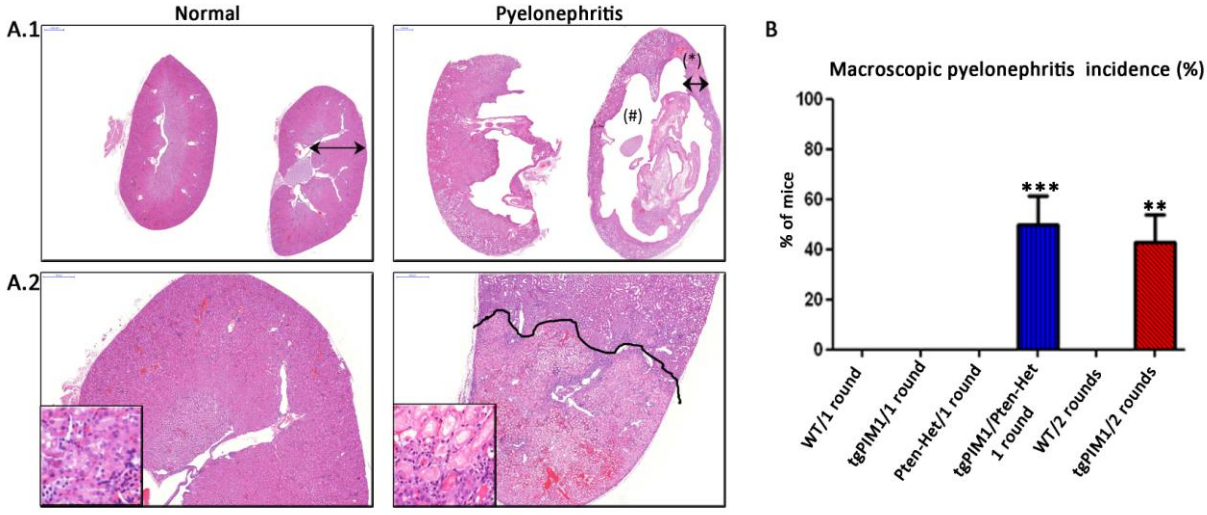

Figure 31. Pyelonephritis incidence in hormone treated mice. **A.1: H&E staining (augmentation 0.5x, panoramic view) of a healthy kidney vs. pyelonephitis.** Kidney of 24 week old wild type animal vs a kidney displaying pyelonephritis of a 24 week old tgPim1 mouse both after 2 rounds of hormone treatment. Note hydronephrosis with pelvic cystic dilatation - (#) and compression and narrowing of the remaining parenchyma (*) **A.2:** H**&E staining of the same kidneys (augmentation 25x).** Note the well demarcated areas of renal infarct where more than one third of the parenchyma is affected. **B: Percentage of pyelonephritis incidence**. Quantification for every genotype after one or 2 rounds of hormone treatment respectively.

4.3.4.1. Senescence as a barrier for further progression to prostate carcinoma

Senescence is a physiological process of proliferative arrest in normal cells after a limited number of cell divisions. This terminal growth arrest is induced by telomeric alterations or different forms of stress including oncogenic transformation. Senescent cells cannot divide even if stimulated with mitogens but they are metabolically active. There are two different forms of senescence i) replicative senescence – due to telomere shortening and ii) accelerated senescence – due to DNA damage, oncogenic mutations like RAS or RAF. Senescence increases markers such as $p21^{WAF1}$ (p21), $p16^{INK4a}$ (p16) and $p19^{ARF}$ (p19) in the cell nucleus and can be detected by immunohistochemistry. As just few of the animals after hormone treatment as well as untreated 10 month old mice display high-grade mPIN lesions or carcinoma we sought to determine the senescence levels in these prostate tissues for markers p21, p16 and p19 (Fig. 32).

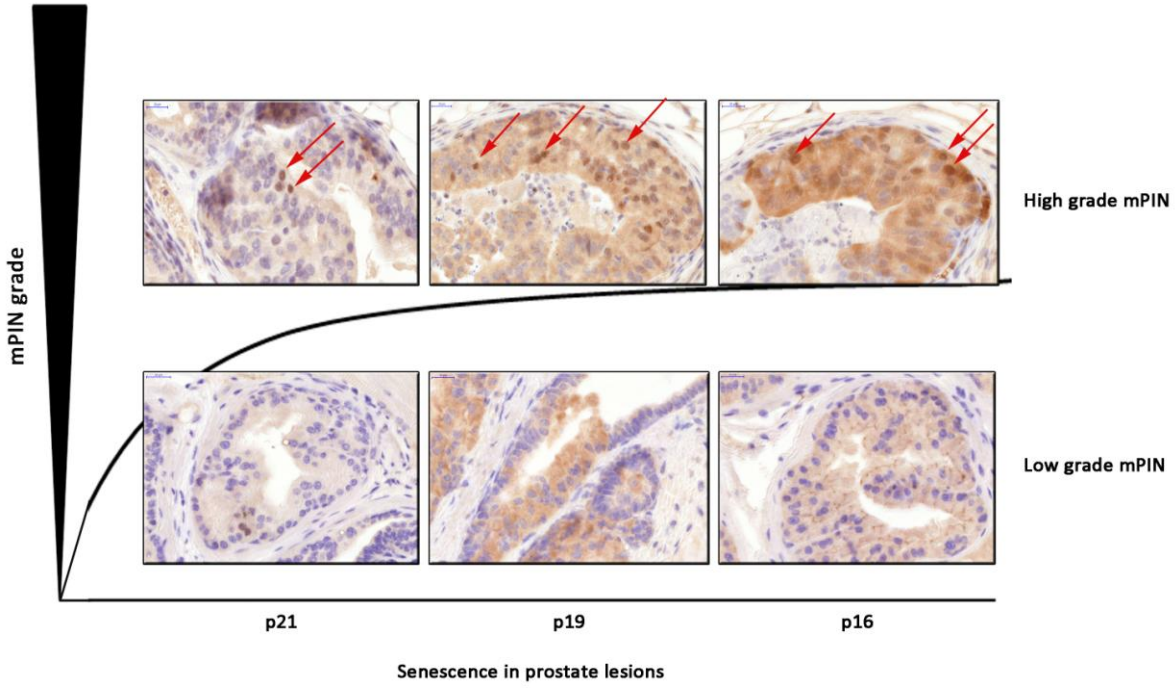

Figure 32. Senescence in Prostate lesions. To determine senescence in prostate lesions, immunohistochemistry for several senescence markers such as p21, p16 and p19 were done in prostate tissue of mice showing high-grade and low-grade mPIN lesions (after hormone treatment as well as in 10 month old mice).

To quantify senescence we used the following grading scale for the number of cells showing senescence markers: s-grade 1 - few cells in 1 lesion (1-5 % positive cells); s-grade 2 - few cells in more than one lesion; s-grade 3 - several cells (5-20 %) in more than one lesion; s-grade 4 - more than 20 % positive cells in more than one lesion; only

considering true senescence if s-grades 3 or 4 were reached in the same animal for at least 2 senescence markers; preferably p16 and p19.

The quantification of all three markers for all grade lesions in all cohorts showed that senescence only appears in high-grade lesions (Fig. 33) of 10-month old untreated mice – Pten-Het and tgPIM1/Pten-Het genotypes. We did not observe high number of cells showing nuclear staining for p16, p19 nor p21 in low-grade mPIN in any cohort. Furthermore, although hormone treated mice displayed high-grade lesions, we did not see senescence markers in these mPIN IV lesions nor in carcinoma (Fig. 34).

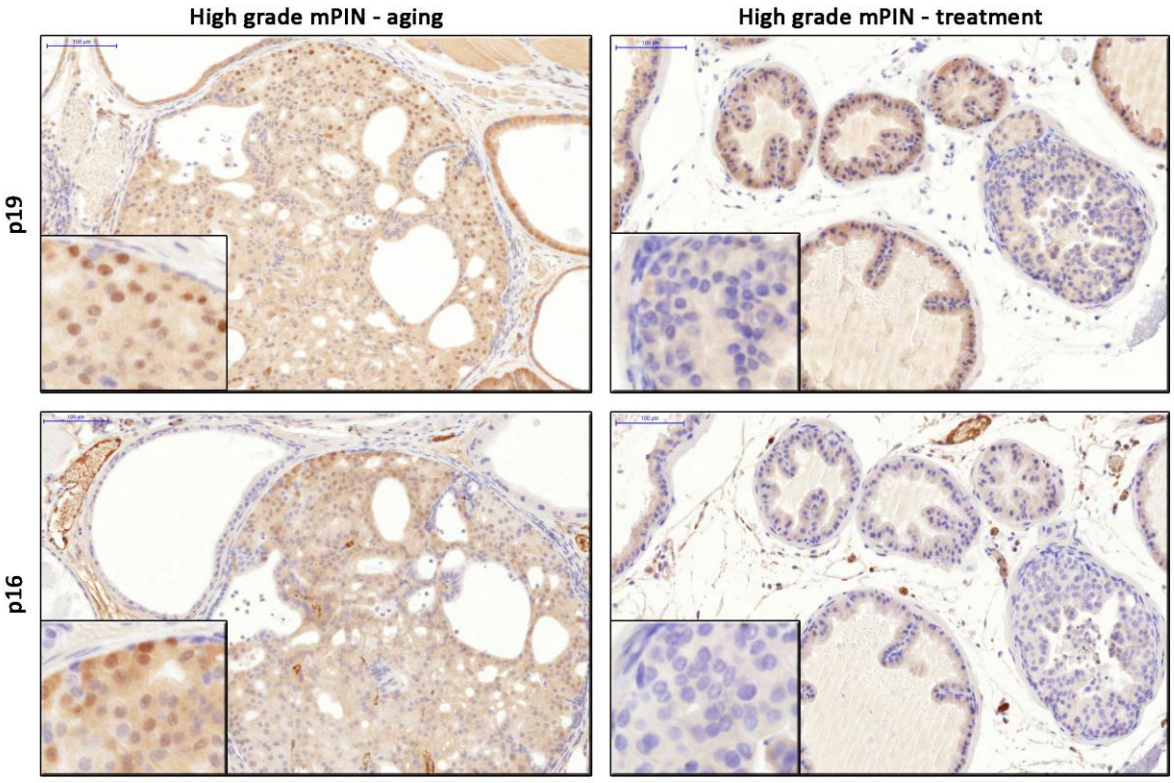

Figure 33. Senescence markers in high-grade lesions – aging versus hormone treatment. Immunohistochemistry for p16 and p19 of high-grade mPIN lesions (mPIN IV) in a 10 month old untreated Pten-Het mouse and a 16 week old hormone treated Pten-Het mouse.

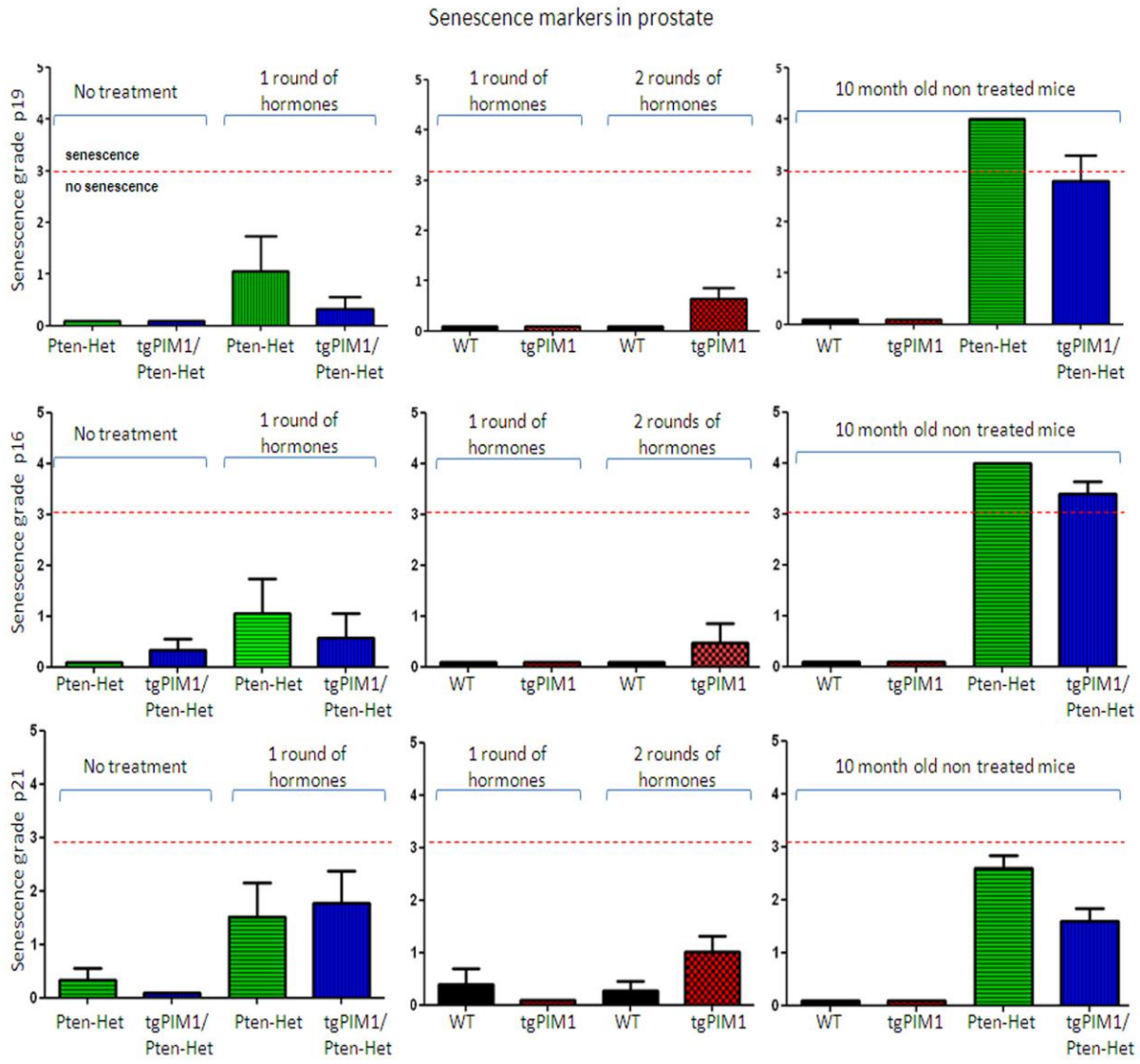

Figure 34. Senescence markers in prostate lesions. To determine senescence in prostate lesions before and after hormone treatment as well as in 10 month old untreated mice, immunohistochemistry for several senescence markers namely p21, p16 and p19 were done in prostate tissue of mice of each genotype using following grading scale for senescence grade (s-grade): s-grade 1 - few cells in 1 lesion (1-5 % positive cells); s-grade 2 - few cells in more than one lesion; s-grade 3 - several cells (5-20 %) in more than one lesion; s-grade 4 - more than 20 % positive cells in more than one lesion; only considering it true senescence if s-grades 3 or 4 were reached in the same animal for at least 2 senescence markers; preferably p16 and p19.

4.3.5. Hormone treatment induces *PIM1* expression in bladder after 2 rounds of treatment.

PSA is supposed to be exclusively expressed in prostate tissue. Nevertheless we detected expression of the *PIM1* transgene in bladder of tgPIM1 mice after two rounds of testosterone/estradiol hormone treatment at the age of 24 weeks (Fig. 35).

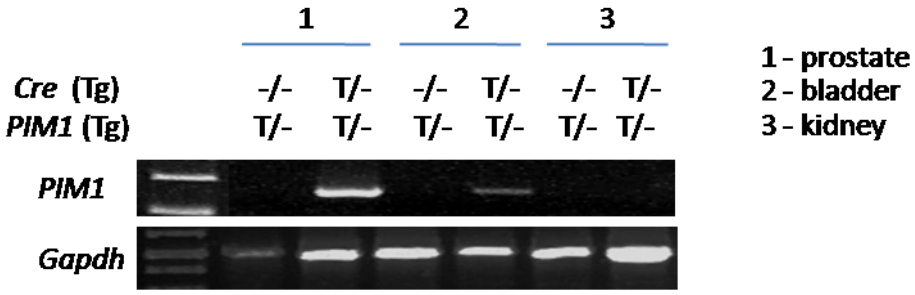

Figure 35. Relative expression of PIM1 in tgPIM1 mice after 2 rounds of hormone treatment. RNA was extracted of different tissues of 24 weeks old mice after 2 rounds of testosterone and estradiol teatment and a reverse transcriptase PCR was performed to obtain cDNA which was amplified using specifically designed primers. PCR fragment length was checked on 1,5 % agarose gels.

4.3.6. Hormone treatment induces hyperplasia in bladder

Hormone treatment protocols, as used in this work, have not been reported to cause urothelial hyperplasia nor severe bladder problems. However we not only detected an increase in bladder size (Fig. 36A) but also urothelial hyperplasia. Whereas untreated animals of all genotypes showed no or only slight hyperplasia in bladder, hormone treatment significantly increased hyperplasia in Pten-Het mice and tgPIM/Pten-Het mice compared to wild type mice (Fig. 36B). Hyperplasia of epithelial cells of bladder tissue that was extended with fixative (10% formalin) at necropsy of bladders before and after hormone treatment was graded using the following grading scale (bladder hyperplasia grade determined bh-grade – table 12): bh-grade 0: normal (2-3 cell layers); bh-grade 1: slight hyperplasia (4 cell layers); bh-grade 2: slight/moderate hyperplasia (5-8 cell layers); bh-grade 3: moderate/severe hyperplasia (9-10 cell layers); bh-grade 4: moderate hyperplasia (11-12 cell layers); bh-grade 5: severe hyperplasia (> 12 cell layers).

Table 12: Classification of bladder hyperplasia in mice after hormone treatment.

bladder hyperplasia grade (bh-grade)	effect on bladder	cell layers
0	normal	2 - 3
1	slight hyperplasia	4
2	slight/moderate hyperplasia	5 - 8
3	moderate hyperplasia	9 - 10
4	moderate/severe hyperplasia	10 - 12
5	severe hyperplasia	> 12

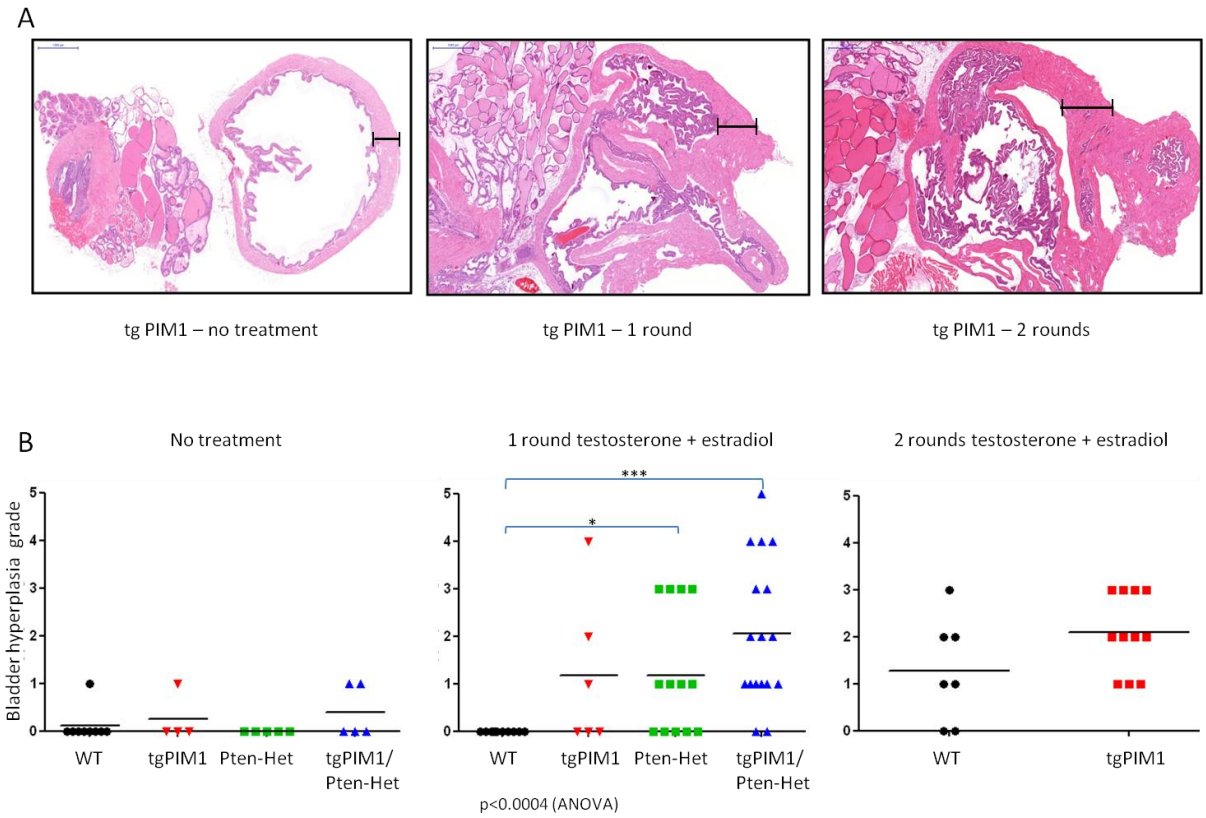

Figure 36. Urothelial hyperplasia incidence in hormone treated mice. To determine the development of urothelial hyperplasia due to hormone treatment, 8 week old untreated mice of each genotype, and mice of corresponding genotypes hormone treated for 1 or 2 rounds were sacrificed and bladder tissue was taken and distended with fixative. **A: Increase of bladder size over treatment course.** H&E stainings of bladders of tgPIM1 mice, before treatment and after 1 or 2 treatment rounds respectively. **B: Urothelial hyperplasia grades.** Hyperplasia of epithelial cells in bladder before and after hormone treatment was graded using the grading scale explained in table 12.

After one treatment round, wild type mice showed no hyperplasia (bh-grade 0), tgPIM1 mice displayed mostly bh-grade 1, reaching the maximum of bh-grade 3 (1 animal, Fig. 36B and 37), Pten-Het mice also only display mostly bh-grade 1 but 3 animals reached bh-grade 3. The increase in urothelial hyperplasia was even more significant in tgPIM1/Pten-Het mice, where several animals displayed bh-grade 4 and 1 animal reached bh-grade 5 (Fig. 36B and 37). After two rounds of hormone treatment, urothelial hyperplasia started to affect also WT animals, as 57 % of this genotype displayed bh-grade 1 or 2. Nevertheless, incidence increase of urothelial hyperplasia in tgPIM1 animals was higher, as 72 % of animals reached bh-grade 2 or 3.

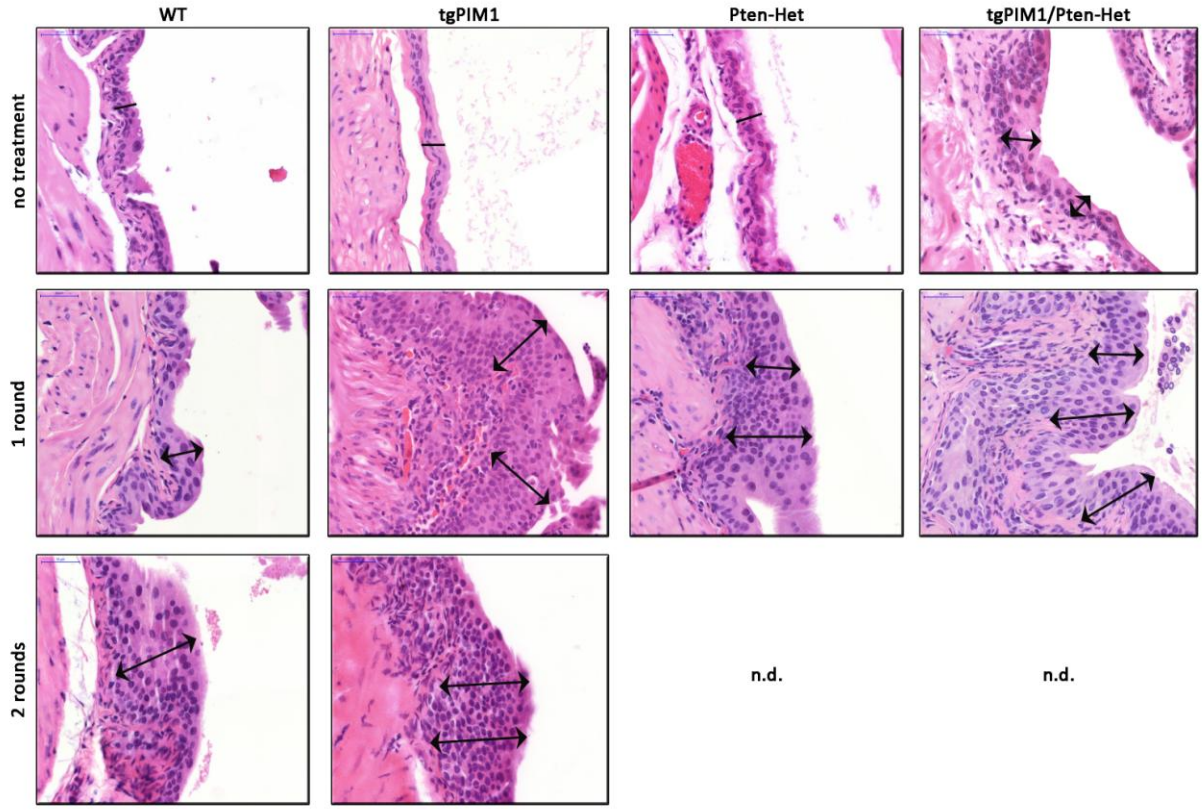

Figure 37. Representative pictures of urothelial hyperplasia developed after hormone treatment. To determine the development of urothelial hyperplasia due to hormone treatment, 8 week old untreated mice of each genotype, and mice of corresponding genotypes hormone treated for 1 or 2 rounds were sacrificed and the bladder was taken. H&E staining of bladder tissue was used for grading (*Table* 12) **No treatment:** WT, tgPIM1 and Pten-Het display bh-grade 0; tgPIM1/Pten-Het) bh-grade 1; **1 round of hormone treatment:** WT) bh-grade 0; tgPIM1) bh-grade 4; Pten-Het) bh-grade 3; tgPIM1/Pten-Het) bh-grade 5; **2 rounds of hormone treatment:** WT) bh-grade 3; tgPIM1) bh-grade 3.

Discussion

5. Discussion

5.1. The essential role of Pim kinases in sarcoma growth and bone invasion

PIM kinases are an active target for drug discovery research, with most compounds focused on the PIM1 isoform due to its known implications in tumourigenesis. However, especially *in vivo*, little is known regarding the specific contribution of each isoform to tumourigenesis. Taking advantage of genetically modified mice, we explored whether the inhibition of specific isoforms is required to prevent sarcomas induced by 3-methylcholanthrene carcinogenic treatment. We found that absence of *Pim2* and *Pim3* greatly reduced sarcoma growth, to a similar extent to the absence of all 3 isoforms. Similar results were obtained in MEFs derived from these knockout mice, where double *Pim2/3* knockout MEFs already showed reduced proliferation and were resistant to oncogenic transformation. To block bone invasion by the tumour, although the absence of all 3 isoforms is necessary to achieve the maximum effect, depletion of *Pim2* and *Pim3* seems to be sufficient to achieve a large reduction of the invasive effect.

We observed that sarcomas arising from *Pim*-defective mice grow significantly more slowly, correlating with reduced proliferation markers, suggesting reduced proliferative capacity. It has been shown that PIM1 phosphorylates CDC25A, thereby increasing its phosphatase activity and the activity of CYCLIN D1-associated kinases, which results in cell cycle progression (Mochizuki, Kitanaka et al. 1999). The CDC25C-associated kinase 1 (C-TAK1) is a potent inhibitor of CDC25C, a protein that actively promotes cell cycle progression at the G2/M phase. By phosphorylating C-TAK1, PIM1 inhibits its activity and eventually advances the cell cycle (Bachmann, Hennemann et al. 2004). Furthermore, PIM1 can phosphorylate $p21^{WAF1}$, another molecule involved in cell cycle progression, at its threonine residues, resulting in its relocation to the cytoplasm and enhancing its protein stability (Wang, Bhattacharya et al. 2002; Zhang, Wang et al. 2007). These effects are associated with increased cell proliferation. Thus, it is tempting to speculate that PIM can promote cell cycle progression and thus eventually contributes to carcinogenesis by modulating the function of molecules that regulate cell cycle progression. Our data showed a reduction of Cyclin D1 in Pim-null tumours, correlating with a decrease in the proliferative capabilities of these tumours. Furthermore, we also observed a partial inhibition of 4E-BP1 phosphorylation and slightly lower levels of pErk in the DKO and TKO tumours (Fig 16). It is possible that the addition of those mild effects contributed to reduced proliferation, slowing the tumour growth rate. However, the most important mechanistic feature observed in our

model is the loss of Gsk3β phosphorylation at Ser9 (inactive form) in most tumours of Pim-depleted mice, but not in MEFs of the same genotype. Absence of Gsk3β Ser9 phosphorylation will maintain high Gsk3β activity, reducing cell cycle transition and glucose metabolism (Vivanco and Sawyers 2002; Carnero 2010). This residue has been shown to be phosphorylated by Akt (Carnero 2010). It is possible that Akt activation lies downstream of Pim, as has been described previously (Hu, Li et al. 2009). Therefore, loss of Pim might abolish Akt activation and subsequent Gsk3β phosphorylation. However, analysis of tumours showed similar levels of Akt activation in Pim-null tumours, suggesting that Gsk3β Ser9 residue phosphorylation depends on a kinase different from Akt. It is possible that PIM itself phosphorylates GSK3β at Ser9 and inactivates the protein, since AKT and PIM share many protein substrates (Amaravadi and Thompson 2005; Brault, Gasser et al. 2010; Nawijn, Alendar et al. 2011). On the other hand, GSK3β is also a substrate of PP2A (Ivaska, Nissinen et al. 2002; Mora, Sabio et al. 2002; Hernandez, Langa et al. 2010), which recently been described as a target of PIM kinases (Chen, Chan et al. 2005). Therefore, loss of PIM kinases might increase the levels of PP2A, leading to GSK3β dephosphorylation. Furthermore, loss of PIM expression might increase levels of PP2A activity, which may mediate the levels of c-MYC and the phosphorylation of proteins needed for increased protein synthesis. Both of these changes could have a significant impact on tumour growth (Chen, Chan et al. 2005). Whatever the the mechanism, it occurs only as a consequence of the tumourigenic process in the absence of Pim, since Pim-null MEFS maintain Gsk3β phosphorylation at the Ser9 residue, suggesting that there is no redundancy in this Gsk3β phosphorylation, and therefore, this protein can be a good therapeutic target for invasion in PIM-dependent tumours. One of the most interesting pieces of data found in our work is the correlation of Pim kinases with the process of bone invasion *in vivo*. Absence of *Pim* kinases blocks the process of bone invasion induced by the 3MC-induced sarcoma, and the genes seem to act in an additive manner, since absence of *Pim2* and *Pim3* produces only a partial effect and the absence of all three is necessary to achieve the maximum effect. In agreement with our data, siRNA interference of PIM1 and PIM2 reduced PC3 migration *in vitro* by around 50%, while inhibition of all 3 PIM kinases by DHPCC-9 (a specific pan-PIM inhibitor) reduced migration of PC3 in vitro by 90% (Santio, Vahakoski et al. 2010). In addition, overexpression of any PIM family member has the opposite effects by enhancing cell motility (Santio, Vahakoski et al. 2010). Silencing of PIM3 was also reported to reduce endothelial cell spreading, migration and vascular tube formation, further supporting that this kinase can stimulate the metastatic and/or angiogenic potential of cancerous cells (Zhang, Wang et al. 2009). In addition, PIM1, but not PIM2, was shown to regulate homing and migration of bone marrow cells, possibly

via phosphorylation-mediated modification of CXCR4 expression in the cell surface (Grundler, Brault et al. 2009). The substrates and signalling pathways regulated by PIM kinases, that contribute to enhancing the motility of adherent cancer cells remain, however, to be elucidated. Recently, the NFAT transcription factors, identified as PIM targets (Rainio, Sandholm et al. 2002) have been implicated in tumour cell migration and invasion (Mancini and Toker 2009). Since NFAT is also a target of GSK3β, it is tempting to speculate that lack of ser9-Gsk3β phosphorylation in Pim tumours contributes to reduced migration by maintaining low levels of NFAT activation.

To determine further the mechanisms of decreased bone invasion we looked at changes in another important factor for bone invasion, MMP9. MMP9 is a gelatinase or type IV collagenase that degrades native collagen type IV, a major component of the basement membrane, and belongs to a subgroup of the MMP family. MMPs participate in normal physiological processes but have been associated with tumour progression, invasion and metastasis. (MacDougall and Matrisian 1995; Coussens, Tinkle et al. 2000; Vande Broek, Asosingh et al. 2004). To determine Mmp9 expression in 3MC sarcoma we extracted protein from the tumour of each genotype and analysed protein expression by Western blot (Fig. 18C). Quantification of Mmp9 protein levels showed a decrease in Mmp9 levels in DKO mice and near absence of Mmp9 in TKO mice, which could explain the decrease in bone invasion in these genotypes. These mechanisms should be further investigated as they again reveal the PIM kinase family to be an interesting drug target.

5.2. Role of PIM 1 in prostate hyperplasia induced by hormone treatment

PIM1 has been implicated in prostate cancer as a prognostic factor (Dhanasekaran, Barrette et al. 2001) Also, recent studies have correlated PIM1 kinase with chemoresistance in prostate cancer cells, which is a common occurrence in more aggressive, hormone-refractory prostate cancers (Chen, Kobayashi et al. 2009/B; Mumenthaler, Ng et al. 2009). However, *PIM1* has also been established to be a supposedly “weak” oncogene with a long latency; for example, in mouse lymphoma. On the other hand, it was also shown that mice overexpressing *Pim1* in T-cells are more susceptible to chemically-induced T-cell lymphoma (Breuer, Slebos et al. 1989; Storer, Cartwright et al. 1995), which is why we decided not only to study mouse prostate intraepithelial neoplasia (mPIN) solely induced by *PIM1* overexpression, but we also wanted to determine if *PIM1* overexpression had an effect in hormone-induced mPIN. As it

has been proved for prostate cancer that PIM1 is most likely to collaborate with MYC in cellular transformation (Zippo, De Robertis et al. 2007), we wanted to explore the possibility of cooperation between *PIM1* overexpression and the loss of *Pten*. Loss of one *Pten* allele is known to induce high-grade prostate lesions within 10 months of age (Wang, Gao et al. 2003). Therefore, to explore whether simultaneous overexpression of PIM1 and loss of one *Pten* allele has an additive or synergistic effect in prostate carcinogenesis we also induced mPIN in mice with only one *Pten* allele overexpressing our transgene (tgPIM1/Pten-Het mice), using Pten-Het mice as comparative controls.

The hormone treatment induced significantly more severe mPIN lesions in tgPIM1 mice - up to carcinoma, over the course of 2 treatment cycles - than in wild type mice with both genotypes starting off with lesion free prostates. This indicates that the sole overexpression of *PIM1* in prostate is sufficient to increase hormone treatment-induced mPIN formation. Mice where one *Pten* allele was inactivated (Pten-Het mice) and mice overexpressing our transgene with only one *Pten* allele (tgPIM1/Pten-Het mice) showed low-grade mPIN lesions before the treatment, significantly increasing incidence in severity and percentage of mice showing these high-grade lesions after one round of hormone treatment compared to wild type and tgPIM1 mice. The fact that one treatment cycle was enough to induce high-grade mPIN lesions in a Pten-Het background shows the malignant potential of *Pten* loss, even though no carcinoma state was detected. And although there are no significant differences in mPIN grade severity of Pten-Het and tgPIM1/Pten-Het mice there is a trend to increased severity, indicating towards cooperation between *Pten* loss and *PIM1* overexpression in hormone-induced mPIN.

It would have been interesting to see if carcinoma developed during following treatment rounds but the protocol had to be interrupted due to high inflammation and subsequent pyelonephritis incidence in tgPIM1/Pten-Het (after the first round) and tgPIM1 mice (after the second round).

PIM1 overexpression was first determined in leukaemia and lymphoma tumours (Cuypers, Selten et al. 1986; Wang, Bhattacharya et al. 2001). However, more recently, PIM1 was found to be increased in solid tumours, including pancreatic and prostate cancer, squamous cell carcinoma, gastric carcinoma, colorectal carcinoma, liver carcinoma (Bachmann and Moroy 2005; Shah, Pang et al. 2008), and recently liposarcoma (Nga, Swe et al. 2010). PIM1 kinase is known to mediate a variety of tumourigenic mechanisms such as preventing apoptosis, inducing genomic instability and increasing proliferation through numerous target proteins, thus fitting perfectly into several cancer hallmarks proposed by Hanahan and Weinberg (Hanahan and Weinberg 2000; Hanahan and Weinberg 2011). For example,

PIM1 is overexpressed in high-grade PIN lesions subverting the mitotic spindle checkpoint, thus inducing genomic instability (Shah, Pang et al. 2008) an early event in the development of PC. On the other hand, overexpression of PIM1 in advanced PC has been described to promote the switch from androgen-dependent to androgen-independent PC, and supports androgen-independent tumour growth through IL6/STAT3 induction (van der Poel, Zevenhoven et al. 2010). Recent studies have also correlated PIM1 kinase with chemoresistance in prostate cancer cells, which is a common occurrence in more aggressive, hormone-refractory prostate cancers (Chen, Kobayashi et al. 2009/B; Mumenthaler, Ng et al. 2009). PIM1 kinase has also been linked to hypoxia-promoted genetic instability in solid tumours facilitating cell survival, resulting in tumours with a more aggressive phenotype (Chen, Kobayashi et al. 2009/A). This suggests that PIM1 can play different roles at different time points in the same human malignancy.

Although the PIM kinases have been identified as oncogenes in transgenic models, by themselves they are only weakly transforming. Our data on PIM1 transgenic animals *in vivo* agree with these works since the increased expression of PIM1 does not induce full tumorigenesis in prostate, but increase the number and grade of premalignant lesions in all tumourigenic settings. In humans, PIM kinases might help the development of neoplasias by adding tumourigenic capabilities to cells and increasing the probability to develop carcinomas. On the other hand, the discovery that PIM expression might protect from apoptosis in hypoxic environments (Chen, Kobayashi et al. 2009/A) may also explain the recurrence of PIM expression in solid tumors. To fully explore this possibility in our model, we need to undertake new experiments in which PIM1 is activated once the tumor (carcinoma) has been formed.

First ectopic expression of SV40 Large T antigen (LTag) in the prostate resulted in the random integration of the transgene and acting as an oncoprotein via suppressive interaction with p53 and pRb. Similarly, LTag was later described to be targeted in prostate by using a region of the C3(1) gene (RAS prostatic steroid binding protein gene). Male C3(1)-LTag mice developed mPIN at 3 months of age, developing locally invasive adenocarcinoma by 10 months (Yoshidome, Shibata et al. 1998). Since then, other transgenics models of large and Small T antigens targeted by different means to the prostate have been developed. All showed similar contributions to prostate cancer development (Valkenburg and Williams 2011). Overexpression of IGF1 in the basal epithelial layer of prostate induced low-grade mPIN as early as 2 months. At 6 months, mice displayed different alterations including high grade mPIN in all prostatic lobes (DiGiovanni, Bol et al. 2000; DiGiovanni, Kiguchi et al. 2000). Myc was also expressed at

different doses in prostate (Jenkins, Qian et al. 1997; Qian, Jenkins et al. 1997), showing a dosage-dependent response in mPIN severity that was dependent on androgens. FGFR1, but not FGFR2, overexpression in prostate produced pronounced hyperproliferation and mPIN, but failed to recapitulate the more aggressive steps of PC (Freeman, Gangula et al. 2003; Freeman, Welm et al. 2003). Overexpression of other Tyrosine kinase receptor such as Erbb2 also induced mPIN and approximately 10% mice showed adenocarcinoma (Li, Szabolcs et al. 2006). Oncogenic Ras expression in prostate did not progress further than mPIN (Scherl, Li et al. 2004), similar to the FGFR1 model.

KO models represent a different strategy. We have to consider that while conditional models may allow tissue specific expression and timed analysis of the full process of tumourigenesis, whole KO models may generate faster growing tumours in other tissues shadowing the relevance of the functional suppression of the gene in prostate. Up to day, more than 10 genes and combinations have been reported being conditionally deleted in prostate (Valkenburg and Williams 2011), most of them produced different grades of mPIN, but only a few have been reported to progress to adenocarcinoma in a small subset of mice, PTEN, APC and combinations of PTEN+Nkx3.1, Ras^{V12}+Catnb or p53+pRb.

In our model, increased expression of PIM1 alone or in combination with loss of one PTEN allele was not able to produce full grown adenocarcinoma (except sporadic ones), but clearly contributed oncogeneically to increase the severity of the mPIN, similar to other models reported. This is also in agreement with the data that *PIM1* has been established to be a supposedly “weak” oncogene with a long latency; for example, in mouse lymphoma. And that PIM1 overexpression in prostate cell lines showed that PIM1 overexpression alone was not sufficient to transform the benign cells to malignancy, but enhanced *in vitro* and *in vivo* the tumourigenic capabilities of tumour cells (Chen, Chan et al. 2005; Kim, Roh et al. 2010). Similarly, mice overexpressing of Pim1 in T-cells are more susceptible to chemically induced lymphoma. On the other hand, it has been recently reported that transgenic mice that express human PIM3 selectively in liver increased the frequency and decreases latency of hepatocellular carcinoma induced with the carcinogen diethylnitrosamine. As in our work, these works also suggest that PIM family members are weak oncogenes, but can contribute to tumourigenesis by selectively enhancing tumourigenic capabilities.

5.3. PIM and inflammation

The hormone treatment used in this work was adapted from a protocol to induce hyperplasia in prostate of rats and dogs used since the 1970ies (DeKlerk, Coffey et al.

1979). This treatment protocol is known to induce mPIN lesions and prostate adenocarcinoma at the ratio of testosterone / oestradiol (10:1) but the exact mechanism how the lesions are induced is still not determined. It is suspected that this happens, at least in part, through prostate inflammation as prostatitis is associated with increased mPIN grade, pointing to a probable initiator role of inflammation in the early steps of prostate cancer (Yatkin, Bernoulli et al. 2009).

It has been established that androgens have an anti-inflammatory role and oestrogens such as oestradiol a pro-inflammatory role in prostatitis (Straub 2007). At the used ratio of 10:1 inflammatory response of wild type and Pten-Het mice seems normal. Although there are small areas of inflammation in up to 20 %, wild type and Pten-Het mice seem to cope with it, having a normal immune response which does not lead to abscesses or pyelonephritis. These small areas of inflammation can be explained by the known fact that testosterone does not always fully repress the inflammatory effects of oestradiol depending on the genetic background of the animal (Yatkin, Bernoulli et al. 2009). However, animals expressing the PIM1 transgene (tgPIM1 and tgPIM1/Pten-Het mice) seem to develop an aggravated immune response after hormone treatment.

Normal prostate tissue contains stromal intraepithelial T- and B-lymphocytes (Theyer, Kramer et al. 1992; Bostwick, de la Roza et al. 2003), macrophages and mast cells. In prostate inflammation, Th1 response (IFN-γ, TNFα) and Th2 response (IL4, 5, 13) are activated as well as PSA, IL6, IL8 and IL10 expression (De Marzo, Platz et al. 2007) and NFκB activation (Colotta, Allavena et al. 2009). As PSA expression is increased by testosterone on one hand, and inflammation on the other, the expression of our transgene PIM1 might also be increased. On the other hand, IL6, NFκB and Stat3 increase endogenous Pim1 expression so that through this positive feedback loop, there would be an excessive amount of PIM1 available in the prostate tissue, which could explain the impaired immune response as PIM1 has been implicated in inflammation recently in several *in vitro* and *in vivo* models (Jackson, Pheneger et al. 2011; Block, Hanke et al. 2012; Shen, Zhao et al. 2012). It is also possible that PSA produced in the prostatic cells diffuses towards inflammatory cells present in the prostate stroma, contributing to transgenic PIM1 activation in these cells. It has been determined that PIM1 and 2 belong to an endogenous pathway that regulates T-cell growth and survival (Wingett, Stone et al. 1995; Owaki, Asakawa et al. 2008; Shen, Zhao et al. 2012). It has also been shown that PIM1 regulates human Th1 cell differentiation (Aho, Lund et al. 2005) and plays a role in immune cell activation and proliferation (Bachmann and Moroy 2005). It also seems that PIM1 contributes to NFκB activation upon TNFα activation (Nihira, Ando et al. 2010) via a

feedback loop, while PIM1 inhibitors inhibit NFκB activation, decrease iNOS production in macrophages and decrease levels of TNFα. These data suggest that PIM1 overexpression could cause the immune response upon hormone treatment in PIM1 transgenic mice. Although the mechanism in this case is not fully clear, we can speculate that excessive PIM1 expression leads to excessive production of certain pro-inflammatory chemokines such as IFNγ and cytokines such as IL6 and NFκB activation and to an impaired T-cell and macrophage response or an excessive oncogenic activation for the expression of two oncogenes such as Pten and PIM1.

5.4. Effects of PIM1 expression on aging prostate

At the age of 10 months, prostates of wild type mice show no lesions. It has been reported that at 10 months of age, PTEN-het mice show high-grade hyperplasia (Wang, Gao et al. 2003). Overexpression of *PIM1* in prostate slightly increases mPIN lesion grade but only low-grade lesions were seen in tgPIM1 mice in 10-months-old mice. On the other hand, Pten-Het mice show mainly high-grade mPIN lesions or microcarcinoma, partly correlating with the published data. Surprisingly, *PIM1* overexpression and *Pten* loss in aging do not seem to cooperate, as although 60 % of the animals display high-grade mPIN lesions, none progressed to carcinoma. This might be explained by senescence found in high-grade lesion in untreated 10-months-old animals.

Here we used the senescence markers $p21^{WAF1}$, $p16^{INK4a}$ and $p19^{ARF}$, only considering true senescence if grade 3 (5-20 % positive cells in more than one lesion) or grade 4 (> 20 % positive cells in more than one lesion) were reached for at least 2 of the 3 senescence markers in the same animal. We did not detect senescence in mPIN lesions of untreated 16-week-old mice nor in hormone-treated animals of any genotype (1^{st} and 2^{nd} treatment rounds), independently of the severity of mPIN lesions. Significantly higher levels of senescence were detected only in high-grade mPIN lesions or carcinoma of 10-months-old Pten-Het and tgPIM1/Pten-Het mice but not in tgPIM1 or wild type mice as senescence seemed to be restricted to high-grade lesions. Interestingly, Pten-Het mice show a slightly higher incidence and higher grade of senescence than tgPIM1/Pten-Het mice, correlating with the higher incidence of high-grade mPIN lesions and carcinoma.

As mentioned in the introduction, senescence is a physiological process of terminal proliferative arrest in normal cells after a limited number of cell divisions and can be induced by telomeric shortening or different forms of stress such as oncogenic mutations. Senescence mechanisms in an inflammatory environment are not fully clear yet. Despite

progressing to high-grade mPIN, hormone-induced hyperplasias did not show senescence markers (we would like to remark that we were unable to detect SA-β-gal staining in mouse tissue, probably due to technical problems). These high-grade mPIN correlated with samples with inflammation processes. It has been described that inflammation might abolish Cyclin Kinase Inhibitors (CKI) expression during senescence, thus facilitating tumourigenesis (Hudson, Shoaibi et al. 1999; De Marzo, Platz et al. 2007; Guerra, Schuhmacher et al. 2007; Zemskova, Lilly et al. 2010). Therefore, it is possible that in high-grade mPIN observed during treatment, p16, p19 and p21 are repressed by inflammation which could have contributed to tumourigenesis if pyelonephritis had not stopped the experiment.

There are different proposals made to explain the role of senescence in tumourigenesis. The most extended is that benign hyperplasias are mostly a result of hyperproliferation of cells subjected to oncogenic stress which in the presence of immortalising events (ie: p53 mutations) can reach malignant status (Chen, Trotman et al. 2005; Larsson 2011). Pandolfi et al proposed that Pten-loss derived pre-neoplasic lesions are a consequence of oncogenic activation, not progressing to malignant grades due to the activation of a senescent programme which is independent of DNA-damage signalling and does not require previous hyperproliferation (Alimonti, Nardella et al. 2010). Our data suggest that senescence markers appear only once the proliferative capability of oncogene stressed cells is exhausted after reaching high grade mPIN and explain lack of senescence markers in low grade mPIN. This will also explain why we have not observed a linear correlation between mPIN and senescence grade.

5.5. Role of PIM 1 in bladder hyperplasia

The hormone treatment used to induce mPIN lesions is not known to induce urothelial hyperplasia. Nevertheless, we detected moderate to severe urothelial hyperplasia in 30 % of tgPIM1/Pten-Het and Pten-Het mice and light to moderate urothelial hyperplasia in 30 % of tgPIM1 mice after one round of hormone treatment. There was no observed urothelial hyperplasia in untreated 10-month old mice.

The PSA/Cre mouse model used in this study has been described to express the induced transgene only in prostate tissue. We did not detect expression of *PIM1* in bladder in untreated 10-week-old mice but there was detectable expression of *PIM1* after 2 rounds of hormone treatment in 24-week-old tgPIM1 mice. As the testosterone increases PSA expression, the levels of testosterone reached by the hormone treatment might be sufficient

to induce PSA expression in bladder or that this diffusible factor reaches the bladder and thus also induces PIM1 expression. This theory is supported by evidence that PSA is found in some bladder carcinoma (Chen, Ho et al. 2008) .

The hormone-induced urothelial hyperplasia grades correlate in each genotype with the hormone-induced mPIN lesion grades, also suggesting as well that in an inflammatory environment PIM1 alone is able to induce hyperplasia. The same stands for the loss of one *Pten* allele. PTEN inactivation has a promoting role in bladder cancer (Puzio-Kuter, Castillo-Martin et al. 2009). And correlating published data, Pten-Het mice show a significant increase in urothelial hyperplasia compared to wild type mice. tgPIM1/Pten-Het mice show an increased severity of hyperplasia in bladder confirming the cooperation between *Pten* loss and transgenic *PIM1* expression in hormone-induced hyperplasia. It has also been published that *PIM1* is involved in bladder cancer as increased PIM1 levels have been detected in bladder carcinoma (Guo, Mao et al. 2010), which correlates with increased bladder hyperplasia in hormone treated tgPIM1 mice.

5.6. PIM as an anticancer drug target.

Besides our work, several other features justify the use of PIM as a cancer target; its overexpression in various types of tumours, and its role in the regulation of pathways considered relevant in cancer, as well as the fact that blocking PIM1 function by introduction of dominant negative PIM1 sensitises pancreatic cancer cells to apoptosis induced by glucose deprivation under hypoxia (Chen, Kobayashi et al. 2009/B). Moreover, dominant negative PIM1 reduces tumourigenicity in pancreatic cancer cells and Hela engraft mouse models. These and other data have led to the synthesis of PIM inhibitors that have recently entered clinical trials.

Inhibitors of PIM are of interest as potential therapeutic agents either alone or in combination (Bullock, Debreczeni et al. 2005; Pogacic, Bullock et al. 2007; Mumenthaler, Ng et al. 2009; Blanco-Aparicio, Collazo et al. 2011); therefore, the understanding of the process that can be targeted by PIM inhibition is of great importance to define the potential activity of these compounds. However, there is some degree of redundancy among PIM kinases that should be studied while defining the specificity of the pharmacological compounds. The levels of expression of the different PIM family members vary among tumour types. PIM1 and PIM2 are mostly overexpressed in leukaemia and lymphomas. PIM1 is also overexpressed in some solid tumours such as prostate, pancreas and colon. PIM3 overexpression has been observed in melanoma, pancreatic and gastric tumours.

The possibility of overlapping substrates and the potential compensatory nature of the different PIM family members as demonstrated by the triple knockout mouse model suggests that the inhibition of all isoforms may be more effective than targeting individual isoforms. In our genetic model, higher activity is achieved in the absence of all family members although sarcoma growth is already significantly reduced in PIM2- and 3-depleted mice.

Since both the PI3K and PIM signalling pathways converge on the regulation of many signalling proteins that are common for AKT and PIM, it is possible that some redundancy among these pathways also occurs in tumours. In fact, It has been described that PIM inhibitors synergise with m-TOR or PI3K inhibitors (Beharry, Zemskova et al. 2009; Blanco-Aparicio, Collazo et al. 2011). Dual treatment with the compounds resulted in decreased phosphorylation of 4E-BP1 and BAD proteins as well as an increase in apoptosis. These data suggest that a combination of drugs that selectively target PI3K/AKT and PIM may have potential in treating tumours.

Conclusions

Conclusions in English

1.) In mouse embryonic fibroblstas (MEFs), loss of *Pim2* and *3* is sufficient to reduce proliferation and render cells resistant to oncogenic transformation.

2.) The absence of *Pim2* and *3* is sufficient to significantly reduce sarcoma growth *in vivo*, but maximum effect is observed with lack of all three isoforms. Pim kinases seem to mediate cell proliferation via Gsk3β, $p27^{kip1}$ and Cylin D1.

3.) Absence of all three isoforms is necessary to achieve maximum effect blocking bone invasion which seems to be related to Gsk3β and Mmp9.

4.) Overexpression of PIM1 under hormonal stress induces high-grade mPIN lesions in prostate and high-grade hyperplasia in bladder but it induces only low-grade mPIN lesions at 10 months of age.

5.) *PIM1* seems to cooperate with *Pten*-loss under hormonal stress, enhancing induced mPIN lesions in prostate and bladder hyperplasia correlating with an inflammatory environment.

6.) Overexpression of *PIM1* and *Pten*-loss induce senescence in high-grade prostate lesions during aging at 10 months, but no progression to carcinoma was observed

7.) *PIM1* overexpression under hormonal stress favours an impaired response to inflammation, leading to pyelonephritis and silencing of $p16^{INK4a}$, $p19^{ARF}$ and $p21^{WAF1}$ as senescence markers

Conclusiones en Español

1.) En MEFs la pérdida de *Pim2* y *3 e*s suficiente para disminuir la proliferación celular y dichas células son resistentes a la transformación oncogénica.

2.) La ausencia de *Pim2* y *3* es suficiente para reducir significativamente el crecimiento de sarcomas *en vivo*, pero el efecto máximo se observa en ausencia de las 3 isoformas. Las Pim quinasas parecen mediar la proliferación celular vía Gsk3β, $p27^{Kip1}$ y Ciclina D1.

3.) Para lograr el máximo bloqueo de la invasión del hueso es necesaria la ausencia de las 3 isoformas de *Pim*, estando dicho efecto relacionado con Gsk3β y Mmp9.

4.) La sobreexpresión de PIM1 bajo estrés hormonal induce neoplasia intraepitelial de alto grado en próstata e hiperplasia de alto grado en vejiga, pero en ratones de 10 meses solamente induce neoplasia intraepitelial de bajo grado.

5.) PIM1 parece cooperar con la pérdida de un alelo de *Pten* bajo estrés hormonal, aumentando las lesiones de neoplasia intraepitelial en próstata y el grado de hiperplasia en vejiga relacionado con un entorno inflamatorio.

6.) La sobreexpresión de PIM1 y pérdida de *Pten* inducen senescencia en lesiones de próstata de alto grado durante el envejecimiento (a los 10 meses), pero no se observó un progreso hacia carcinoma.

7.) La sobreexpressión de PIM1 bajo estrés hormonal favorece un aumento de inflamación local que lleva a pielonefritis y a silenciamiento de los marcadores de senescencia $p16^{INK4a}$, $p19^{ARF}$ y $p21^{WAF1}$

References

References

1. Abate-Shen, C. and M. M. Shen (2002). "Mouse models of prostate carcinogenesis." Trends Genet 18(5): S1-5.
2. Acton, D., J. Domen, et al. (1992). "Collaboration of pim-1 and bcl-2 in lymphomagenesis." Curr Top Microbiol Immunol 182: 293-8.
3. Aho, T. L., R. J. Lund, et al. (2005). "Expression of human pim family genes is selectively up-regulated by cytokines promoting T helper type 1, but not T helper type 2, cell differentiation." Immunology 116(1): 82-8.
4. Aho, T. L., J. Sandholm, et al. (2006). "Pim-1 kinase phosphorylates RUNX family transcription factors and enhances their activity." BMC Cell Biol 7: 21.
5. Alcorta, D. A., Y. Xiong, et al. (1996). "Involvement of the cyclin-dependent kinase inhibitor p16 (INK4a) in replicative senescence of normal human fibroblasts." Proc Natl Acad Sci U S A 93(24): 13742-7.
6. Alimonti, A., C. Nardella, et al. (2010). "A novel type of cellular senescence that can be enhanced in mouse models and human tumor xenografts to suppress prostate tumorigenesis." J Clin Invest 120(3): 681-93.
7. Allen, J. D. and A. Berns (1996). "Complementation tagging of cooperating oncogenes in knockout mice." Semin Cancer Biol 7(5): 299-306.
8. Allen, J. D., E. Verhoeven, et al. (1997). "Pim-2 transgene induces lymphoid tumors, exhibiting potent synergy with c-myc." Oncogene 15(10): 1133-41.
9. Amaravadi, R. and C. B. Thompson (2005). "The survival kinases Akt and Pim as potential pharmacological targets." J Clin Invest 115(10): 2618-24.
10. Bachmann, M., H. Hennemann, et al. (2004). "The oncogenic serine/threonine kinase Pim-1 phosphorylates and inhibits the activity of Cdc25C-associated kinase 1 (C-TAK1): a novel role for Pim-1 at the G2/M cell cycle checkpoint." J Biol Chem 279(46): 48319-28.
11. Bachmann, M. and T. Moroy (2005). "The serine/threonine kinase Pim-1." Int J Biochem Cell Biol 37(4): 726-30.
12. Becker, C., M. C. Fantini, et al. (2004). "TGF-beta suppresses tumor progression in colon cancer by inhibition of IL-6 trans-signaling." Immunity 21(4): 491-501.
13. Beharry, Z., M. Zemskova, et al. (2009). "Novel benzylidene-thiazolidine-2,4-diones inhibit Pim protein kinase activity and induce cell cycle arrest in leukemia and prostate cancer cells." Mol Cancer Ther 8(6): 1473-83.
14. Bhattacharya, N., Z. Wang, et al. (2002). "Pim-1 associates with protein complexes necessary for mitosis." Chromosoma 111(2): 80-95.
15. Blanco-Aparicio, C., A. M. Collazo, et al. (2011). "Pim 1 kinase inhibitor ETP-45299 suppresses cellular proliferation and synergizes with PI3K inhibition." Cancer Lett 300(2): 145-53.
16. Blanco-Aparicio, C., O. Renner, et al. (2007). "PTEN, more than the AKT pathway." Carcinogenesis 28(7): 1379-86.
17. Block, K. M., N. T. Hanke, et al. (2012). "IL-6 Stimulates STAT3 and Pim-1 Kinase in Pancreatic Cancer Cell Lines." Pancreas.
18. Borg, K. E., M. Zhang, et al. (1999). "Prolactin regulation of pim-1 expression: positive and negative promoter elements." Endocrinology 140(12): 5659-68.
19. Borrello, M. G., L. Alberti, et al. (2005). "Induction of a proinflammatory program in normal human thyrocytes by the RET/PTC1 oncogene." Proc Natl Acad Sci U S A 102(41): 14825-30.
20. Bostwick, D. G., G. de la Roza, et al. (2003). "Intraepithelial and stromal lymphocytes in the normal human prostate." Prostate 55(3): 187-93.

21. Brault, L., C. Gasser, et al. (2010). "PIM serine/threonine kinases in the pathogenesis and therapy of hematologic malignancies and solid cancers." Haematologica 95(6): 1004-15.

22. Breuer, M., R. Slebos, et al. (1989). "Very high frequency of lymphoma induction by a chemical carcinogen in pim-1 transgenic mice." Nature 340(6228): 61-3.

23. Breuer, M., E. Wientjens, et al. (1991). "Carcinogen-induced lymphomagenesis in pim-1 transgenic mice: dose dependence and involvement of myc and ras." Cancer Res 51(3): 958-63.

24. Bullock, A. N., J. Debreczeni, et al. (2005). "Structure and substrate specificity of the Pim-1 kinase." J Biol Chem 280(50): 41675-82.

25. Campisi, J. (2001). "Cellular senescence as a tumor-suppressor mechanism." Trends Cell Biol 11(11): S27-31.

26. Campisi, J., S. H. Kim, et al. (2001). "Cellular senescence, cancer and aging: the telomere connection." Exp Gerontol 36(10): 1619-37.

27. Cardiff, R. D., A. Rosner, et al. (2004). "Validation: the new challenge for pathology." Toxicol Pathol 32 Suppl 1: 31-9.

28. Carnero, A. (2010). "The PKB/AKT pathway in cancer." Curr Pharm Des 16(1): 34-44.

29. Colotta, F., P. Allavena, et al. (2009). "Cancer-related inflammation, the seventh hallmark of cancer: links to genetic instability." Carcinogenesis 30(7): 1073-81.

30. Coussens, L. M., C. L. Tinkle, et al. (2000). "MMP-9 supplied by bone marrow-derived cells contributes to skin carcinogenesis." Cell 103(3): 481-90.

31. Culig, Z. and M. Puhr (2011). "Interleukin-6: A multifunctional targetable cytokine in human prostate cancer." Mol Cell Endocrinol.

32. Culjkovic, B., I. Topisirovic, et al. (2006). "eIF4E is a central node of an RNA regulon that governs cellular proliferation." J Cell Biol 175(3): 415-26.

33. Cuypers, H. T., G. Selten, et al. (1986). "Assignment of the human homologue of Pim-1, a mouse gene implicated in leukemogenesis, to the pter-q12 region of chromosome 6." Hum Genet 72(3): 262-5.

34. Cuypers, H. T., G. Selten, et al. (1984). "Murine leukemia virus-induced T-cell lymphomagenesis: integration of proviruses in a distinct chromosomal region." Cell 37(1): 141-50.

35. Chen, J., M. Kobayashi, et al. (2009)/A. "Hypoxia-mediated up-regulation of Pim-1 contributes to solid tumor formation." Am J Pathol 175(1): 400-11.

36. Chen, J., M. Kobayashi, et al. (2009)/B. "Pim-1 plays a pivotal role in hypoxia-induced chemoresistance." Oncogene 28(28): 2581-92.

37. Chen, J. C., C. L. Ho, et al. (2008). "Immunohistochemical detection of prostate-specific antigen expression in primary urothelial carcinoma of the urinary bladder." Anticancer Res 28(6B): 4149-54.

38. Chen, L. S., S. Redkar, et al. (2009). "Pim kinase inhibitor, SGI-1776, induces apoptosis in chronic lymphocytic leukemia cells." Blood 114(19): 4150-7.

39. Chen, W. W., D. C. Chan, et al. (2005). "Pim family kinases enhance tumor growth of prostate cancer cells." Mol Cancer Res 3(8): 443-51.

40. Chen, Z., L. C. Trotman, et al. (2005). "Crucial role of p53-dependent cellular senescence in suppression of Pten-deficient tumorigenesis." Nature 436(7051): 725-30.

41. Chiang, W. F., C. Y. Yen, et al. (2006). "Up-regulation of a serine-threonine kinase proto-oncogene Pim-1 in oral squamous cell carcinoma." Int J Oral Maxillofac Surg 35(8): 740-5.

42. Dautry, F., D. Weil, et al. (1988). "Regulation of pim and myb mRNA accumulation by interleukin 2 and interleukin 3 in murine hematopoietic cell lines." J Biol Chem 263(33): 17615-20.

43. Dave, S. S., K. Fu, et al. (2006). "Molecular diagnosis of Burkitt's lymphoma." N Engl J Med 354(23): 2431-42.

44. De Marzo, A. M., E. A. Platz, et al. (2007). "Inflammation in prostate carcinogenesis." Nat Rev Cancer 7(4): 256-69.

45. DeKlerk, D. P., D. S. Coffey, et al. (1979). "Comparison of spontaneous and experimentally induced canine prostatic hyperplasia." J Clin Invest 64(3): 842-9.

46. Denis, L. and G. P. Murphy (1993). "Overview of phase III trials on combined androgen treatment in patients with metastatic prostate cancer." Cancer 72(12 Suppl): 3888-95.

47. Dhanasekaran, S. M., T. R. Barrette, et al. (2001). "Delineation of prognostic biomarkers in prostate cancer." Nature 412(6849): 822-6.

48. DiGiovanni, J., D. K. Bol, et al. (2000). "Constitutive expression of insulin-like growth factor-1 in epidermal basal cells of transgenic mice leads to spontaneous tumor promotion." Cancer Res 60(6): 1561-70.

49. DiGiovanni, J., K. Kiguchi, et al. (2000). "Deregulated expression of insulin-like growth factor 1 in prostate epithelium leads to neoplasia in transgenic mice." Proc Natl Acad Sci U S A 97(7): 3455-60.

50. Domen, J., N. M. van der Lugt, et al. (1993). "Analysis of Pim-1 function in mutant mice." Leukemia 7 Suppl 2: S108-12.

51. Eichmann, A., L. Yuan, et al. (2000). "Developmental expression of pim kinases suggests functions also outside of the hematopoietic system." Oncogene 19(9): 1215-24.

52. Evans, K. E. and S. W. Fox (2007). "Interleukin-10 inhibits osteoclastogenesis by reducing NFATc1 expression and preventing its translocation to the nucleus." BMC Cell Biol 8: 4.

53. Fearon, E. R. and B. Vogelstein (1990). "A genetic model for colorectal tumorigenesis." Cell 61(5): 759-67.

54. Fizazi, K., L. A. Martinez, et al. (2002). "The association of p21((WAF-1/CIP1)) with progression to androgen-independent prostate cancer." Clin Cancer Res 8(3): 775-81.

55. Fox, C. J., P. S. Hammerman, et al. (2003). "The serine/threonine kinase Pim-2 is a transcriptionally regulated apoptotic inhibitor." Genes Dev 17(15): 1841-54.

56. Freeman, K. W., R. D. Gangula, et al. (2003). "Conditional activation of fibroblast growth factor receptor (FGFR) 1, but not FGFR2, in prostate cancer cells leads to increased osteopontin induction, extracellular signal-regulated kinase activation, and in vivo proliferation." Cancer Res 63(19): 6237-43.

57. Freeman, K. W., B. E. Welm, et al. (2003). "Inducible prostate intraepithelial neoplasia with reversible hyperplasia in conditional FGFR1-expressing mice." Cancer Res 63(23): 8256-63.

58. Gong, J., J. Wang, et al. (2009). "Serine/threonine kinase Pim-2 promotes liver tumorigenesis induction through mediating survival and preventing apoptosis of liver cell." J Surg Res 153(1): 17-22.

59. Grundler, R., L. Brault, et al. (2009). "Dissection of PIM serine/threonine kinases in FLT3-ITD-induced leukemogenesis reveals PIM1 as regulator of CXCL12-CXCR4-mediated homing and migration." J Exp Med 206(9): 1957-70.

60. Guerra, C., A. J. Schuhmacher, et al. (2007). "Chronic pancreatitis is essential for induction of pancreatic ductal adenocarcinoma by K-Ras oncogenes in adult mice." Cancer Cell 11(3): 291-302.

61. Guo, S., X. Mao, et al. (2010). "Overexpression of Pim-1 in bladder cancer." J Exp Clin Cancer Res 29: 161.

62. Halvorsen, O. J., J. Hostmark, et al. (2000). "Prognostic significance of p16 and CDK4 proteins in localized prostate carcinoma." Cancer 88(2): 416-24.

63. Hanahan, D. and R. A. Weinberg (2000). "The hallmarks of cancer." Cell 100(1): 57-70.

64. Hanahan, D. and R. A. Weinberg (2011). "Hallmarks of cancer: the next generation." Cell 144(5): 646-74.

65. Hernandez, F., E. Langa, et al. (2010). "Regulation of GSK3 isoforms by phosphatases PP1 and PP2A." Mol Cell Biochem 344(1-2): 211-5.

66. Hogan, C., C. Hutchison, et al. (2008). "Elevated levels of oncogenic protein kinase Pim-1 induce the p53 pathway in cultured cells and correlate with increased Mdm2 in mantle cell lymphoma." J Biol Chem 283(26): 18012-23.

67. Hoover, D. S., D. G. Wingett, et al. (1997). "Pim-1 protein expression is regulated by its 5'-untranslated region and translation initiation factor elF-4E." Cell Growth Differ 8(12): 1371-80.

68. Hsi, E. D., S. H. Jung, et al. (2008). "Ki67 and PIM1 expression predict outcome in mantle cell lymphoma treated with high dose therapy, stem cell transplantation and rituximab: a Cancer and Leukemia Group B 59909 correlative science study." Leuk Lymphoma 49(11): 2081-90.

69. Hu, X. F., J. Li, et al. (2009). "PIM-1-specific mAb suppresses human and mouse tumor growth by decreasing PIM-1 levels, reducing Akt phosphorylation, and activating apoptosis." J Clin Invest 119(2): 362-75.

70. Hudson, J. D., M. A. Shoaibi, et al. (1999). "A proinflammatory cytokine inhibits p53 tumor suppressor activity." J Exp Med 190(10): 1375-82.

71. Isaac, M., A. Siu, et al. "The oncogenic PIM kinase family regulates drug resistance through multiple mechanisms." Drug Resist Updat 14(4-5): 203-11.

72. Ishibashi, Y., H. Maita, et al. (2001). "Pim-1 translocates sorting nexin 6/TRAF4-associated factor 2 from cytoplasm to nucleus." FEBS Lett 506(1): 33-8.

73. Ivaska, J., L. Nissinen, et al. (2002). "Integrin alpha 2 beta 1 promotes activation of protein phosphatase 2A and dephosphorylation of Akt and glycogen synthase kinase 3 beta." Mol Cell Biol 22(5): 1352-9.

74. Jackson, L. J., J. A. Pheneger, et al. (2011). "The role of PIM kinases in human and mouse CD4+ T cell activation and inflammatory bowel disease." Cell Immunol 272(2): 200-13.

75. Jaffe, E. S., N. L. Harris, et al. (2008). "Classification of lymphoid neoplasms: the microscope as a tool for disease discovery." Blood 112(12): 4384-99.

76. Jenkins, R. B., J. Qian, et al. (1997). "Detection of c-myc oncogene amplification and chromosomal anomalies in metastatic prostatic carcinoma by fluorescence in situ hybridization." Cancer Res 57(3): 524-31.

77. Kim, J., M. Roh, et al. (2010). "Pim1 promotes human prostate cancer cell tumorigenicity and c-MYC transcriptional activity." BMC Cancer 10: 248.

78. Koike, N., H. Maita, et al. (2000). "Identification of heterochromatin protein 1 (HP1) as a phosphorylation target by Pim-1 kinase and the effect of phosphorylation on the transcriptional repression function of HP1(1)." FEBS Lett 467(1): 17-21.

79. Kortylewski, M., M. Kujawski, et al. (2005). "Inhibiting Stat3 signaling in the hematopoietic system elicits multicomponent antitumor immunity." Nat Med 11(12): 1314-21.

80. Kortylewski, M., H. Xin, et al. (2009). "Regulation of the IL-23 and IL-12 balance by Stat3 signaling in the tumor microenvironment." Cancer Cell 15(2): 114-23.

81. Laird, P. W., N. M. van der Lugt, et al. (1993). "In vivo analysis of Pim-1 deficiency." Nucleic Acids Res 21(20): 4750-5.

82. Larsson, L. G. (2011). "Oncogene- and tumor suppressor gene-mediated suppression of cellular senescence." Semin Cancer Biol 21(6): 367-76.

83. Lee, C. T., P. Capodieci, et al. (1999). "Overexpression of the cyclin-dependent kinase inhibitor p16 is associated with tumor recurrence in human prostate cancer." Clin Cancer Res 5(5): 977-83.

84. Li, Z., M. Szabolcs, et al. (2006). "Prostatic intraepithelial neoplasia and adenocarcinoma in mice expressing a probasin-Neu oncogenic transgene." Carcinogenesis 27(5): 1054-67.

85. Lin, W. W. and M. Karin (2007). "A cytokine-mediated link between innate immunity, inflammation, and cancer." J Clin Invest 117(5): 1175-83.

86. Lin, Y. W., Z. M. Beharry, et al. (2010). "A small molecule inhibitor of Pim protein kinases blocks the growth of precursor T-cell lymphoblastic leukemia/lymphoma." Blood 115(4): 824-33.

87. Lopez-Ramos, M., R. Prudent, et al. (2010). "New potent dual inhibitors of CK2 and Pim kinases: discovery and structural insights." FASEB J 24(9): 3171-85.

88. MacDougall, J. R. and L. M. Matrisian (1995). "Contributions of tumor and stromal matrix metalloproteinases to tumor progression, invasion and metastasis." Cancer Metastasis Rev 14(4): 351-62.

89. Magnuson, N. S., Z. Wang, et al. (2010). "Why target PIM1 for cancer diagnosis and treatment?" Future Oncol 6(9): 1461-78.

90. Mancini, M. and A. Toker (2009). "NFAT proteins: emerging roles in cancer progression." Nat Rev Cancer 9(11): 810-20.

91. Mantovani, A. (2009). "Cancer: Inflaming metastasis." Nature 457(7225): 36-7.

92. Mantovani, A., P. Allavena, et al. (2008). "Cancer-related inflammation." Nature 454(7203): 436-44.

93. McCubrey, J. A., L. S. Steelman, et al. (2007). "Roles of the Raf/MEK/ERK pathway in cell growth, malignant transformation and drug resistance." Biochim Biophys Acta 1773(8): 1263-84.

94. Mikkers, H., M. Nawijn, et al. (2004). "Mice deficient for all PIM kinases display reduced body size and impaired responses to hematopoietic growth factors." Mol Cell Biol 24(13): 6104-15.

95. Mizuno, K., T. Shirogane, et al. (2001). "Regulation of Pim-1 by Hsp90." Biochem Biophys Res Commun 281(3): 663-9.

96. Mochizuki, T., C. Kitanaka, et al. (1999). "Physical and functional interactions between Pim-1 kinase and Cdc25A phosphatase. Implications for the Pim-1-mediated activation of the c-Myc signaling pathway." J Biol Chem 274(26): 18659-66.

97. Mora, A., G. Sabio, et al. (2002). "Lithium blocks the PKB and GSK3 dephosphorylation induced by ceramide through protein phosphatase-2A." Cell Signal 14(6): 557-62.

98. Morishita, D., R. Katayama, et al. (2008). "Pim kinases promote cell cycle progression by phosphorylating and down-regulating p27Kip1 at the transcriptional and posttranscriptional levels." Cancer Res 68(13): 5076-85.

99. Moroy, T., S. Verbeek, et al. (1991). "E mu N- and E mu L-myc cooperate with E mu pim-1 to generate lymphoid tumors at high frequency in double-transgenic mice." Oncogene 6(11): 1941-8.

100. Mukaida, N., Y. Y. Wang, et al. (2011). "Roles of Pim-3, a novel survival kinase, in tumorigenesis." Cancer Sci.

101. Mumenthaler, S. M., P. Y. Ng, et al. (2009). "Pharmacologic inhibition of Pim kinases alters prostate cancer cell growth and resensitizes chemoresistant cells to taxanes." Mol Cancer Ther 8(10): 2882-93.

102. Naugler, W. E. and M. Karin (2008). "The wolf in sheep's clothing: the role of interleukin-6 in immunity, inflammation and cancer." Trends Mol Med 14(3): 109-19.

103. Nawijn, M. C., A. Alendar, et al. (2011). "For better or for worse: the role of Pim oncogenes in tumorigenesis." Nat Rev Cancer 11(1): 23-34.

104. Nga, M. E., N. N. Swe, et al. (2010). "PIM-1 kinase expression in adipocytic neoplasms: diagnostic and biological implications." Int J Exp Pathol 91(1): 34-43.

105. Nihira, K., Y. Ando, et al. (2010). "Pim-1 controls NF-kappaB signalling by stabilizing RelA/p65." Cell Death Differ 17(4): 689-98.

106. Noda, A., Y. Ning, et al. (1994). "Cloning of senescent cell-derived inhibitors of DNA synthesis using an expression screen." Exp Cell Res 211(1): 90-8.

107. Osman, I., M. Drobnjak, et al. (1999). "Inactivation of the p53 pathway in prostate cancer: impact on tumor progression." Clin Cancer Res 5(8): 2082-8.

108. Owaki, T., M. Asakawa, et al. (2008). "STAT3 is indispensable to IL-27-mediated cell proliferation but not to IL-27-induced Th1 differentiation and suppression of proinflammatory cytokine production." J Immunol 180(5): 2903-11.

109. Park, J. H., J. E. Walls, et al. (2002). "Prostatic intraepithelial neoplasia in genetically engineered mice." Am J Pathol 161(2): 727-35.

110. Paukku, K. and O. Silvennoinen (2004). "STATs as critical mediators of signal transduction and transcription: lessons learned from STAT5." Cytokine Growth Factor Rev 15(6): 435-55.

111. Pogacic, V., A. N. Bullock, et al. (2007). "Structural analysis identifies imidazo[1,2-b]pyridazines as PIM kinase inhibitors with in vitro antileukemic activity." Cancer Res 67(14): 6916-24.

112. Popivanova, B. K., Y. Y. Li, et al. (2007). "Proto-oncogene, Pim-3 with serine/threonine kinase activity, is aberrantly expressed in human colon cancer cells and can prevent Bad-mediated apoptosis." Cancer Sci 98(3): 321-8.

113. Poulsen, C. B., R. Borup, et al. (2005). "Microarray-based classification of diffuse large B-cell lymphoma." Eur J Haematol 74(6): 453-65.

114. Powell, W. C., R. D. Cardiff, et al. (2003). "Mouse strains for prostate tumorigenesis based on genes altered in human prostate cancer." Curr Drug Targets 4(3): 263-79.

115. Pulciani, S., E. Santos, et al. (1982). "Oncogenes in human tumor cell lines: molecular cloning of a transforming gene from human bladder carcinoma cells." Proc Natl Acad Sci U S A 79(9): 2845-9.

116. Puzio-Kuter, A. M., M. Castillo-Martin, et al. (2009). "Inactivation of p53 and Pten promotes invasive bladder cancer." Genes Dev 23(6): 675-80.

117. Qian, J., R. B. Jenkins, et al. (1997). "Detection of chromosomal anomalies and c-myc gene amplification in the cribriform pattern of prostatic intraepithelial neoplasia and carcinoma by fluorescence in situ hybridization." Mod Pathol 10(11): 1113-9.

118. Qian, K. C., L. Wang, et al. (2005). "Structural basis of constitutive activity and a unique nucleotide binding mode of human Pim-1 kinase." J Biol Chem 280(7): 6130-7.

119. Rainio, E. M., J. Sandholm, et al. (2002). "Cutting edge: Transcriptional activity of NFATc1 is enhanced by the Pim-1 kinase." J Immunol 168(4): 1524-7.

120. Reiser-Erkan, C., M. Erkan, et al. (2008). "Hypoxia-inducible proto-oncogene Pim-1 is a prognostic marker in pancreatic ductal adenocarcinoma." Cancer Biol Ther 7(9): 1352-9.

121. Roh, M., B. Gary, et al. (2003). "Overexpression of the oncogenic kinase Pim-1 leads to genomic instability." Cancer Res 63(23): 8079-84.

122. Roninson, I. B. (2003). "Tumor cell senescence in cancer treatment." Cancer Res 63(11): 2705-15.

123. Roy-Burman, P., H. Wu, et al. (2004). "Genetically defined mouse models that mimic natural aspects of human prostate cancer development." Endocr Relat Cancer 11(2): 225-54.

124. Santio, N. M., R. L. Vahakoski, et al. (2010). "Pim-selective inhibitor DHPCC-9 reveals Pim kinases as potent stimulators of cancer cell migration and invasion." Mol Cancer 9: 279.

125. Scherl, A., J. F. Li, et al. (2004). "Prostatic intraepithelial neoplasia and intestinal metaplasia in prostates of probasin-RAS transgenic mice." Prostate 59(4): 448-59.

126. Selten, G., H. T. Cuypers, et al. (1986). "The primary structure of the putative oncogene pim-1 shows extensive homology with protein kinases." Cell 46(4): 603-11.

127. Shah, N., B. Pang, et al. (2008). "Potential roles for the PIM1 kinase in human cancer - a molecular and therapeutic appraisal." Eur J Cancer 44(15): 2144-51.

128. Shappell, S. B., G. V. Thomas, et al. (2004). "Prostate pathology of genetically engineered mice: definitions and classification. The consensus report from the Bar Harbor meeting of the Mouse Models of Human Cancer Consortium Prostate Pathology Committee." Cancer Res 64(6): 2270-305.

129. Shay, K. P., Z. Wang, et al. (2005). "Pim-1 kinase stability is regulated by heat shock proteins and the ubiquitin-proteasome pathway." Mol Cancer Res 3(3): 170-81.

130. Shen, Y. M., Y. Zhao, et al. (2012). "Inhibition of Pim-1 Kinase Ameliorates Dextran Sodium Sulfate-Induced Colitis in Mice." Dig Dis Sci.

131. Siu, A., C. Virtanen, et al. (2011). "PIM kinase isoform specific regulation of MIG6 expression and EGFR signaling in prostate cancer cells." Oncotarget 2(12): 1134-44.

132. Song, J. H., K. Kandasamy, et al. (2011). "The BH3 mimetic ABT-737 induces cancer cell senescence." Cancer Res 71(2): 506-15.

133. Storer, R. D., M. E. Cartwright, et al. (1995). "Short-term carcinogenesis bioassay of genotoxic procarcinogens in PIM transgenic mice." Carcinogenesis 16(2): 285-93.

134. Straub, R. H. (2007). "The complex role of estrogens in inflammation." Endocr Rev 28(5): 521-74.

135. Swords, R., K. Kelly, et al. (2011). "The Pim kinases: new targets for drug development." Curr Drug Targets 12(14): 2059-66.

136. Tamburini, J., A. S. Green, et al. (2009). "Protein synthesis is resistant to rapamycin and constitutes a promising therapeutic target in acute myeloid leukemia." Blood 114(8): 1618-27.

137. Theyer, G., G. Kramer, et al. (1992). "Phenotypic characterization of infiltrating leukocytes in benign prostatic hyperplasia." Lab Invest 66(1): 96-107.

138. Valdman, A., X. Fang, et al. (2004). "Pim-1 expression in prostatic intraepithelial neoplasia and human prostate cancer." Prostate 60(4): 367-71.

139. Valkenburg, K. C. and B. O. Williams (2011). "Mouse models of prostate cancer." Prostate Cancer 2011: 895238.

140. van der Poel, H. G., J. Zevenhoven, et al. (2010). "Pim1 regulates androgen-dependent survival signaling in prostate cancer cells." Urol Int 84(2): 212-20.

141. van Lohuizen, M., S. Verbeek, et al. (1989). "Predisposition to lymphomagenesis in pim-1 transgenic mice: cooperation with c-myc and N-myc in murine leukemia virus-induced tumors." Cell 56(4): 673-82.

142. Vande Broek, I., K. Asosingh, et al. (2004). "Bone marrow endothelial cells increase the invasiveness of human multiple myeloma cells through upregulation of MMP-9: evidence for a role of hepatocyte growth factor." Leukemia 18(5): 976-82.

143. Vivanco, I. and C. L. Sawyers (2002). "The phosphatidylinositol 3-Kinase AKT pathway in human cancer." Nat Rev Cancer 2(7): 489-501.

144. Wang, J., J. Kim, et al. (2010). "Pim1 kinase synergizes with c-MYC to induce advanced prostate carcinoma." Oncogene 29(17): 2477-87.

145. Wang, S., J. Gao, et al. (2003). "Prostate-specific deletion of the murine Pten tumor suppressor gene leads to metastatic prostate cancer." Cancer Cell 4(3): 209-21.

146. Wang, Z., N. Bhattacharya, et al. (2002). "Phosphorylation of the cell cycle inhibitor p21Cip1/WAF1 by Pim-1 kinase." Biochim Biophys Acta 1593(1): 45-55.

147. Wang, Z., N. Bhattacharya, et al. (2001). "Pim-1: a serine/threonine kinase with a role in cell survival, proliferation, differentiation and tumorigenesis." J Vet Sci 2(3): 167-79.

148. Warnecke-Eberz, U., E. Bollschweiler, et al. (2009). "Prognostic impact of protein overexpression of the proto-oncogene PIM-1 in gastric cancer." Anticancer Res 29(11): 4451-5.

149. White, E. (2003). "The pims and outs of survival signaling: role for the Pim-2 protein kinase in the suppression of apoptosis by cytokines." Genes Dev 17(15): 1813-6.

150. Wingett, D., D. Stone, et al. (1995). "Expression of the pim-1 protooncogene: differential inducibility between alpha/beta- and gamma/delta-T cells and B cells." Cell Immunol 162(1): 123-30.

151. Winn, L. M., W. Lei, et al. (2003). "Pim-1 phosphorylates the DNA binding domain of c-Myb." Cell Cycle 2(3): 258-62.

152. Wu, Y., Y. Y. Wang, et al. (2010). "Accelerated hepatocellular carcinoma development in mice expressing the Pim-3 transgene selectively in the liver." Oncogene 29(15): 2228-37.

153. Xie, Y., K. Xu, et al. (2006). "The 44 kDa Pim-1 kinase directly interacts with tyrosine kinase Etk/BMX and protects human prostate cancer cells from apoptosis induced by chemotherapeutic drugs." Oncogene 25(1): 70-8.

154. Yatkin, E., J. Bernoulli, et al. (2009). "Inflammation and epithelial alterations in rat prostate: impact of the androgen to oestrogen ratio." Int J Androl 32(4): 399-410.

155. Yoshidome, K., M. A. Shibata, et al. (1998). "Genetic alterations in the development of mammary and prostate cancer in the C3(1)/Tag transgenic mouse model." Int J Oncol 12(2): 449-53.

156. Yu, H., M. Kortylewski, et al. (2007). "Crosstalk between cancer and immune cells: role of STAT3 in the tumour microenvironment." Nat Rev Immunol 7(1): 41-51.

157. Zemskova, M., M. B. Lilly, et al. (2010). "p53-dependent induction of prostate cancer cell senescence by the PIM1 protein kinase." Mol Cancer Res 8(8): 1126-41.

158. Zemskova, M., E. Sahakian, et al. (2008). "The PIM1 kinase is a critical component of a survival pathway activated by docetaxel and promotes survival of docetaxel-treated prostate cancer cells." J Biol Chem 283(30): 20635-44.

159. Zhang, P., H. Wang, et al. (2009). "Pim-3 is expressed in endothelial cells and promotes vascular tube formation." J Cell Physiol 220(1): 82-90.

160. Zhang, Y., Z. Wang, et al. (2008). "Pim kinase-dependent inhibition of c-Myc degradation." Oncogene 27(35): 4809-19.

161. Zhang, Y., Z. Wang, et al. (2007). "Pim-1 kinase-dependent phosphorylation of p21Cip1/WAF1 regulates its stability and cellular localization in H1299 cells." Mol Cancer Res 5(9): 909-22.

162. Zhao, Y., M. S. Hamza, et al. (2008). "Kruppel-like factor 5 modulates p53-independent apoptosis through Pim1 survival kinase in cancer cells." Oncogene 27(1): 1-8.

163. Zippo, A., A. De Robertis, et al. (2007). "PIM1-dependent phosphorylation of histone H3 at serine 10 is required for MYC-dependent transcriptional activation and oncogenic transformation." Nat Cell Biol 9(8): 932-44.

Appendix

Appendix

A) Materials

Table A: Equipment

Product	Manufacturer
10 cm Ø tissue culture plate	Falcon, BD
12 well plate	Falcon
24 well plare	Falcon
30 cm Ø tissue culture plate	Falcon, BD
6 cm Ø plate	Falcon, BD
6 well plate	Falcon
biosafety tissue culture hood	ICN Biomedicals Gelaire
blotting device	BioRad
blotting paper	Albet
cell counting chamber	Brand
centrifuge megafuge 1.0 R	Heraeus
centrifuge RC5C	Sorvall instruments
conical tube 15 ml	Falcon
conical tube 50 ml	Falcon
digital camera	Olympus C-5050
elisa reader	Labsystems multiskan Biochromatic
erlenmeyer flask	Pyrex
filter paper	Albet
gel electroporesis device	BioRad
glass pasteur pipette	Brand
glass bottle (1 l; 0.5 l)	Schott
incubator	NuAire
latex gloves	T&C
measuring cylinder	Pyrex
microcentrifuge tubes	Eppendorf
microvave	Moulinex
multichannel pipette	Micronic
parafilm	American national can
PCR machine	Biometra
phase contrast microscope	Nikon
pipette help acuboy	Technomara
power supply	BioRad

precision balance	Cobos
PVDF membrane	Millipore
rocking platform	Elmi
round bottom tube 13 ml	Sarstedt
sterile pipette (2 ml; 5 ml; 10 ml; 25 ml)	Falcon, BD
thermoblock	P-Selecta
thermomixer	eppendorf
top-table centrifuge	Hettich
Vortex	Scientific industries
x-ray film cassette	Rego
x-ray flim	Kodak

Table B: Chemicals

Product	Manufacturer
1x PBS	at research facility
Acetic acid	Merck
Acrylamide	BioRad
Agarose	Gibco
Ammoniumperoxodisulphate (APS)	Fluka
Ampicillin	Sigma
Aprotinin from bovine lung	Sigma
beta-Mercaptoethanol	Calbiochem
Bovine serum albumine (BSA)	Roche
Bromphenol Blue	Merk
Chloroform	Merck
Coomassie Brillant Blue	BioRad
Desoxycholate (Methyl 7-Acetylchenodesoxcholate)	Fluka
Dimethylsofoxid (DMSO)	Sigma
D-MEM medium	Gibco
dNTP	Pharmacia
DTT	Sigma
EDTA	Sigma
EGTA	Merk
Ethanol 96%	Merck
Fetal calf serum	ICN Biomedicals
Formaldehyde	Merck
Glycerin	AppliChem
Glycerol	Merk

Glycine	Sigma
Isopropanol	Merck
Klenow enzyme	Roche
Leupeptin (in Trifluoroacetate salt)	Sigma
L-Glutamine	Gibco
Lipofectamine	Invitrogen
Methanol	Merck
Methylene blue	Merck
Milk powder	Nestle
NP-40 (Nonidet-P 40)	Fluka
Oligonucleotide Primers	Sigma
Phenol	Merck
Plus reagent	Invitrogen
PMSF	AppliChem
Ponceau S	Sigma
Pre-stained broad range protein marker	BioRad
Prime-It II; random labelling kit	Stratagene
Proteinase K	Roche
Puromycin	Invitrogen
Restriction enzymes	Roche
Rnasin	Promega
SDS	BioRad
Sodium acetate	Merck
Sodium Chloride	Merk
Sodium hydroxide	Merk
sodium ortho-vanadate	Sigma
T4-DNA Ligase	Roche
Temed (tetra-methyl-ethylenediamine)	BioRad
Tris Base	USB
Tris-Hcl	USB
Trypan blue	AppliChem
Trypsin-EDTA	Gibco
Tween 20	Sigma

Buffer and Solutions

1.) Western Blot

Running Buffer (5x):
1000 ml H_20
0.1225 M Tris base (15.15 g)
0.96 M Glycine (72.2 g)
0.5 % SDS (5 g)

TBS (1x):
1000 ml H_20
150 mM NaCl (9.74 g)
50 mM Tris-HCl pH 7.4 (20 ml Tris-HCl 1 M)

Washing Buffer:
1000 ml TBS
0.1 % BSA (1 g)
0.05 % Tween 20 (0.5 ml)
0.02 % Thimerosal[1]

Blocking Buffer:
1000 ml TBS
5 % Milkpowder (50 g)
1 % BSA (10 g)
0.02 % Thimerosal (optional[1])

Transfer Buffer:
800 ml H_2O
25 mM Tris (3 g)
190 mM Gycine (14.4 g)
20 % Methanol (200 ml)

Sample Buffer (4x):
12.5 ml Tris 1 M pH 6.9
20 ml Gycerol
20 ml SDS 20 %
5 ml Bromphenol Blue 0.4 %
Prepare aliquots of 950 µl and store them at –20 ºC; before use. add 50 µl Mecaptoethanol to aliquot.

Ripa Buffer:
8.4 ml H_2O
50 mM Tris-HCl pH 8.0
150 mM NacCl
1% NP-40 (1 ml)
0.5 % Desoxycholate (0.5 ml)
0.1 % SDS (0.1 ml)
Immediately before use add protease inhibitors to ripa buffer (1:40 v/v)

[1] augments storing time for up to one month

Protease Inhibitor (40x): 20 mM PMSF
40 mM O_4VNa(sodium ortho-vanadate)
40 µg/ml Aprotinin
40 µg/ml Leupeptin

NP-40 High Salt Buffer: 20 mM Hepes pH 7.9
1 mM EDTA
400 mM NaCl
25 % Glycerol
0.1 % NP-40

TB-buffer: 0.41 M pH 6.7 Pipes (2,43 ml)[2]
0.5 M $MnCl_2$ (11 ml)
1 M $CaCl_2$ (1,5 ml)
3M KCl (8,33 ml)
77 ml H_2O

The TB-Buffer needs to be filtered and stored at 4 ºC. The pH has to be adjusted to pH 6.7.

2.) RNA:

NP-40 Lysis Buffer: 10 mM Tris-hydroxymethyl-aminomethane (Tris-HCl) pH=8,0
150 mM NaCl
1.5 mM $MgCl_2$
0.5% v/v Nonidet P-40 (NP-40)

TE (Tris-EDTA): 10 mM Tris-HCl pH=8.0
1 mM EDTA pH=8.0
store at room temperature.

RNasin: placental RNase inhibitor (see also II.1.); requires 5 mM dithiotreitol (DTT) for optimal activity); available from Promega, Boehringer Mannheim and other suppliers; usually 40 U/µl; store at -20^{O}C.

3.) DNA:

TAE-Buffer (1x): 40 mM Tris-base,
20 mM acetic acid,
1 mM EDTA pH=8.0

TBE-Buffer (1x): 89 mM Tris-base
89 mM Boric acid
2 mM EDTA pH=8.0

[2] Due to its acid pH the Pipes may does not dissolve well. If that is the case NaOH lentils need to be added until the Pipes dissolves and the pH has to be adjusted afterwards to pH 6.7 with NaOH before the $MnCl_2$ is added.

Publications

This work gave rise to several publications:

Maja Narlik-Grassow, Carmen Blanco-Aparicio, Yolanda Cecilia, Sandra Peregrina, Beatriz Garcia-Serelde, Sandra Moñoz-Galvan, Marta Cañamero and Amancio Carnero. "The essential role of PIM kinases in sarcoma growth and bone invasion." Carcinogenesis, accepted 02.05.2012

Maja Narlik-Grassow, Carmen Blanco-Aparicio, Marta Cañamero, Yolanda Cecilia, Oliver Renner, Amancio Carnero. "PIM1 kinase gain of function contributes to prostate tumorigenesis *in vivo*." In progress

Oliver Renner, Carmen Blanco-Aparicio, **Maja Grassow**, Marta Cañamero, Juan F. Leal, Amancio Carmero; "Activation of phosphatidylinositol 3-kinase by membrane localization of p110alpha predisposes mammary glands to neoplastic transformation." Cancer Res. 2008 Dec 1;68(23):9643-53.